UiT
THE ARCTIC
UNIVERSITY
OF NORWAY

Faculty of Health Sciences
Department of Pharmacy
Natural Products and Medicinal Chemistry Research Group

Large scale cultivation of microalgae at Finnfjord AS: The effect of addition of CO_2 and flue gas on lipid production and fatty acid composition

—

Marte Ramskjell

Master's thesis in Pharmacy, May 2018

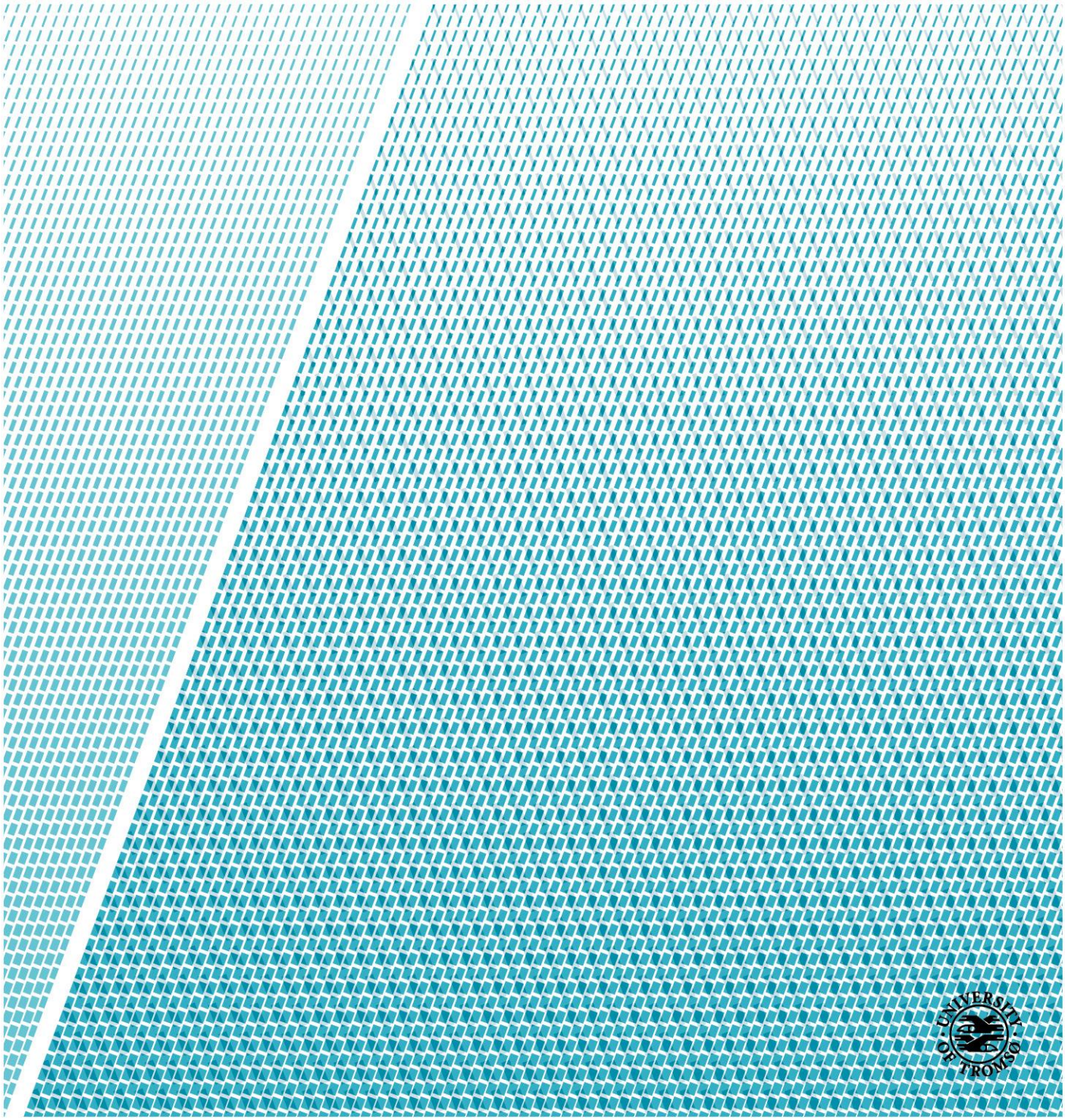

Acknowledgement

The work presented in this thesis was carried out at the Natural Products and Medicinal Chemistry Research Group, Department of Pharmacy (IFA), UiT The Arctic University of Norway in collaboration with the Norwegian College of Fishery Science (NFH) and Finnfjord AS in the period from August 2017 to May 2018. Supervisors were Associate Professor Terje Vasskog (IFA), Associate Professor Terkel Hansen (IFA) and PhD Candidate Jon Brage Svenning (NFH).

First of all, I would like to express my deepest gratitude to my main supervisor Terje Vasskog. This thesis would not have been possible without your dedicated assistance, guidance and support throughout the period. Thanks for always finding time to help me. I would also like to thank my co-supervisor Terkel Hansen for helping with the picolinyl derivatization and the development of the GC/MS method.

I wish to express my gratitude to my external supervisor Jon B. Svenning for helping me with the biology part of the thesis and for letting me participate in the cultivation and harvesting at Finnfjord. I would also like to thank PhD Candidate Lars Dalheim, my unofficial external co-supervisor, who, together with Jon, helped me with the lipid extraction and preparation of FAMEs. A special thanks to the engineers who carried out the cultivation and harvesting of the algae. To Professor Hans C. Eilertsen and the rest of the project team, thank you for letting me be a part of this exciting project.

I would also like to thank my classmate Simen, who also worked with analysis of fatty acids in microalgae. Most of the lab work was done in collaboration with him. Thanks for being a great discussion partner and good company at the lab.

Finally, I must show my appreciation to my family, boyfriend and friends for supporting and encouraging me throughout this period. Thanks!

Tromsø, May 2018
Marte Ramskjell

Abstract

Background: This master's thesis was a part of a project involving mass cultivation of microalgae at the smelting plant Finnfjord AS. Microalgae are primary producers of the important omega-3 long-chain polyunsaturated fatty acids EPA and DHA. At Finnfjord, the algae use CO_2 from the flue gas for their production of lipid and protein rich biomass. The algal biomass can potentially function well as fish feed for the aquaculture industry. In this thesis, the main goal was to investigate how the addition of flue gas affects the lipid content and fatty acid composition of the algae.

Method: Two algal species were included in the project. *Porosira glacialis* was cultivated with and without addition of CO_2 and flue gas (from Finnfjord), and *Chaetoceros furcellatus* was cultivated with and without addition of CO_2. From freeze-dried algal biomass, the lipids were extracted. Fatty acids were isolated from larger lipids and derivatized to fatty acid methyl esters (FAMEs) by methylation/transesterification, for quantitative analysis, and further derivatized to picolinyl derivatives for structure elucidation. To analyze the fatty acid derivatives, GC/MS with EI and full scan mode was applied. For identifying molecular ions of FAMEs, a method using GC/MS with CI and SIR was developed. In addition, GC/MS/MS with a product ions scan approach was also tested.

Results: The content of polyunsaturated fatty acids, including EPA, were generally high in all the algae samples, and the omega-3/omega-6 ratio was also particularly high. The addition of CO_2 and flue gas had a small impact on lipid content and fatty acid composition of the algae. Most importantly, the proportion of unsaturated fatty acids was not reduced by the addition of flue gas, and the lipid content was only slightly reduced. The double bond positions of all the fatty acids in the algae, except 18:3, were determined. GC/MS with CI and SIR appeared to be useful for determination of molecular ions of FAMEs. The method provided better sensitivity and selectivity compared to EI and full scan mode. GC/MS/MS with a product ion scan approach was, on the contrary, unsuccessful for analysis of both FAMEs and picolinyl derivatives.

Conclusion: Based on the lipid content and fatty acid profile of the algae, the use of algal biomass as fish feed for the aquaculture industry seems promising.

Table of contents

Abbreviations

AA	Arachidonic acid
A_a/A_{IS}	Ratio between peak area of the analyte and the internal standard
ALA	Alpha-linolenic acid
amu	Atomic mass unit
CACI	Covalent adduct chemical ionization
CAS	Chemical Abstracts Service
Cf.	*Chaetoceros furcellatus*
CI	Chemical ionization
CID	Collision-induced dissociation
DCM	Dichloromethane
DHA	Docosahexaenoic acid
EI	Electron ionization
EPA	Eicosapentaenoic acid
eV	Electron volt
FA	Fatty acid
FAME	Fatty acid methyl ester
x g	Times gravity
GC	Gas chromatography
IS	Internal standard
LA	Linoleic acid
LC-PUFA	Long-chain polyunsaturated fatty acid
M	mol/L
MeOH	Methanol
MRM	Multiple reaction monitoring
MS	Mass spectrometry
MS/MS	Tandem mass spectrometry
MUFA	Monounsaturated fatty acid
m/z	Mass-to-charge ratio
n.d.	Not detectable
Pg.	*Porosira glacialis*
PUFA	Polyunsaturated fatty acid
Q1	First mass filter of a triple quadrupole
Q2	Collision cell of a triple quadrupole
Q3	Second mass filter of a triple quadrupole
QqQ	Triple quadrupole
RSD	Relative standard deviation
SD	Standard deviation
SFA	Saturated fatty acid
SIR	Selected ion recording

SLE	Solid-liquid extraction
sp.	Species
SS	Stock solution
TAG	Triglycerides
TFA	Total fatty acids
THF	Tetrahydrofuran
UFA	Unsaturated fatty acid
v/v	Volume/volume

1 Introduction

1.1 Background

In 2015, a collaborative project involving mass cultivation of microalgae was established between Finnfjord AS and UiT The Arctic University of Norway. The smelting plant Finnfjord AS, located at Finnsnes in Northern Norway, produces approximately 100,000 tonnes of ferrosilicon per year. This creates large CO_2 emissions, which are both harmful for the environment and expensive for the company. The smelting plant has an annual emission of 300,000 tonnes of CO_2. Diatoms, which are photosynthetic microalgae, use CO_2 from the flue gas for their production of lipid and protein rich biomass. This is positive both in terms of reduced CO_2 emissions and increased biomass production. The biomass can potentially function well as fish feed for the aquaculture industry.

The content of Norwegian fish feed has changed over the past decades. In 1990, about 90% of the ingredients in salmon feed had marine sources, while in 2013, this number was reduced to roughly 30% [1]. A large proportion is being replaced by ingredients of plant origin, which contain small amounts of omega-3 long-chain polyunsaturated fatty acids (LC-PUFAs). Plant ingredients also have a high omega-6/omega-3 ratio. This will not give the same beneficial health effects to the end consumers, i.e. humans, as fish feed of marine origin with high omega-3/omega-6 ratio. Currently available sources of the important omega-3 fatty acids EPA and DHA will not be adequate to meet future needs [2]. Therefore, alternative sustainable sources of EPA and DHA are sought. Since microalgae are primary producers of omega-3 LC-PUFAs, they are a promising candidate for this purpose.

In conventional mass cultivation of microalgae, small (approx. 5 µm diameter) warm-water strains, such as *Chlorella* or *Nannochloropsis*, are mainly used. Due to certain adaptations, such species may reach much higher cell densities compared to larger cells. High densities result in high levels of self-shading, which causes short light depth into the cultivation tanks. As a result, bioreactors with large surface area to volume ratios are required. The Finnfjord/UiT project uses large cold-water diatom species, which have much smaller surface to volume ratios. This gives a lower self-shading level, which in turn gives longer light depth. Thus, cultivation tanks with much larger volume to surface area ratios can be employed. The cold-water diatoms used in this project are physiologically adapted to the northern conditions, i.e. the low temperature

and the winter darkness. To survive the darkness, the algae are highly effective lipid producers. The lipid profile of cold-water diatoms is generally highly unsaturated [3, 4].

This work is part of an upscaling of a successful pilot project, where photobioreactors with a total volume of 26,000 L were applied. This is now being extended to preindustrial scale, with a photobioreactor containing 300,000 L. Using large northern cold-water diatoms, Finnfjord AS has ambitions to become the world's first carbon neutral smelting plant.

In this thesis, the main goal was to investigate how the addition of flue gas affects the lipid content and fatty acid composition of the diatoms used in the Finnfjord/UiT project, as well as developing a chemical analysis method for this purpose.

1.2 Lipids

Lipids are a class of biological compounds and can be defined as substances that are soluble in organic solvents and often insoluble in water. Various types of lipids can be very different in terms of structure and function. Some lipids are completely non-polar (e.g. triglycerides and waxes), while others are amphipathic, which means that they have both a polar and a non-polar part (e.g. fatty acids and phospholipids)[5, p. 93].

1.2.1 Fatty acids

Fatty acids consist of a hydrocarbon chain with a carboxyl group at one end. The length of the chain varies. Fatty acids can either occur as free fatty acids or as a part of larger lipids (e.g. phospholipids or triglycerides).

A fatty acid can be saturated or unsaturated. Unsaturated fatty acids (UFAs) contain one or more double bonds in the hydrocarbon chain. Saturated fatty acids (SFAs), on the other hand, have no double bonds in the chain. Monounsaturated fatty acids (MUFAs) contain one double bond, while polyunsaturated fatty acids (PUFAs) contain two or more double bonds.

The physical properties of fatty acids are determined by the number of double bonds and the length of the chain. A shorter chain and more double bonds give increased polarity and a lower melting point, and vice versa, a longer chain and fewer double bonds give reduced polarity and a higher melting point [5, p. 93-96].

1.2.1.1 Nomenclature

When describing fatty acids, the number of carbon atoms and the number of double bonds in the chain, as well as the location of the double bonds, are given. The position of double bonds can be expressed in two ways; with either delta (Δ) or omega (ω or n). Delta indicates the number of carbon atoms from the carboxyl end, while omega indicates the number of carbon atoms from the omega end (i.e. the opposite end). For instance, eicosapentaenoic acid (EPA) can be expressed as 20:5 n-3 or 20:5 Δ5,8,11,14,17. This fatty acid has 20 carbon atoms and five double bonds (Figure 1).

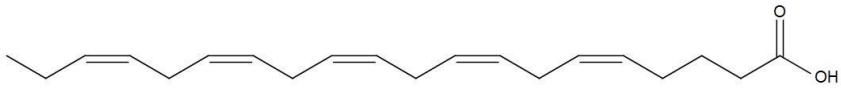

Figure 1 - Eicosapentaenoic acid (20:5 n-3)

A double bond has either cis or trans configuration (Figure 2). It can also be expressed as Z or E configuration. The configuration is specified in the systematic name of the fatty acids. Cis configuration gives a "bend" in the hydrocarbon chain.

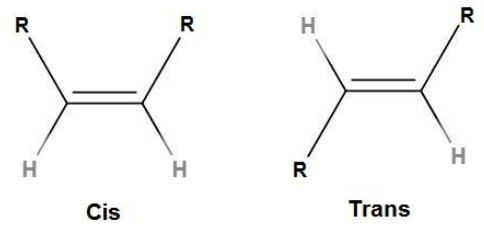

Figure 2 - The difference between cis and trans configuration. R = hydrocarbon chain.

1.2.1.2 Long-chain polyunsaturated fatty acids

Since mammals, including humans, lack the necessary enzymes to synthesize long-chain polyunsaturated fatty acids (LC-PUFA), it must be administered through the diet [6]. Alpha-linolenic acid (ALA, 18:3 n-3) and linoleic acid (LA, 18:2 n-6) are essential fatty acids. When humans receive ALA and LA through diet, these fatty acids can be metabolized into three important LC-PUFAs; arachidonic acid (AA, 20:4 n-6), eicosapentaenoic acid (EPA, 20:5 n-3) and docosahexaenoic acid (DHA, 22:6 n-3)[7]. However, the conversion to EPA and DHA occurs with low efficiency, and therefore it is recommended to receive these fatty acids also from other sources [8]. Microalgae can be a direct source of EPA and DHA [9].

LC-PUFAs have many important functions in the body. They have an important role as components of phospholipids, which are structural components in biological membranes. They are also precursors of eicosanoids (including prostaglandins and thromboxanes), which play a key role in the regulation of, among other things, the immune system and coagulation [6, 8].

1.2.1.3 Omega-6/omega-3 ratio

As mentioned, AA, EPA and DHA can be formed from the essential fatty acids LA and ALA. This occurs via two metabolic pathways; the omega-6 and the omega-3 pathway (Figure 3). These pathways compete for the same enzymes (desaturates and elongases). For this reason, a high omega-6/omega-3 ratio will limit the metabolic production of the omega-3 fatty acids EPA and DHA [7].

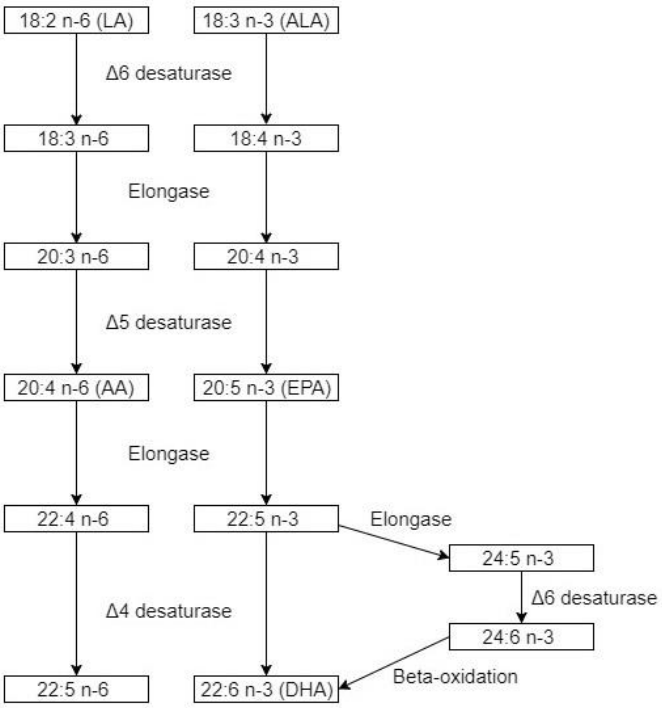

Figure 3 - The metabolic pathways of omega-3 and omega-6 PUFAs.

1.2.2 Triglycerides

Triglycerides (TAGs), or triacylglycerols, are lipids consisting of glycerol and three fatty acids. The fatty acids are bound to the hydroxyl groups via ester bonds. Compared to free fatty acids, TAGs are more non-polar. Since the three fatty acids are often different, many combinations of fatty acids are possible. The fatty acid composition varies according to the origin of the TAG.

In humans, TAGs act as energy storage. When energy is needed by the body, glycerol and fatty acids are released via hydrolysis of the ester bonds [5, p. 96-98].

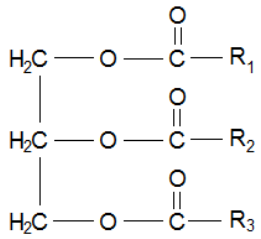

Figure 4 - The general structure of TAGs. R_1, R_2, R_3 = fatty acid.

1.2.3 Phospholipids

Biological membranes consist of a bilayer of lipids, primarily phospholipids. Phospholipids are amphipathic, i.e. they have a polar and a non-polar region, which is an essential characteristic of membrane lipids. Phospholipids are divided into two main groups; glycerophospholipids and sphingolipids.

1.2.3.1 Glycerophospholipids

Glycerophospholipids consist of a glycerol backbone with two fatty acids (often one saturated and one unsaturated fatty acid) and phosphate attached to it. Glycerophospholipids can be divided into different groups based on which head group that further is bound to the phosphate group. Examples of head groups are choline, glycerol, ethanolamine and serine. The head group together with phosphate is the polar region of the molecule, while the two fatty acids constitute the non-polar region [10, p. 350-351].

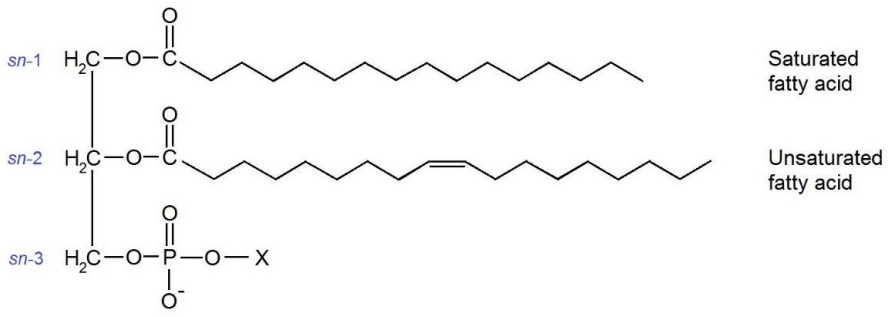

Figure 5 - The general structure of glycerophospholipids. X = head group.

1.2.3.2 Sphingolipids

Unlike glycerophospholipids, sphingolipids do not contain glycerol. Sphingolipids consist of sphingosine, a fatty acid and a head group. Phosphocholine is an example of a head group [10, p. 352-353].

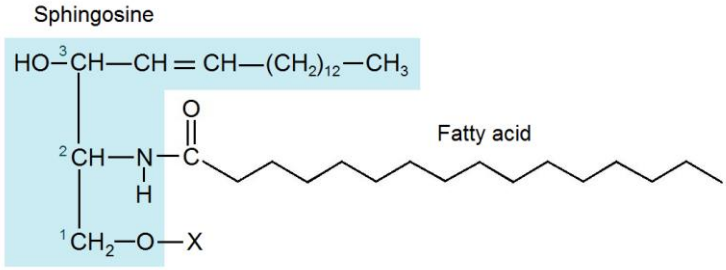

Figure 6 - The general structure of sphingolipids. X = head group.

1.2.4 Glycolipids

Glycolipids are membrane lipids, the structure of which has many similarities with phospholipids, but instead of phosphate, the lipids contain a carbohydrate [5, p. 98-99]. In algae, glycolipids are located mainly in photosynthetic membranes [9].

1.3 Marine diatoms

Diatoms (Bacillariophyceae) are an algae class within the division Heterokontophyta. This is an important group of phytoplankton that dominates in cold and temperate sea areas, like in the Norwegian coastal areas [11, p. 11, 12]. There are at least 30,000, and probably approximately 100,000 species of diatoms, according to estimations made by Mann and Vanormelingen [13].

Diatoms are unicellular eukaryotic organisms, the size of which varies from about 2 µm to over 5 mm. The cell wall is a two-part siliceous shell consisting of silicic acid ("glass"). Diatoms can be divided into two main groups; centric (order Biddulphiales) and pennate (order Bacillariales). Centric diatoms have a circular shape, while pennate diatoms are rod-shaped. Diatoms often form colonies [11, p. 112-114].

Figure 7 - Coscinodiscus sp. Example of a centric diatom (photo: Jon B. Svenning)

Figure 8 - Navicula sp. Example of a pennate diatom (photo: Gunilla K. Eriksen)

1.3.1 Diatoms as lipid producers

Diatoms are photosynthetic organisms containing chloroplast. Algae account for as much as 40% of the global photosynthesis [14]. As mentioned, diatoms are important *de novo* producers of LC-PUFAs [9], which means that other marine organisms of all trophic levels directly or indirectly receive LC-PUFAs from algae.

In order to grow, the algae need light, inorganic nutrients (nitrogen, phosphate and silicate), dissolved CO_2 and trace metals (e.g. iron) [15]. When the algae are stressed by lack of nutrients, CO_2 or light, they alter from an exponential growth phase to a stationary phase (resting phase), and the algae shift from producing and consuming lipids, to storing lipids, resulting in accumulation of lipids in the algae [16-18]. The proportion of polar lipids, such as phospholipids, which are important for cell division, increases during the exponential growth phase, while the proportion of neutral lipids, such as TAGs, increases during the stationary phase [19].

1.3.2 *Porosira glacialis*

In this project, the algal species *Porosira glacialis* was studied. *P. glacialis* is a centric diatom belonging to the family Thalassiosiraceae. These algae have a relatively large cell size, with a diameter of approximately 30-40 µm [11, p. 124-130]. The species can be found during the spring bloom along the northern Norwegian coast and in the Barents Sea, but it is not a dominant species [12].

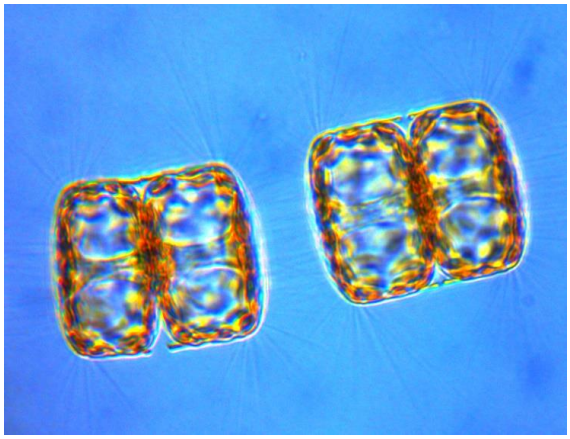

Figure 9 - Porosira glacialis (photo: Richard Ingebrigtsen)

1.3.3 *Chaetoceros furcellatus*

The algal species *Chaetoceros furcellatus* was also included in this project. *C. furcellatus* is a centric diatom belonging to the family Chaetocerotaceae. The apical axis of the algae is 8-20 µm, which means that the cell size is smaller than for *P. glacialis*. As shown in Figure 10, the algae exist in chains [11, p. 122-173]. *C. furcellatus* is one of the main species during the spring bloom along the northern Norwegian coast and in the Barents Sea [12].

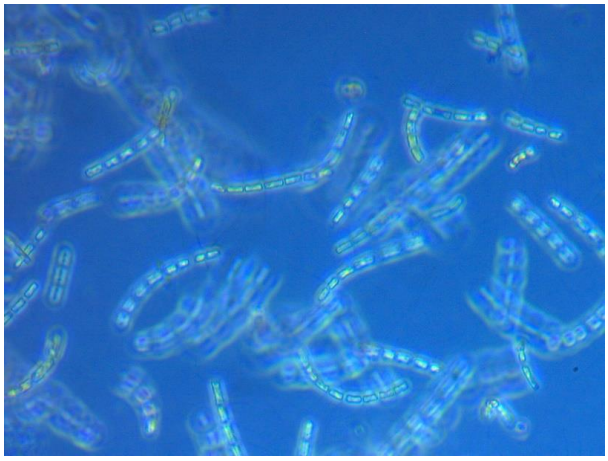

Figure 10 - Chaetoceros furcellatus (photo: Martina Uradnikova).

1.4 Lipid extraction

In order to analyze the fatty acids, all lipids must first be isolated from the algal biomass. When having a solid sample, solid-liquid extraction (SLE) is an appropriate approach for sample preparation. SLE is used to extract the analyte from a mixture of solids using an extracting solvent. The solid sample is powdered and a solvent is added. After shaking, the analyte is extracted from the solid phase to the solvent. The extract containing the analyte can then be collected [20, p. 275-287].

1.5 Derivatization of fatty acids

1.5.1 Methylation/transesterification

All analyses in this project were performed using GC/MS. Due to the low volatility of fatty acids, they need to be derivatized to be analyzed by GC. The methylation/transesterification has two purposes: to isolate fatty acids from larger lipids, such as phospholipids and TAGs, and to form fatty acid methyl esters (FAMEs). FAMEs are formed by methylation of free fatty acids and transesterification of larger lipids, using methanol and an acidic catalyst. During methylation, the fatty acid is protonated and an oxonium ion is formed. The oxonium ion reacts with methanol and forms an intermediate, which, after loss of a proton, forms a FAME (Figure 11) [21]. FAMEs are more volatile and thermally stable than fatty acids, which are important characteristics when running GC.

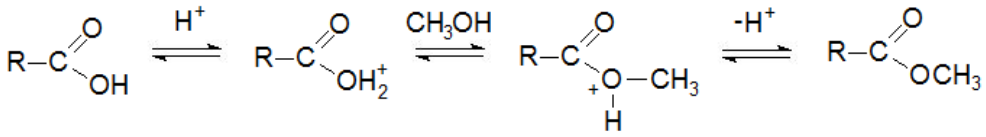

Figure 11 – Acid-catalyzed methylation of fatty acids. R = hydrocarbon chain.

FAMEs are well-suited for quantitative analysis on GC/MS, but because it is difficult to distinguish between isomeric FAMEs, for instance in the case of unsaturated fatty acids with double bonds in different positions, FAMEs are unsuitable for identification of fatty acids.

However, it is possible to identify fatty acids using FAMEs if standards of the compounds are available and retention time is thus known.

1.5.2 Picolinyl derivatization

Picolinyl derivatization transform FAMEs to picolinyl esters, also called 3-pyridylcarbinol esters. When picolinyl esters are ionized in the mass spectrometer, an electron will be removed from the nitrogen of the pyridine ring. This attracts a proton from the fatty acid chain, which leads to cleavage of the chain. The probability of where this proton is taken from depends on the structure of the fatty acid chain. The result is a fragmentation pattern that makes it possible to determine double bond positions [22]. Picolinyl derivatives of fatty acids are therefore well-suited for identification of fatty acids.

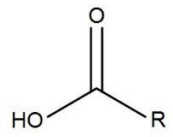

Figure 12 - The structure of fatty acids. R = hydrocarbon chain.

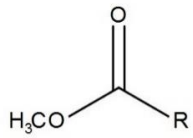

Figure 13 - The structure of FAMEs. R = hydrocarbon chain.

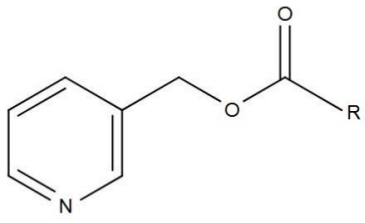

Figure 14 - The structure of picolinyl esters. R = hydrocarbon chain.

1.6 Gas chromatography

In order to analyze the fatty acid derivatives, the different compounds need to be separated. Chromatography is a collective term for separation methods based on the analyte distribution between a stationary phase and a mobile phase. In gas chromatography (GC), the mobile phase is an inert gas, called carrier gas, and the stationary phase is usually a liquid.

The apparatus consists of an injector system, a column and a detector. In addition, a container with carrier gas is required. Common carrier gases are helium, hydrogen and nitrogen. The carrier gas enters the injector system and goes through the column, which is placed in a hot air oven. The column contains the stationary phase.

Sample solution is injected into the injector, where the constituents evaporate. Then the carrier gas "carries" the analytes through the column. The analytes are distributed between the carrier gas and the stationary phase. For polar stationary phases, the solubility of the analyte in the stationary phase affects the analyte velocity through the column, which means that compounds which are more soluble in the stationary phase will remain for a longer time in the column than compounds which are less soluble. The retention time of an analyte, i.e. the time the analyte uses through the column, also depends on the boiling point of the analyte. The boiling point matters because the analyte must be in gas phase to move through the column. For non-polar stationary phases, only the boiling point affects the retention time. As a result, various analytes are eluted at different points in time. The analytes are registered by the detector, and a chromatogram is formed. The chromatogram shows detector response as a function of retention time.

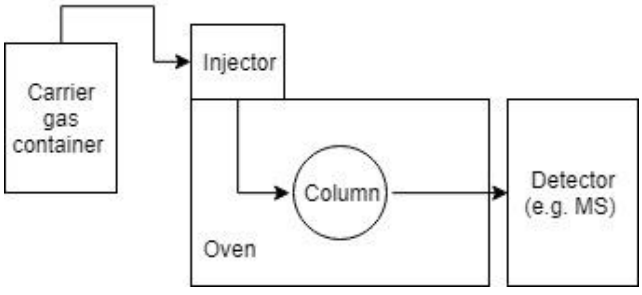

Figure 15 - Overview of a gas chromatograph

The column temperature is an important parameter. By increasing the temperature, the analyte volatility increases, which gives shorter retention time. The column temperature can either be

constant throughout the analysis (isothermal analysis) or it can change during the analysis (temperature gradient). Compared to isothermal analysis, an appropriate temperature program will provide shorter analysis time while maintaining good separation of analytes.

GC is suitable for volatile and thermally stable compounds, or compounds that can be made volatile and thermally stable by derivatization [23, p. 200-214].

1.6.1 Split/splitless injection

For both split and splitless injection, the same injector is used. When using split injection, only a portion of the sample from the injector goes into the column, while the rest is vented out. Splitless injection involves that the sample is injected slowly. In contrast to split injection, 100% of the sample enters the column. The column temperature should be at least 10 °C below the boiling point of the solvent in which the analytes are dissolved. The solvent will then condense and form a thin film in the first part of the column, and the analytes are trapped in a narrow band in the condensed solvent. As the column temperature rises, the solvent and analytes evaporate [23, p. 210-212].

1.7 Mass spectrometry

A mass spectrometer can be used as detector for GC. Mass spectrometry (MS) is an analytical method that measures the molecular mass of chemical compounds and/or their fragments, and it can be used for both quantitative analysis and identification. A mass spectrometer consists of an inlet, an ion source, one or several mass filters, a detector and a computer. The sample enters the mass spectrometer through the inlet. In the ion source, the analyte molecules are ionized to molecular ions, which might further be decomposed into smaller fragment ions. The mass filter separates the ions according to their mass-to-charge ratio (*m/z*). After the ions are separated, they are registered by the detector, which sends signal to the computer. In the mass spectrum, *m/z* is plotted against relative intensity.

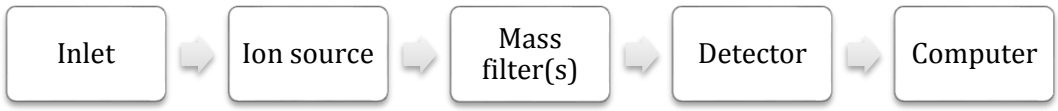

Figure 16 - Overview of a mass spectrometer

1.7.1 Ion source

In order for the analytes to be detected by the MS, the molecules must be charged. In the ion source, an analyte is ionized to either a positive or a negative ion, called molecular ion. This molecular ion might further be decomposed into smaller fragment ions. Two commonly used ionization methods are electron ionization (EI) and chemical ionization (CI).

1.7.1.1 Electron ionization

Electron ionization (EI) takes place under vacuum. Neutral molecules in gas phase enter the ion source, where the molecules are bombarded by an electron beam. The energy of the electron beam is usually 70 eV. The electrons are released from a filament and accelerated in an electric field. One electron is then "knocked out" of the molecule (M), and a positively charged radical ion ($M^{\cdot +}$), i.e. the molecular ion, is formed:

$$M + e^- \rightarrow M^{\cdot +} + 2e^-$$

EI is considered a hard ionization method, i.e. it gives a high degree of fragmentation, which can result in low intensity of the molecular ion.

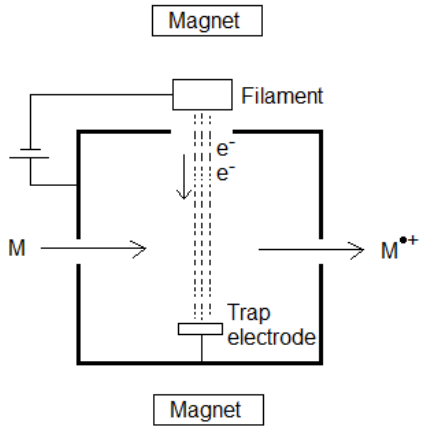

Figure 17 - Electron ionization (EI)

1.7.1.2 Chemical ionization

Chemical ionization (CI) is a soft ionization technique, which means that the molecular ion is fragmented to a lesser extent compared to EI. This ionization method is suitable if EI provides a molecular ion with low intensity, or if the molecular ion is absent. CI is quite similar to EI, but a reagent gas (often methane) is added to the ion source. The reagent gas will be ionized by the electron beam. Further, the ions formed will react with additional reagent gas molecules, which results in highly reactive ions (CH_5^+ and $C_2H_5^+$ are formed when using methane as reagent gas). When these ions react with the analyte, a charged quasi-molecular ion with either one additional proton ($[M+H]^+$) or one proton less ($[M-H]^+$) is formed. CI can produce both positive and negative ions [23, p. 252-263].

1.7.2 Mass filter

A mass filter separates the ions according to mass-to-charge ratio (*m/z*). In this project, a quadrupole was used as mass filter.

A quadrupole consists of four parallel cylindrical electrodes connected in pairs, and to these electrodes an electrical field is applied (Figure 18). The ions from the ion source are sent into

the electrical field. By varying the voltage on the electrodes, only selected ions will pass through and reach the detector [23, p. 267-271].

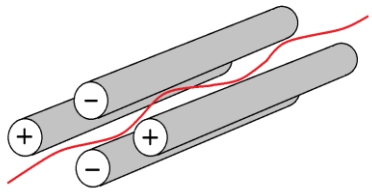

Figure 18 – A quadrupole mass filter.

The mass spectrometer can either be set to scan over a mass range or to detect specific masses. When using *full scan mode*, a wide mass range is scanned. *Selected ion recording* (SIR) is used to measure one single or a few specific masses. In quantitative analysis, for instance, SIR is often used. If SIR does not provide sufficient sensitivity or specificity, *multiple reaction monitoring* (MRM) can be applied. MRM is a tandem mass spectrometry (MS/MS) mode. For this purpose, a triple quadrupole (QqQ) is used. The QqQ consists of three quadrupoles connected in series; two quadrupole mass filters with a collision cell between. The first quadrupole (Q1) is locked to a selected characteristic mass of the analyte, which is called the precursor ion. In the collision cell (Q2), the precursor ion collides with an inert collision gas (e.g. nitrogen or argon) and decomposes into product ions. This process is called collision-induced dissociation (CID). Only selected product ions get past the last quadrupole (Q3) [23, p. 271-273]. In addition to MRM, there are several other MS/MS modes. In a *product ion scan*, only the selected precursor ion gets past Q1, and product ions formed in the collision cell are scanned through Q3. In a *precursor ion scan*, only a selected product ion gets past Q3, and precursor ions of the product ion are detected in Q1. In *neutral loss scan*, Q1 and Q3 are both scanned simultaneously, but only ions providing the selected neutral loss (from Q1 to Q3) are detected [24].

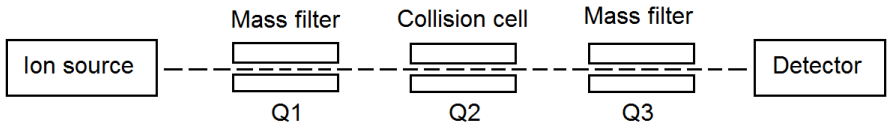

Figure 19 - Triple quadrupole (QqQ).

1.8 Internal standard

When performing quantitative analysis by GC/MS, it is necessary to use an internal standard (IS). The purpose of using an internal standard is to correct for loss of analyte during the sample preparation and analysis. A known concentration of the internal standard is added to the sample solution prior to sample preparation. Internal standard is used both for setting up the calibration curve and for quantification of samples. A calibration curve shows the relationship between analyte concentration and the ratio between peak area of the analyte and the internal standard (A_a/A_{IS}). The calibration curve can thus be used to determine the analyte concentration in samples.

There are certain criteria that apply when selecting an internal standard:

- The IS must follow the analytes in all stages of the sample preparation;
- it must be possible to separate the IS from the analytes;
- the IS cannot be naturally present in the samples;
- the IS must be stable;
- it is beneficial if the molecular structure resembles that of the analyte;
- and it must be available in pure form.

2 Aim of the thesis

This thesis had two main purposes:

- ✓ Investigate how the addition of CO_2 and flue gas affect total lipid content and fatty acid composition of the algae
- ✓ Determine double bond positions of unsaturated fatty acids in the algae

To reach the main goals, a set of subgoals was established:

- ✓ Develop a GC/MS method for analysis of FAMEs and picolinyl derivatives of fatty acids
- ✓ Test whether CI can be used to determine the molecular ion of FAMEs
- ✓ Evaluate whether a MS/MS product ion scan approach could be useful for fatty acid analysis

3 Materials and methods

3.1 Chemicals

Table 1 – Chemicals and solvents

Substance	**Purity**	**CAS number**	**Supplier**
Dichloromethane	≥99.9%	75-09-2	Sigma-Aldrich Inc., St. Louis, MO, USA
Heptane	>99%	142-82-5	Merck, Darmstadt, Germany
Methanol	≥99.9%	67-56-1	Sigma-Aldrich Inc., St. Louis, MO, USA
Potassium *tert*-butoxide (1 M in THF)		865-47-4	Sigma-Aldrich Inc., St. Louis, MO, USA
3-pyridinemethanol	98%	100-55-0	Sigma-Aldrich Inc., St. Louis, MO, USA
Sodium chloride		7647-14-5	Merck, Darmstadt, Germany
Sulfuric acid	96%	7664-93-9	Merck, Darmstadt, Germany
18.2 MΩ Milli-Q water			Merck Millipore, Billerica, MA, USA

3.1.1 Standards

Table 2 - Standards

Fatty acid/FAME			Purity	CAS number	Supplier
Tetradecanoic acid	14:0		>99%	544-63-8	Larodan AB, Solna, Sweden
Hexadecanoic acid	16:0		>99%	57-10-3	
9(Z)-hexadecenoic acid	16:1	n-7	>99%	373-49-9	
9(Z),12(Z)-hexadecadienoic acid	16:2	n-4	>98%	5070-03-01	
7(Z),10(Z),13(Z)-hexadecatrienoic acid	16:3	n-3	>98%	7561-64-0	
Methyl 6(Z),9(Z),12(Z),15(Z)-hexadecatetraenoate	16:4	n-1	>98%	94035-78-6	
Octadecanoic acid	18:0		>99%	57-11-4	
Methyl oleate	18:1	n-9	>99%	112-62-9	
Linoleic acid	18:2	n-6	>99%	60-33-3	
Linolenic acid	18:3	n-3	>99%	463-40-1	
6(Z),9(Z),12(Z),15(Z)-octadecatetraenoic acid	18:4	n-3	>97%	20290-75-9	
Eicosanoic acid	20:0		>99%	506-30-9	
Arachidonic acid	20:4	n-6	>99%	506-32-1	
5(Z),8(Z),11(Z),14(Z),17(Z)-eicosapentaenoic acid	20:5	n-3	>99%	10417-94-4	
Docosanoic acid	22:0		>99%	112-85-6	
4(Z),7(Z),10(Z),13(Z),16(Z),19(Z)-docosahexaenoic acid	22:6	n-3	>99%	6217-54-5	
Tetracosanoic acid	24:0		>99%	557-59-5	
15(Z)-tetracosenoic acid	24:1	n-9	>99%	506-37-6	

3.1.2 Internal standards

Table 3 - Internal standards

Fatty acid	Purity	CAS number	Supplier
Isopalmitic acid	≥98%	4669-02-7	Sigma-Aldrich Inc., St. Louis, MO, USA
19-methylarachidic acid	~98%	59708-73-5	

3.2 Materials

Table 4 – Materials used for lipid extraction, methylation/transesterification and picolinyl derivatization

Usage/description	Name of equipment	Supplier
Analytical balance	Sartorius Entris 224I-1S	Sartorius, Göttingen, Germany
Centrifuge	Heraeus Megafuge 16R Centrifuge	Thermo Fisher Scientific, Waltham, MA, USA
Centrifuge tubes	Thermo Scientific Nunc 15mL conical centrifuge tubes	Thermo Fisher Scientific, Waltham, MA, USA
Drying oven	Termaks Laboratory drying oven	Termaks AS, Bergen, Norway
DURAN glass tubes	DURAN culture tubes, GL14 and GL18, with screw cap	DURAN Group, Mainz, Germany
Eppendorf pipettes	Eppendorf Research plus pipettes	Eppendorf, Hamburg, Germany
Freeze dryer	FreeZone 4.5 Liter Freeze Dry Systems 7750030	Labconco, Kansas City, MO, USA
GC/MS vials	12x32mm glass screw neck vial, quick thread, LectraBond cap, PTFE/silicone septa.	Waters, Milford, MA, USA
Glass Pasteur pipettes 150 mm		VWR International, West Chester, PA, USA
Glass vials	Glass vials, rolled rim, with snap-cap, 10mL	Assistent, Sondheim, Germany
Nitrogen	Nitrogen 5.0	AGA AS, Oslo, Norway
Nitrogen evaporator	Stuart Sample Concentrator, SBHCONC/1	Cole-Parmer, UK
Vortexer	Vortex 1	IKA Works, Staufen, Germany

3.3 Collection and storage of algae

Algal species included in the project were *Porosira glacialis* and *Chaetoceros furcellatus*. *P. glacialis* was originally collected in the Barents Sea (76.3 °N) in May 2014. *C. furcellatus* was collected on the coast of Svalbard (78.4 °N) in May 2007. Since then, the algae have been stored in the plankton lab at the Norwegian College of Fishery Science (NFH) at UiT The Arctic University of Norway.

3.4 Cultivation and harvesting of algae

The cultivation and harvesting of algae was carried out by technicians at the Norwegian College of Fishery Science (NFH).

At NFH, both algal species were cultivated both with and without supply of CO_2; three parallels with and without CO_2 addition (a total of six cultivations) of *P. glacialis* and one parallel with and without CO_2 addition (a total of two cultivations) of *C. furcellatus*. *P. glacialis* was also cultivated in a photobioreactor with and without addition of flue gas at Finnfjord AS. All algae samples were harvested during the exponential growth phase.

3.4.1 Cultivation with and without CO_2 aeration

From a stock culture, algal cell density was measured. The stock culture was diluted with filtered and pasteurized seawater so that a solution of 50 L with 700,000 cells/L (for *P. glacialis*) and 100 L with 7,000,000 cells/L (for *C. furcellatus*) was obtained in 100-liter plexiglass columns. The following inorganic nutrients were added to the cultures: 0.1 g/L Kristalon flower (Yara Norge, Oslo, Norway) and 1 mL/L silicate solution (35 g/L sodium metasilicate pentahydrate, Sigma-Aldrich). To add CO_2 and prevent sedimentation of algae, technical air with and without 3% CO_2 was continuously added to the bottom of the column (0.7 L/min, 0.013 Bar). The cultivation took place in temperature and light controlled rooms (temperature: 6 °C, light: 60 µmol photons $m^{-2}s^{-1}$). Each column was illuminated by three LED light strips (Northlight). Chlorophyll a, cell density and pH were measured several times during cultivation; when the culture was initiated, Mondays, Wednesdays and Fridays, until a cell density of 6,000,000 cells/L (for *P. glacialis*) and 60,000,000 cells/L (for the much smaller *C. furcellatus*) was obtained. These densities were calculated prior to the cultivation by technicians

at NFH based on the biomass requirement for lipid analyses. Biomass was then harvested using a 20 µm pore size plankton mesh and centrifuged at 1917 x g (Heraeus Megafuge 8R, Thermo Scientific) for 5 minutes. After centrifugation, the supernatant was discarded. Finally, the algal biomass was frozen in liquid nitrogen and stored in a freezer at -80 °C.

Figure 20 - Cultivation of P. glacialis at The Norwegian college of Fishery Science (NFH).

3.4.2 Mass cultivation at Finnfjord AS

The algae were cultivated in nutrient replete conditions in a 6,000 L fiberglass tank. The culture was maintained at approximately 10,000,000 cells/L by daily dilutions using sea water at ambient temperature (approx. 2 °C) filtered through 1 µm polypropylene filters (model GX01-9 7/8, GE Power & Water, Minnetonka, MN, USA). The culture was irradiated by a LED light source (Daylight White 300W LED, JM Hansen, Tromsø, Norway) set to 200 W. The following inorganic nutrients were added daily to the culture: 0.25 g/L Kristalon flower and 1 mL/L silicate solution (35 g/L sodium metasilicate pentahydrate). In order to prevent sedimentation of algae, ambient air was continuously added to the bottom of the tank.

The algae with added flue gas were cultivated and harvested using the following procedure: Before the addition of flue gas, the pH of the culture was roughly 8.1. Each day, flue gas containing 7-8% CO_2 was added for a few hours, until the pH of the culture was reduced to

roughly 7.4. This was repeated for six days. Biomass was then harvested using a 20 µm pore size plankton mesh. The sample material was transferred to 50 mL Falcon centrifuge tubes (VWR International), which were frozen in liquid nitrogen and stored in a freezer at -40 °C.

Overall, harvesting was carried out once before and once after addition of flue gas.

Figure 21 - The 6,000 L bioreactor where P. glacialis was cultivated at Finnfjord AS.

3.5 Lipid extraction

In this project, a modified version of the Folch method [25] was used to extract lipids from the algae samples. For each algae sample, i.e. *P. glacialis* with and without added CO_2, *C. furcellatus* with and without added CO_2 and *P. glacialis* with and without added flue gas, three parallels were prepared.

Prior to the lipid extraction, all algae samples were freeze-dried and crushed with a glass rod. Approximately 100 mg of pulverized sample material was weighed into a centrifuge tube (exact mass was noted). 2 mL of DCM-MeOH (2:1) and 2 mL of 5% NaCl in Milli-Q water were added to the sample. The sample was shaken for a few seconds, and then centrifuged at 2000 x g for 5 minutes. A layer of solid biomass was formed between the water phase and the organic phase. The water phase (i.e. the upper phase) was discarded. The extractant (i.e. the lower phase) was transferred to a pre-weighed glass vial. The same volume of DCM-MeOH (2:1) and 5% NaCl in Milli-Q water were added to the residual biomass in the centrifuge tube, and the extraction was repeated. The extractant was transferred to the same glass vial as for the first run. Solvents were then evaporated under nitrogen. Finally, the glass vial was weighed to determine the lipid mass.

3.6 Preparation of FAMEs

Extracted and dried lipids were dissolved in DCM-MeOH (2:1), giving a concentration of 10 mg/mL. In a Duran glass tube, 100 µL of extract, 100 µL of 100 µg/mL IS solution and 800 µL of DCM were mixed. 2 mL of 10% H_2SO_4 in MeOH was added to the sample. The sample was then heated at 100 °C for 1 hour. After the sample was cooled to room temperature, 3 mL of heptane and 3 mL of 5% NaCl in Milli-Q water were added. The sample was shaken well. After phase separation, the heptane phase (i.e. the upper phase) was transferred to a GC/MS vial and evaporated under nitrogen. Finally, 0.5 mL of heptane was used to dissolve the sample before analysis.

3.7 Preparation of picolinyl derivatives

For picolinyl derivatization of FAMEs, the method of Dubois et al. [26] with some adjustments was used.

After the preparation of FAMEs, one parallel of each algae sample (FAMEs in 0.5 mL heptane) was transferred to a Duran glass tube, and then evaporated under nitrogen. The derivatization reagent was prepared as follows: in the ratio 1:2 (v/v), potassium *tert*-butoxide (1 M in THF) and 3-pyridinemethanol were mixed. The sample was dissolved in 1 mL of DCM, and 0.25 mL of derivatization reagent was added. Then the sample was heated at 45 °C for 45 minutes. After the sample was cooled to room temperature, 1 mL of Milli-Q water and 2 mL of heptane were added, and the solvents were mixed on a vortexer. After phase separation, the organic phase (i.e. the upper phase) was transferred to a new Duran glass tube. 1 mL of 5% NaCl in Milli-Q water was added to the organic phase, and the solvents were again mixed on a vortexer. After phase separation, the organic phase was transferred to a GC/MS vial and evaporated under nitrogen. Finally, 1 mL of heptane was added to dissolve the sample before analysis.

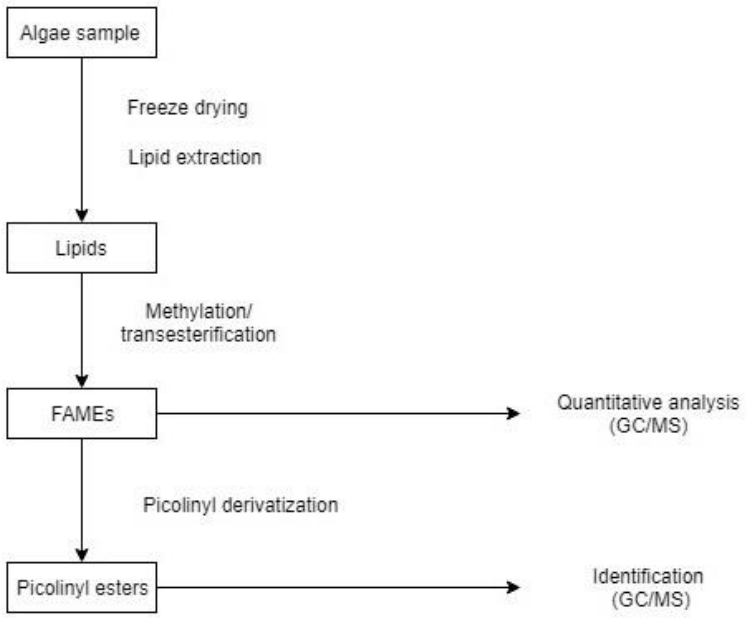

Figure 22 - Flowchart of the sample preparation process

3.8 Calibration curves

3.8.1 Stock solution

Solutions of each FA/FAME standard (Table 2) were prepared using volumetric flasks of appropriate volume. Solvents used were heptane, DCM and MeOH (in various ratios depending on solubility). For each FA/FAME, a volume corresponding to an amount of 1 mg FA/FAME was added to a 1 mL volumetric flask, where all the fatty acids and FAMEs were mixed. The volume was adjusted to 1 mL by evaporation using nitrogen and addition of heptane-DCM (1:1), giving a concentration of 1 mg/mL. Two concentrations of the stock solution were prepared; 1000 µg/mL (SS1) and 100 µg/mL (SS2). For preparing SS2, SS1 was diluted 1:10 with DCM.

3.8.2 Internal standards

The internal standards used were isopalmitic acid (IS1) and 19-methylarachidic acid (IS2). IS1 and IS2 are saturated branched chain fatty acids that do not occur naturally in the algae. For quantitative analysis, the fatty acids 14:0, 16:0, 16:1, 16:2, 16:3, 16:4, 18:0 and 18:1 were quantified with IS1 as internal standard, while the remaining fatty acids were quantified with IS2 as internal standard.

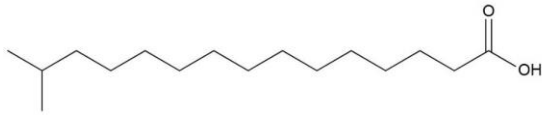

Figure 23 - Isopalmitic acid (IS1)

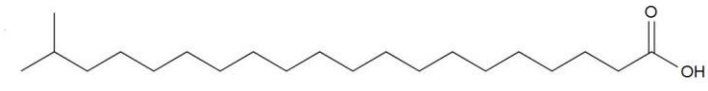

Figure 24 - 19-methylarachidic acid (IS2)

Solutions of IS1 and IS2 were prepared using volumetric flasks of 1 and 2 mL. Solvents used were heptane for IS1 and heptane-DCM (1:1) for IS2. To prepare the IS solution, 20 µL of 10 mg/mL IS1, 40 µL of 5 mg/mL IS2 and 1.94 mL of heptane were mixed, giving a concentration of 100 µg/mL.

3.8.3 Standard solutions

For the calibration curves, three parallels of seven different concentration levels (10, 25, 50, 100, 250, 500 and 1000 µg/mL) were prepared. 100 µL of IS solution was added to all standard solutions, and DCM was used to obtain a final volume of 1 mL. The preparation of each standard solution is shown in Appendix 1. The standard solutions with concentration 10 and 25 µg/mL were prepared at a later date and from a new stock solution, which was prepared in the same manner as for the other stock solution. In addition, from a stock solution containing only the fatty acid 20:5, standard solutions with concentration 2500 and 5000 µg/mL were prepared.

Further, the fatty acids in the standard solutions were methylated using the same procedure as for the algae samples.

3.8.4 Analysis of standard samples

Each parallel of standard solution was injected three times on GC/MS, giving nine injections for each concentration. The samples were run with increasing concentration to minimize carry-over effects. When going from highest to lowest concentration, two blank samples were run to avoid carry-over.

3.8.5 Calibration curves

A calibration curve was set up for each FAME. Based on the fatty acid concentration in the algae samples, different concentration ranges were used for different FAMEs. For 14:0, 16:0, 16:1, 16:2, 16:3, 16:4, 18:4, 20:0, 22:0 and 24:0, the concentration range was set to 10-1000 µg/mL. For 18:0, 18:1, 18:2, 18:3 and 24:1, the concentration range was 10-250 µg/mL. For 20:4 and 22:6, the concentration range was 25-1000 µg/mL. And finally, for 20:5, the concentration range was 25-5000 µg/mL.

In the calibration curves, the ratio between peak area of the FAME standard and the internal standard (A_a/A_{IS}) was plotted against the concentration.

3.9 Analysis of algae samples

For each algae sample, i.e. *P. glacialis* with and without added CO_2, *C. furcellatus* with and without added CO_2 and *P. glacialis* with and without added flue gas, three parallels were prepared. First, the fatty acids in the samples were derivatized to FAMEs. For quantitative analysis, each parallel was injected twice on GC/MS. Two blank samples were run between each triplicate of an algae sample.

One parallel of each algae sample was further picolinyl derivatized, giving six algae samples of picolinyl derivatives. Each sample was injected once on GC/MS. Between each sample, a blank sample was run. Due to difficulties in interpreting some of the mass spectra, the samples were concentrated by evaporation from 1 mL to 0.1 mL.

3.10 GC/MS analysis

All analyses were performed using GC/MS. The instrument consisted of an Agilent 6890N Network GC System combined with a Waters Quattro micro GC Mass Spectrometer.

3.10.1 Materials

Table 5 - Equipment used for GC/MS analysis

Usage/description		**Name of equipment**	**Supplier**
Software		MassLynx V4.1	Waters, Milford, MA, USA
GC	Apparatus	6890N Network GC System	Agilent Technologies, Santa Clara, CA, USA
	Carrier gas	Helium 5.0	AGA AS, Oslo, Norway
	Injector	7683B Series Injector (split/splitless)	Agilent Technologies, Santa Clara, CA, USA
	Column	TG-FAMEWAX, length 30m, I.D. 0.25mm, film 0.25µm, max temp. 20-250°C.	Thermo Fisher Scientific, Waltham, MA, USA
MS	Apparatus	Waters Quattro micro GC	Waters, Milford, MA, USA
	Reagent gas	Methane 5.0	AGA AS, Oslo, Norway
	Collision gas	Argon 5.0	AGA AS, Oslo, Norway

3.10.2 Method development

The GC column used from the beginning was TG-FAMEWAX. Various temperature programs were tested for the FAMEs and the picolinyl derivatives in order to achieve acceptable chromatographic separation. Due to the high molecular weight and polarity of the picolinyl derivatives compared to the FAMEs, the peaks of the longest fatty acids were remarkably broad in the chromatogram. For the standard sample shown in Figure 25, the picolinyl derivative of the fatty acid 22:6 was not even detectable. Trying to solve this problem, another column was tested with the purpose of using it for analysis of picolinyl derivatives. ZB-FAME (Phenomenex Inc., Torrance, CA, USA) is a capillary column containing a high-cyanopropyl polar stationary phase that tolerates higher temperatures (max. 280 °C) than the TG-FAMEWAX column. The ZB-FAME column provided improved sensitivity and more narrow peaks for the longest fatty acids. However, the separation was poor for several fatty acids, and the fatty acids were eluted in an unpredictable order (see Figure 26), which could have been a problem considering that some of the fatty acids in the algae samples did not have the same double bond positions as their corresponding fatty acid in the standard samples. Also, compared to the other column, the mass spectra were more challenging to interpret. For these reasons, the ZB-FAME column was not further used.

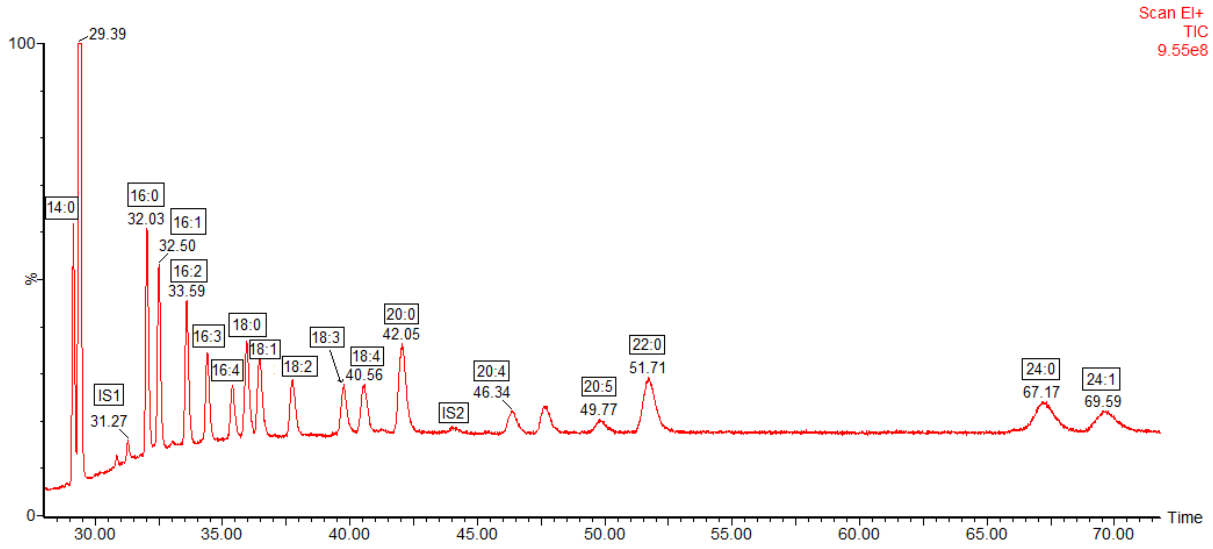

Figure 25 - Chromatogram of the picolinyl derivatives in a 200 µg/mL standard sample. TG-FAMEWAX column. The peak at 29.39 minutes was most likely a byproduct of the reagent used for the picolinyl derivatization.

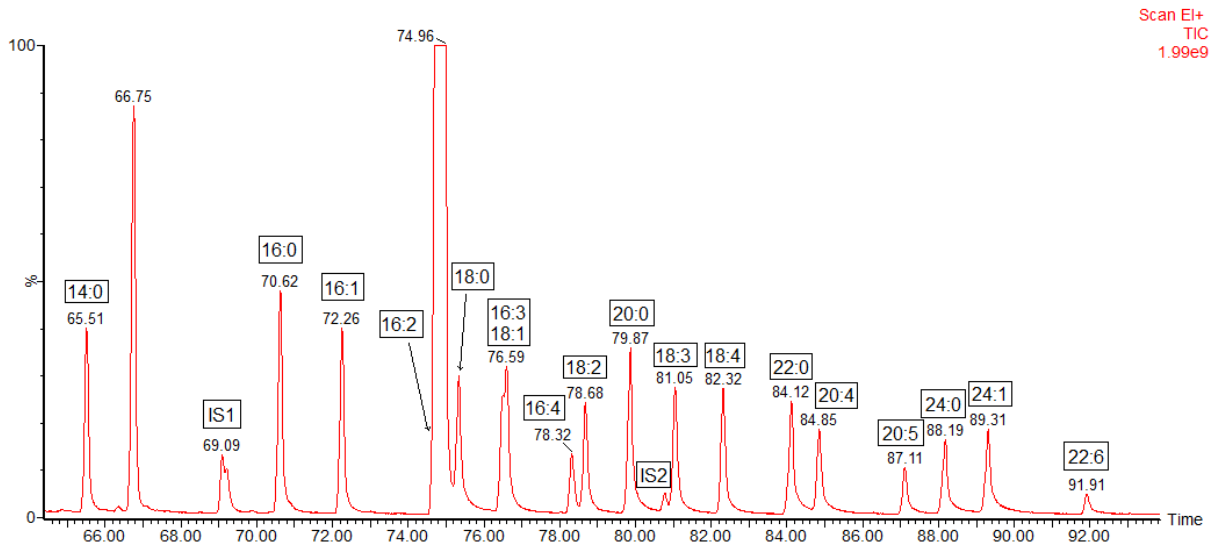

Figure 26 - Chromatogram of the picolinyl derivatives in a 375 µg/mL standard sample. ZB-FAME column. Compared to the TG-FAMEWAX column, the sensitivity was improved. The peak at 74.96 minutes was the same compound as the peak at 29.39 minutes in Figure 25. IS1 co-eluted with an unknown compound.

After switching back to the TG-FAMEWAX column, problems with baseline drift and tailing occurred. Cutting off the end of the column did not solve the problem. However, after changing the flow rate of the carrier gas from 1.0 to 1.4 mL/min, the problem disappeared.

Furthermore, when the standard samples were run, there was an issue with carry-over of long-chain saturated FAMEs (18:0, 20:0, IS2, 22:0 and 24:0). To try to solve the problem, the following were tested: using DCM as washing solvent A, using DCM-MeOH-heptane (1:1:1) as washing solvent A, increasing the number of syringe washes from one to five and increasing the injector temperature from 250 to 350 °C. All these changes except for the former were retained. Changing the injector temperature solved the carry-over issue. A possible explanation for this is the low volatility of these long-chain saturated FAMEs compared to the rest of the FAMEs.

For the picolinyl derivatives, the broad peaks of the longest fatty acids remained a problem. However, by concentrating the algae samples, it was possible to interpret the mass spectra of most fatty acids.

3.10.3 GC

GC conditions used for all analyses are listed in Table 6.

Table 6 - GC conditions

Injector	Mode	Splitless
	Injector temperature (°C)	350
	Injection volume (µL)	1
Carrier gas	Gas	Helium
	Flow rate (mL/min)	1.4 (constant)
Solvents	Sample solvent	Heptane
	Washing solvents	A = heptane-DCM-MeOH (1:1:1) B = heptane

3.10.3.1 Column

Both FAMEs and picolinyl derivatives of the fatty acids were analyzed using a TG-FAMEWAX capillary column, which has a polar stationary phase of polyethylene glycol. The column provided a predictable retention order and good separation for most FAMEs and picolinyl derivatives.

3.10.3.2 Temperature program

Table 7 and Figure 27 show the temperature programs used to achieve acceptable chromatographic separation.

Table 7 - Temperature programs used to analyze FAMEs and picolinyl derivatives.

FAMEs	Initial temp.: 70 °C. Initial time: 2 min. Rate: 2 °C/min. Final temp.: 226 °C. Hold time: 0 min. Rate: 6 °C/min. Final temp.: 250 °C. Hold time: 2 min. Total time: 86 min.
Picolinyl derivatives	Initial temp.: 60 °C. Initial time: 2 min. Rate: 10 °C/min. Final temp.: 150 °C. Hold time: 0 min. Rate: 5 °C/min. Final temp.: 250 °C. Hold time: 50 min. Total time: 81 min.

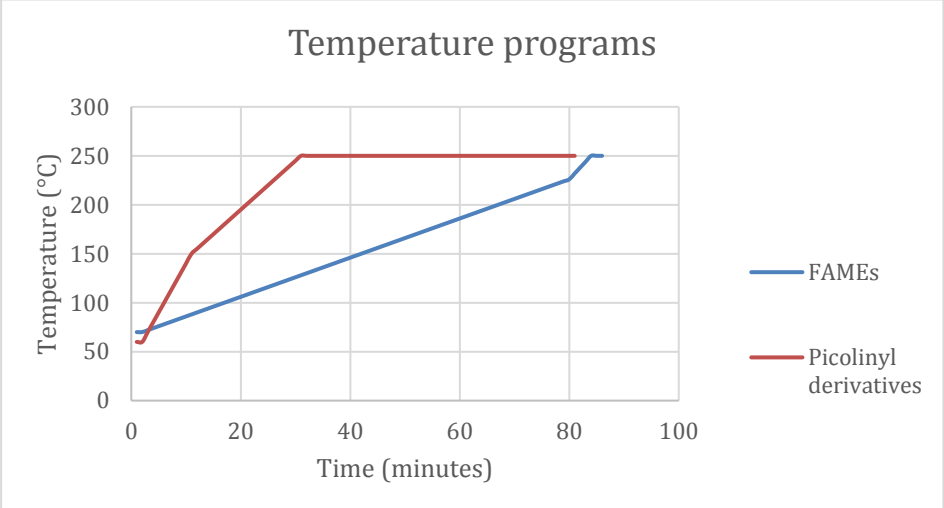

Figure 27 - Temperature programs used to analyze FAMEs and picolinyl derivatives.

3.10.4 MS

MS conditions used for all analyses are listed in Table 8.

3.10.4.1 Ion source

EI was employed to analyze all the algae samples (FAMEs and picolinyl derivatives) and the standard samples for the calibration curves. However, when using EI, the molecular ion can be weak or missing for some of the FAMEs. To determine the molecular ion of the FAMEs in the algae samples, positive CI was also used.

Table 8 - MS conditions

	EI	**CI**
Electron energy (eV)	70	70
Trap (µA)	200	
Emission (µA)		200
Repeller (V)	1.6	
Extraction lens (V)	7	1
Focus lens 1 (V)	120	120
Focus lens 3 (V)	29	40
Source temperature (°C)	200	200
CI reagent gas		Methane
CI gas flow (%)		70
Resolution (LM1 and HM1)	14.5	14.5
Resolution (LM2 and HM2)	14.5	14.5
Ion energy 1	1	3.0
Ion energy 2	2.5	2.5
Entrance	50	50
Collision	2	2
Exit	50	50
Multiplier	400	500

3.10.4.2 Scan mode

The mass spectrometer contained a triple quadrupole. All standard samples for the calibration curves and all algae samples were analyzed in full scan mode (see Table 9).

Table 9 – MS parameters for full scan analysis of FAMEs and picolinyl derivatives.

	FAMEs	**Picolinyl derivatives**
Mass (*m/z*)	45.5-400	80-500
Time (min)	5-86	3.5-81
Scan time (sec)	0.4	0.6

For the analyses with chemical ionization, selected ion recording (SIR) was employed to achieve better sensitivity. Masses included are listed in Table 10. These masses correspond to the mass of the molecular ion plus a proton ($[M+H]^+$).

Table 10 – MS parameters for SIR analysis of FAMEs.

FAME	***m/z***	**Retention time window (min)**	**Dwell (sec)**
14:0	243.00	30.00-35.00	0.3
IS1 and 16:0	271.00	36.00-43.00	0.3
16:1	269.00	41.10-45.00	0.3
16:2	267.00	42.00-44.50	0.3
16:3	265.00	44.50-47.00	0.3
16:4	263.00	46.00-49.50	0.3
18:0	299.00	48.50-51.00	0.3
18:1	297.00	49.70-52.00	0.3
18:2	295.00	51.00-53.00	0.3
18:3	293.00	51.70-54.70	0.3
18:4	291.00	53.00-57.00	0.3
20:0	327.00	56.50-60.00	0.3
IS2	341.00	58.00-62.00	0.3
20:4	319.00	60.00-63.00	0.3
20:5	317.00	61.00-67.00	0.3
22:0	355.00	64.00-69.00	0.3
22:6	343.00	68.00-74.00	0.3
24:0	383.00	71.00-75.00	0.3
24:1	381.00	72.00-75.00	0.3

A tandem mass spectrometry (MS/MS) product ion scan approach was tested on standard samples of both FAMEs and picolinyl derivatives to determine whether this method could be applicable for fatty acid analysis. Only selected fatty acid derivatives were analyzed, the masses of which are listed in Table 11. Collision-induced dissociation (CID) was employed to obtain fragmentation of the selected precursor ions. The following collision energies were tested: 15, 30, 40 and 50 V. As for the ionization mode, both EI and CI were tested.

Table 11 – MS/MS parameters for product ion scan analysis of FAMEs and picolinyl derivatives.

FA	**FAMEs**			**Picolinyl derivatives**		
	Precursor ion (*m/z*)		***m/z* range**	**Precursor ion (*m/z*)**		***m/z* range**
	EI	**CI**		**EI**	**CI**	
16:0	270.00	271.00	45.50-280.00	347.00	348.00	50.00-350.00
16:1	268.00	269.00		345.00	346.00	
16:2	266.00	267.00		343.00	344.00	
16:3	264.00	265.00		341.00	342.00	
16:4	262.00	263.00		339.00	340.00	
18:0	298.00	299.00	45.50-300.00	375.00	376.00	50.00-380.00
18:1	296.00	297.00		373.00	374.00	
18:2	294.00	295.00		371.00	372.00	
18:3	292.00	293.00		369.00	370.00	
18:4	290.00	291.00		367.00	368.00	

3.11 Quantification

For each FAME in an algae sample, the ratio A_a/A_{IS} was obtained by dividing the peak area of the FAME by the peak area of the internal standard. The fatty acid concentration in the algae sample was then determined using the calibration curve of the FAME. From these concentrations, the proportion of total fatty acids (% TFA) was calculated for each fatty acid.

3.12 Statistical analysis

The data for lipid content and fatty acid composition were analyzed using Microsoft Excel® and IBM SPSS® Statistics 25. An independent samples t-test was used to determine whether there is a statistical significant difference in mean lipid content before and after addition of CO_2 and flue gas. For the fatty acid composition, an independent samples t-test was used to compare mean proportion of total fatty acids for each fatty acid before and after addition of CO_2 and flue gas. Significance level was set to 0.05.

3.13 Interpretation of mass spectra

In the mass spectrum, picolinyl derivatives of fatty acids have characteristic fragmentation patterns which make it possible to locate double bond positions. In addition to searching for fragmentation patterns, the mass spectra were also compared to reference mass spectra obtained from the website "the Lipid Web" [27].

The characteristic fragment ions at *m/z* = 92, 108, 151 and 164 are often prominent for picolinyl derivatives of fatty acids. Because the molecule contains one nitrogen atom, the molecular ion is always odd-numbered and most fragment ions are even-numbered. Ions with masses lower than 92 are usually not important for the interpretation, as they are mainly fragments of the pyridine ring and are thus similar for all picolinyl esters. At the omega end of the fatty acid chain, loss of the terminal methyl group is seen. For the picolinyl derivative of 16:0 (Figure 28 and Figure 29), for instance, there is loss of a methyl group between *m/z* = 332 and 347. When there are no double bonds present in the fatty acid chain, a series of fragment ions 14 amu apart is observed. This represents the loss of methylene groups.

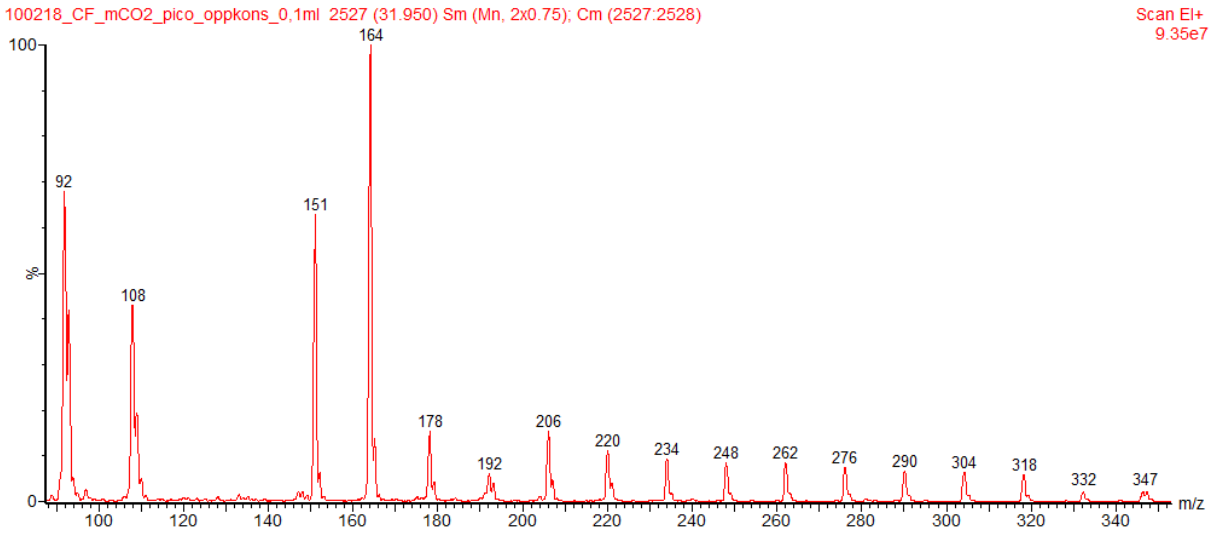

Figure 28 - Mass spectrum of 3-pyridylcarbinyl hexadecanoate (16:0)

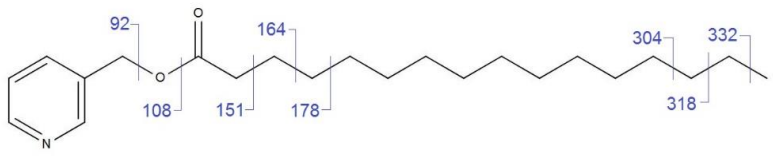

Figure 29 - Structure of 3-pyridylcarbinyl hexadecanoate (16:0). Selected fragment ions are marked.

For picolinyl derivatives of MUFAs, a gap of 26 or 40 amu, which represents the position of the double bond, is observed. 40 amu equals to 26 amu (the two carbons sharing a double bond) plus 14 amu (the methylene group next to the double bond). When there is only one double bond in the fatty acid chain, a doublet of prominent ions (*) 14 amu apart appears at the distal side of the double bond. For the picolinyl derivative of 16:1 n-5, there is a gap of 40 amu between *m/z* = 248 and 288 and a doublet at *m/z* = 302 and 316 (Figure 30 and Figure 31). For the picolinyl derivative of 16:1 n-7, there is a gap of 26 amu between *m/z* = 234 and 260 and a doublet at *m/z* = 274 and 288 (Figure 30 and Figure 32).

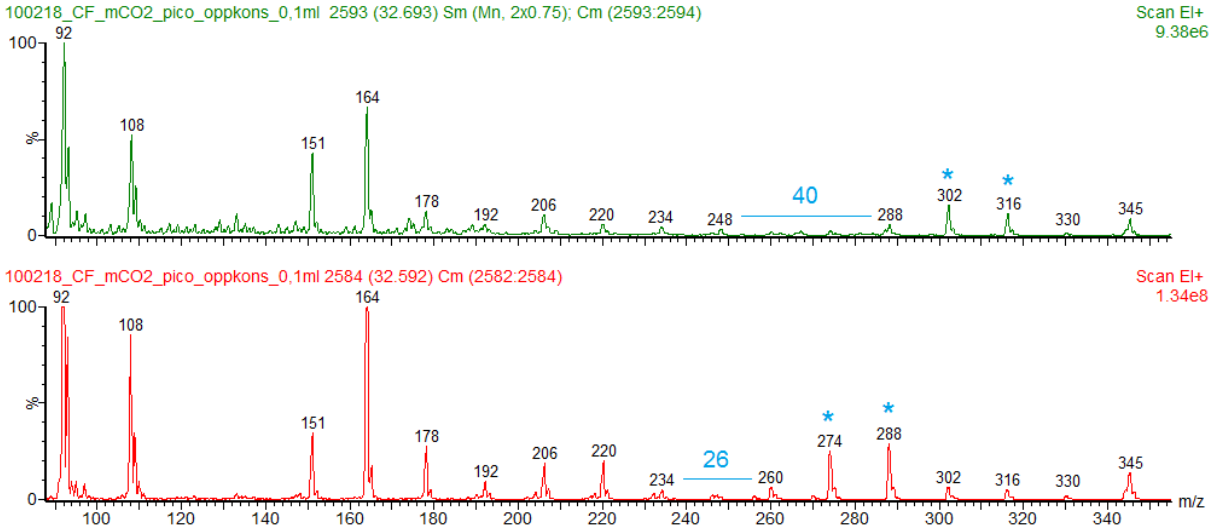

Figure 30 - Mass spectrum of 3-pyridylcarbinyl 11(Z)-hexadecenoate (16:1 n-5), at the top, and 3-pyridylcarbinyl 9(Z)-hexadecenoate (16:1 n-7), at the bottom.

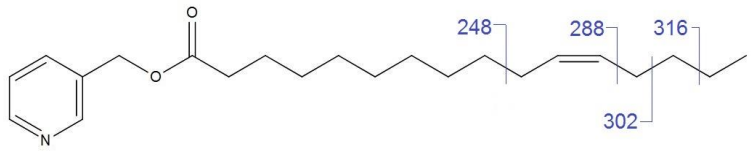

Figure 31 - Structure of 3-pyridylcarbinyl 11(Z)-hexadecenoate (16:1 n-5). Selected fragment ions are marked.

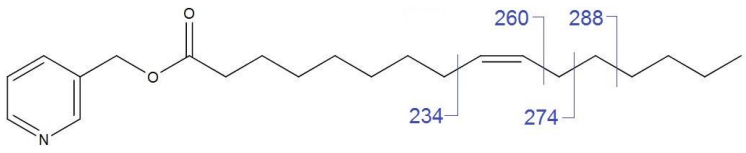

Figure 32 - Structure of 3-pyridylcarbinyl 9(Z)-hexadecenoate (16:1 n-7). Selected fragment ions are marked.

For picolinyl derivatives of PUFAs, double bond positions can be found by locating gaps of 26 and 40 amu. Figure 33 and Figure 34 show an example of methylene-interrupted double bonds, which means that there is a methylene group between the double bonds. The gap of 26 amu between *m/z* = 274 and 300 represents the position of the terminal double bond, while the gap of 26 amu between *m/z* = 234 and 260 represents the position of the internal double bond. However, sometimes it might be easier to discover gaps of 40 amu, as between *m/z* = 220 and 260 (or 234 and 274), and between *m/z* = 260 and 300 (or 274 and 314), but then it is more challenging to determine the exact positions of the double bonds. A series of gaps of 40 amu indicates that the double bonds in the fatty acid chain are methylene-interrupted. In that case, if a gap of 26 amu is located, the positions of the remaining double bonds can thus be determined. Also, it may be useful to compare the mass spectrum to reference mass spectra.

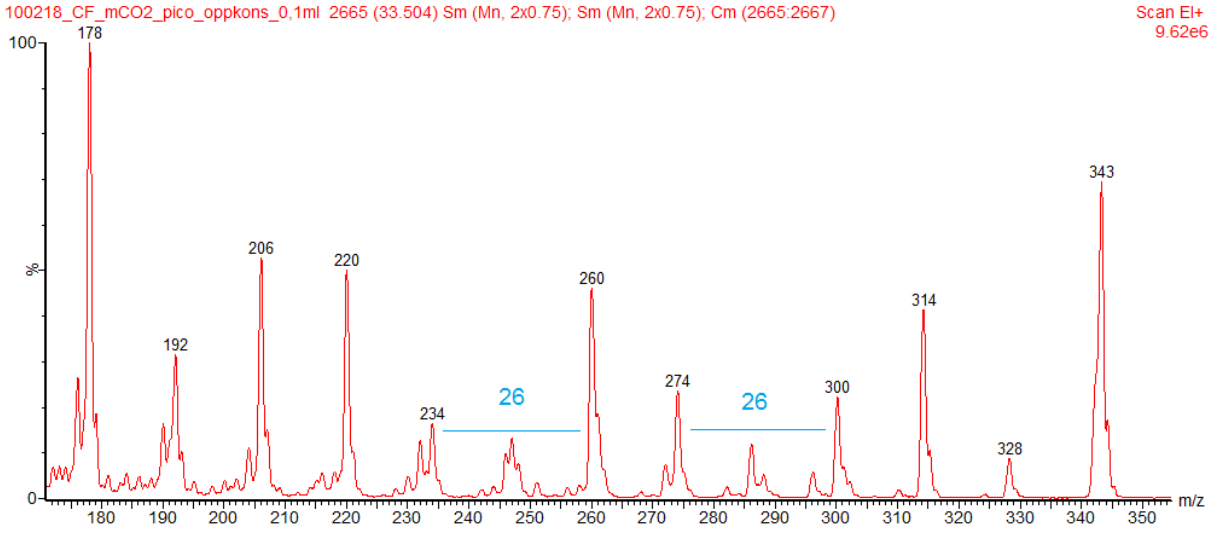

Figure 33 - Mass spectrum of 3-pyridylcarbinyl 9(Z),12(Z)-hexadecadienoate (16:2 n-4)

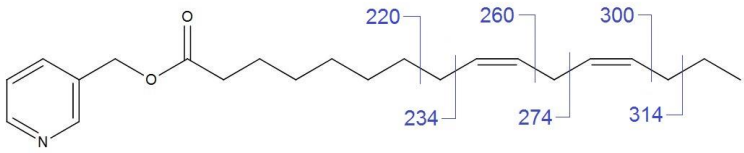

Figure 34 - Structure of 3-pyridylcarbinyl 9(Z),12(Z)-hexadecadienoate (16:2 n-4). Selected fragment ions are marked.

4 Results and discussion

4.1 Total lipid content

Total lipid content of the algae was determined gravimetrically after the lipid extraction. To estimate the lipid content, the weight of extracted lipids was divided by the weight of dry algal biomass. The weight of biomass and lipids can be found in Appendix 2. Table 12 shows the total lipid content of each algae sample. The results are also presented in Figure 35.

Table 12 - Total lipid content of P. glacialis (Pg.) before and after addition of CO_2 and flue gas and C. furcellatus (Cf.) before and after addition of CO_2.

Species	Sample	Mean (%)	SD (%)	RSD (%)
Pg.	Before CO_2	9.26	0.15	1.67
	After CO_2	10.46*	0.59	5.62
	Before flue gas	8.52	0.23	2.73
	After flue gas	7.27*	0.22	2.98
Cf.	Before CO_2	4.31	0.51	11.76
	After CO_2	4.48	0.28	5.80

***** statistically significant difference before and after addition of CO_2 or flue gas (t-test, 95% level, α=0.05, n=3)

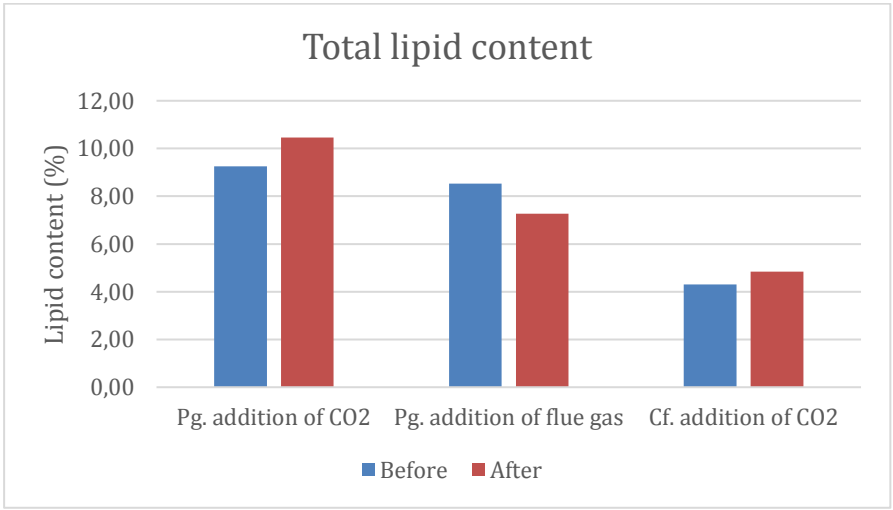

Figure 35 - The bar chart shows how the total lipid content of the algae is affected by the addition of CO_2 and flue gas

Regarding the algal growth, both the addition of CO_2 and flue gas resulted in an increased growth rate. The addition of flue gas also increased the maximum algal cell density of the culture.

For *P. glacialis*, the total lipid content increased from 9.26% to 10.46% ($p = 0.027$) as a result of the addition of CO_2. This is consistent with the results of a similar study done by Artamonova et al. [28], in which case the total lipid content of *P. glacialis* increased from 8.91% to 10.57% ($p < 0.05$) in response to CO_2 aeration. An important difference between these two studies, though, is that Artamonova et al. used ambient air containing 20-25% CO_2 for short intervals each day, while in the present study, air containing 3% CO_2 was added continuously throughout the cultivation.

Addition of flue gas (containing 7-8% CO_2) from Finnfjord resulted, on the other hand, in a reduction from 8.52% to 7.27% ($p = 0.002$) in total lipid content. At the time of writing, there have been few studies published on how flue gas affects the lipid content of microalgae, and no studies on *P. glacialis*. A study by Yoo et al. [29] found that addition of real flue gas (containing 5.5% CO_2) from a heating generator burning liquefied petroleum gas led to an increase in total lipid productivity (1.9-fold and 3.7-fold, respectively) for the microalgae *Botryococcus braunii* and *Scenedesmus* sp., which are in contradiction with the results of the present study. Kao et al. [30] demonstrated how the addition of three types of flue gases from a steel plant (containing approx. 25% CO_2) affected the lipid content of *Chlorella* sp. Compared to the control (with added ambient air), which had a lipid content of 34.0%, coke-oven flue gas gave a lower lipid content (26.4%), hot stove flue gas provided a higher lipid content (35.2%) and power plant flue gas gave a barely lower lipid content (33.8%). This suggests that the resulting lipid content may vary depending on the composition of the flue gas.

For the much smaller *C. furcellatus*, the lipid content was not significantly affected by the addition of CO_2. No previous studies were found on this species. However, de Castro Araújo and Garcia [31] reported that the lipid content of *Chaetoceros wighamii*, which is of the same genus as *C. furcellatus*, was not influenced by the addition of CO_2. In accordance with this, Artamonova et al. [28] demonstrated that there was no significant change in the lipid content of *Attheya longicornis* in response to CO_2 aeration (20-25% CO_2). According to a study by Wang et al. [32], on the contrary, the lipid content of *Chaetoceros muelleri* was significantly increased ($p < 0.05$) in response to CO_2 aeration (10-30% CO_2). Similarly, Tang et al. [33]

reported that the addition of CO_2 (10-50% CO_2) increased the lipid content of both *Scenedesmus obliquus* and *Chlorella pyrenoidosa*.

The results of the present study suggest that the addition of air containing 3% CO_2 slightly increases the lipid content of both algal species. The addition of flue gas, on the contrary, resulted in a slight decrease in the lipid content of *P. glacialis*. Ideally, an increased or unchanged lipid content would have been preferred, however, the reduction in lipid content was in average only 15%, and with an increased algal growth rate and the positive effects on climate gas release from the smelting plant, this should be acceptable.

4.2 Fatty acid composition

For the standard samples, there were three parallels of each concentration (10, 25, 50, 100, 250, 500 and 1000 µg/mL), and each parallel was injected three times on GC/MS. An example of a chromatogram of a standard sample is shown in Figure 36. Chromatograms of standard samples of the remaining concentration levels can be found in Appendix 3, and the calibration curves of all the FAMEs are shown in Appendix 4. The R^2 values of the calibration curves ranged from 0.9605 to 0.9963.

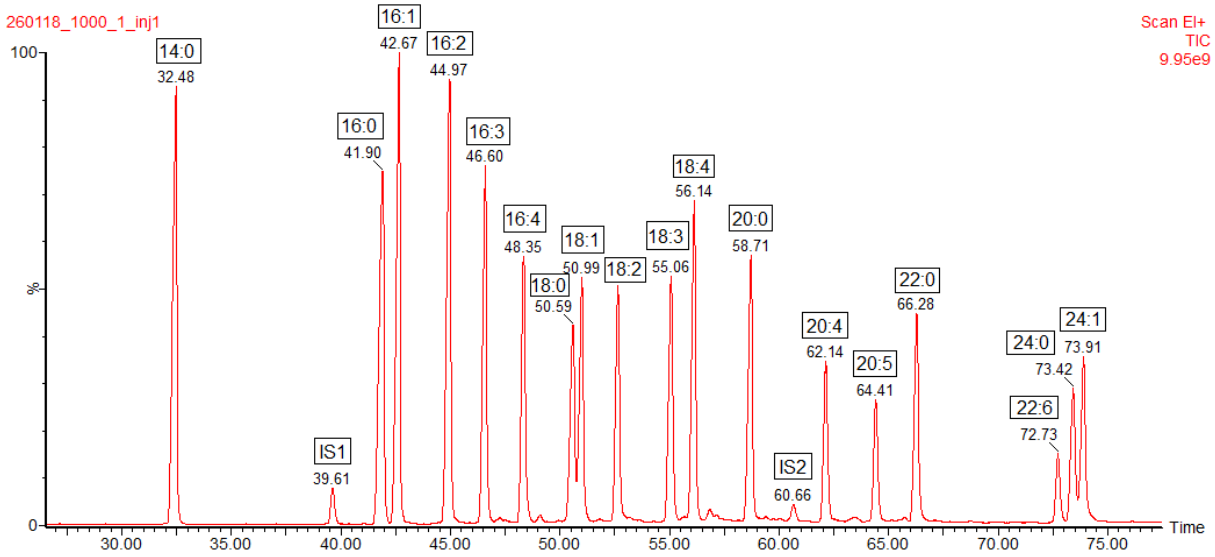

Figure 36 - Chromatogram of the FAMEs in a standard sample with concentration 1000 µg/mL

For the six algae samples, there were three parallels of each sample, and each parallel was injected twice on GC/MS. Chromatograms of the FAMEs in the algae sample are shown in Figure 37 - 42.

In the chromatograms of all the algae samples, one peak consisted of two overlapping peaks. The FAMEs that co-eluted were 16:1 n-5 and 16:2 n-7, both of which were not present in the standard samples. For all six algae samples it was estimated how much each compound contributed to the total peak area. The detector response was relatively similar for 16:1 and 16:2 in the standard samples. For a few standard samples, the peak area of the molecular ions (*m/z* = 266 and 268) of these FAMEs were compared. For the FAME 16:2, this area was in average 2.3 times greater than for 16:1. Further, for each algae sample, the peak containing both FAMEs

was analyzed. Taking the ratio of 2.3 into account, the peak areas of the two molecular ions were compared to determine the proportion each FAME contributed to the total peak area (see Table 13 and Appendix 5). By using these proportions, it was possible to estimate the approximate peak area of these FAMEs in the algae samples. Obviously, this is not a proper method for finding exact peak areas, and the measurements are therefore only semi-quantitative.

Table 13 – Estimated proportions of the peak containing both 16:1 n-5 and 16:2 n-7

Algae sample	**Proportion of the peak (%)**	
	16:1	**16:2**
Pg. before CO_2	48.5	51.5
Pg. after CO_2	72.7	27.3
Pg. before flue gas	52.8	47.2
Pg. after flue gas	49.8	50.2
Cf. before CO_2	18.5	81.5
Cf. after CO_2	18.6	81.4

Based on the estimates presented in Table 13, it appeared that there were minor changes in the proportions of 16:1 n-5 and 16:2 n-7 by the addition of flue gas to *P. glacialis* and by the addition of CO_2 to *C. furcellatus*. However, for *P. glacialis*, the proportion of 16:1 n-5 increased from 48.5% to 72.7% by the addition of CO_2.

Figure 37 and Figure 38 show the chromatograms of FAMEs present in the algae samples of *P. glacialis* before and after addition of CO_2. As a result of the addition of CO_2, an obvious reduction of the FAME 16:3 and increase of the FAME 16:4 can be seen.

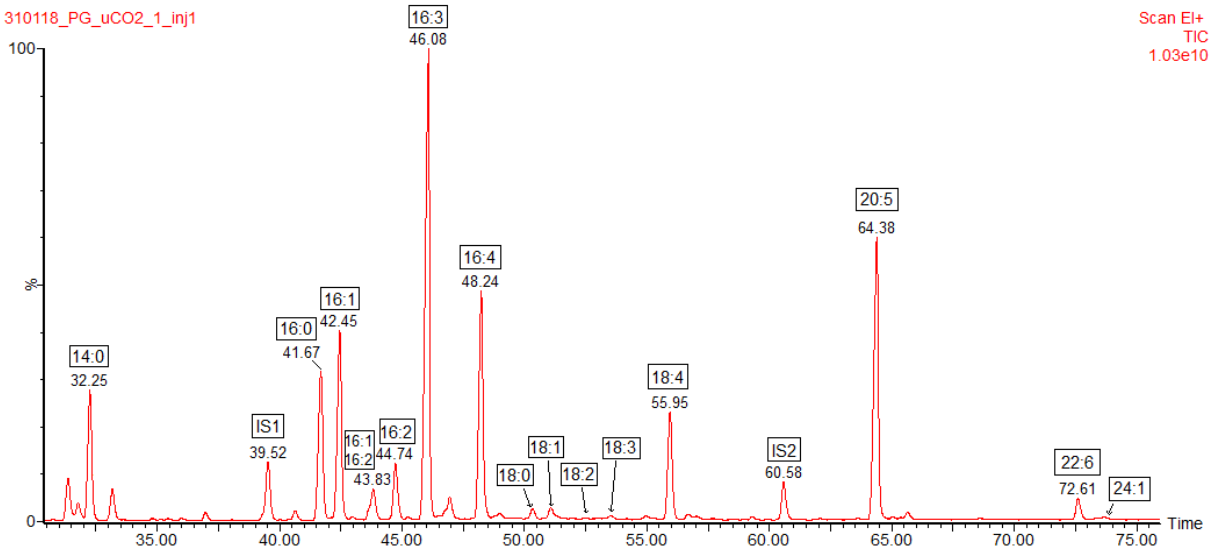

Figure 37 - Chromatogram of the FAMEs in P. glacialis before addition of CO_2

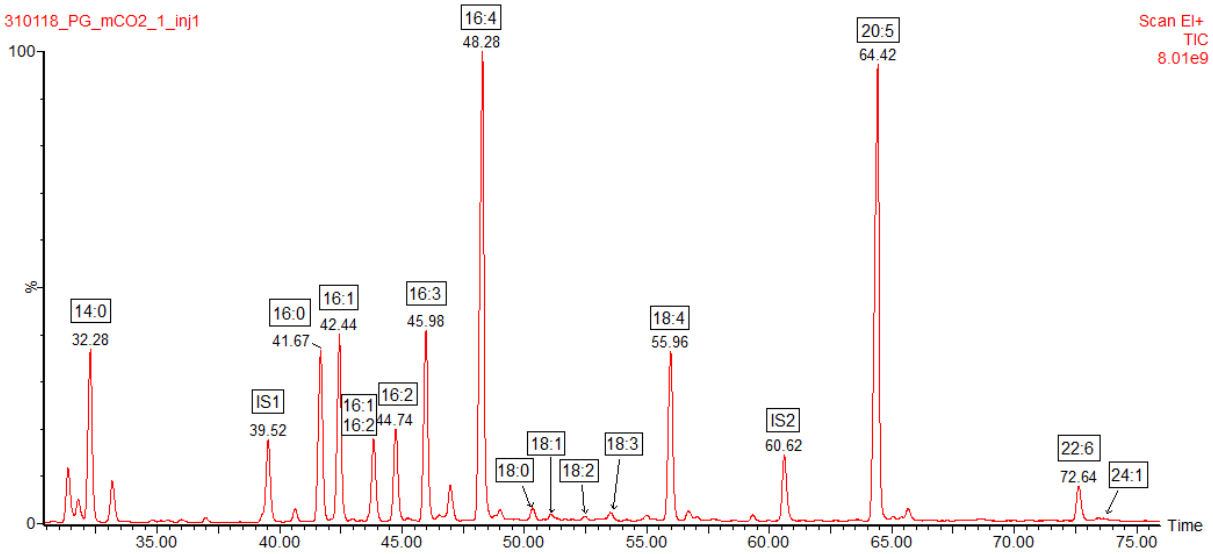

Figure 38 - Chromatogram of the FAMEs in P. glacialis after addition of CO_2

The chromatograms of FAMEs present in the algae samples of *P. glacialis* before and after addition of flue gas are shown in Figure 39 and Figure 40. As a result of the addition of flue gas, no major changes in the relative peak areas of the FAMEs were observed.

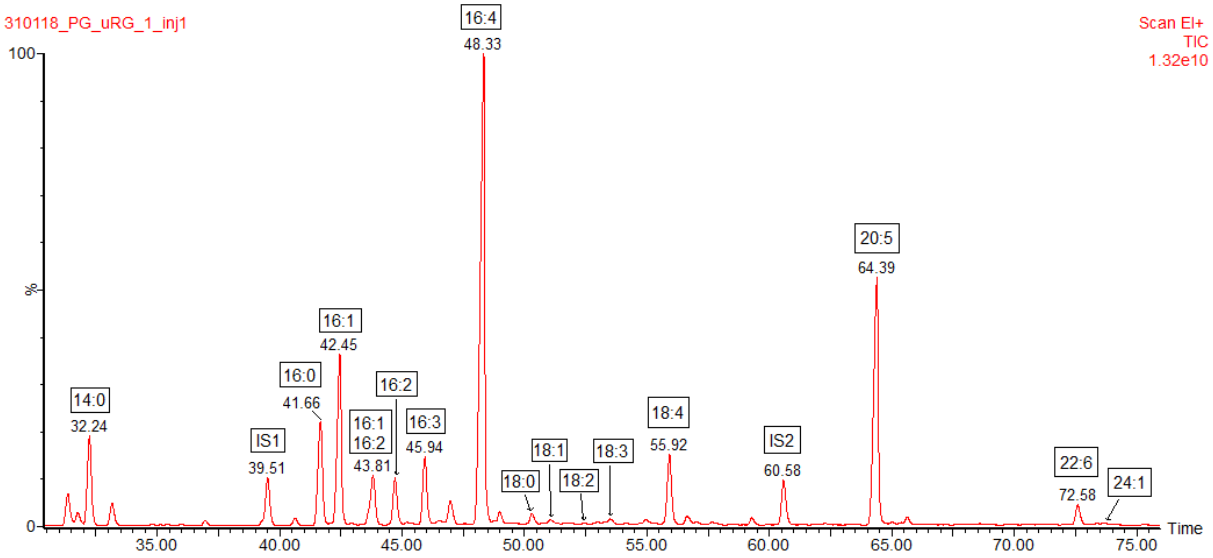

Figure 39 - Chromatogram of the FAMEs in P. glacialis before addition of flue gas

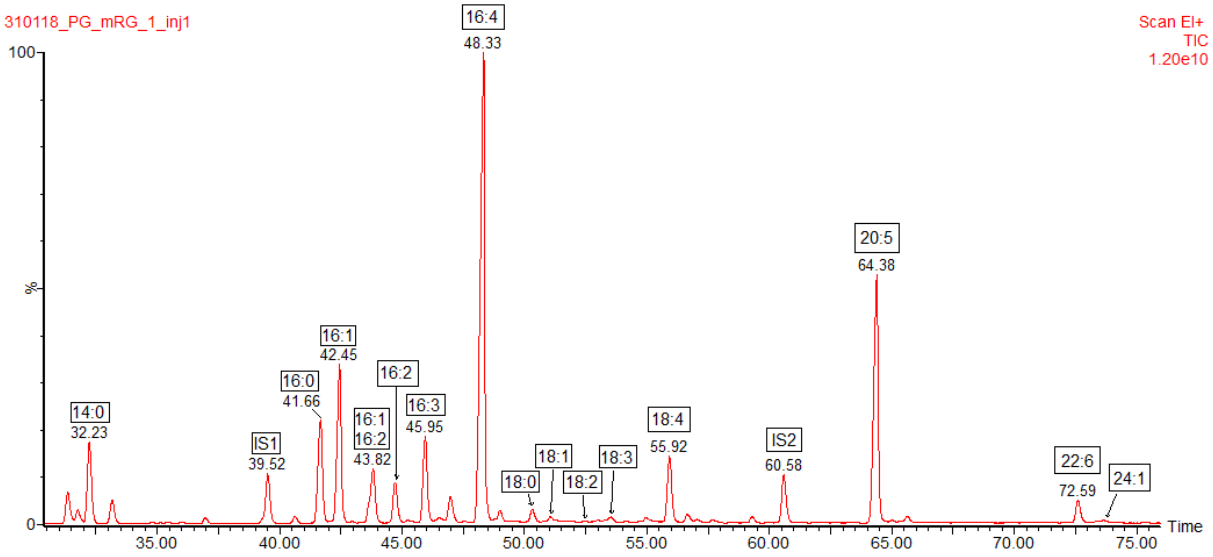

Figure 40 - Chromatogram of the FAMEs in P. glacialis after addition of flue gas

Figure 41 and Figure 42 show the chromatograms of FAMEs present in the algae samples of *C. furcellatus* before and after addition of CO_2. No major changes in the relative peak areas of the FAMEs were observed as a result of the addition of CO_2.

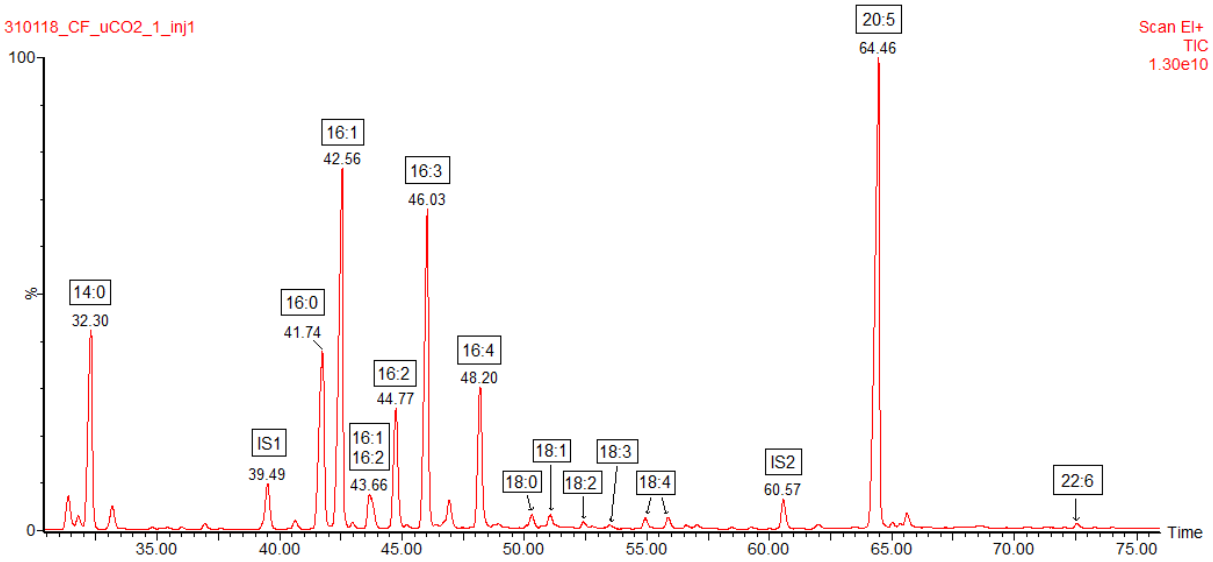

Figure 41 - Chromatogram of the FAMEs in C. furcellatus before addition of CO_2

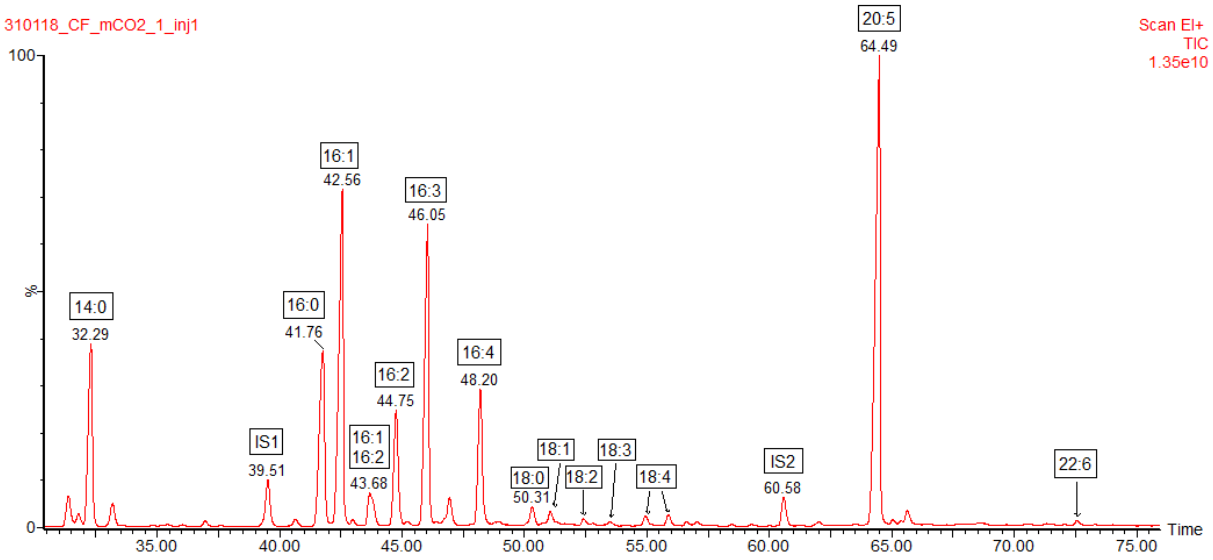

Figure 42 - Chromatogram of the FAMEs in C. furcellatus after addition of CO_2

4.2.1 Fatty acid composition of *P. glacialis* before and after addition of CO_2 and flue gas

Table 14 - Fatty acid composition of P. glacialis before and after addition of CO_2 and flue gas. For each fatty acid, proportion of total fatty acids (mean ± SD) is presented. n.d.: not detectable.

Fatty acid	***Pg.* before CO_2 (% TFA)**	***Pg.* after CO_2 (% TFA)**	***Pg.* before flue gas (% TFA)**	***Pg.* after flue gas (% TFA)**
14:0	3.80 ± 0.14	4.51 ± 0.35*	3.92 ± 0.06	3.80 ± 0.06*
16:0	4.80 ± 0.12	4.60 ± 0.10*	4.53 ± 0.09	4.53 ± 0.09
16:1 (1)	5.83 ± 0.24	5.25 ± 0.64	6.92 ± 0.13	6.59 ± 0.06*
16:1 (2)	0.95 ± 0.02	1.93 ± 0.11*	1.67 ± 0.02	1.79 ± 0.01*
16:2 (1)	1.09 ± 0.03	1.14 ± 0.05	1.65 ± 0.02	1.90 ± 0.02*
16:2 (2)	2.21 ± 0.23	2.62 ± 0.21*	2.36 ± 0.03	2.25 ± 0.02*
16:3	18.06 ± 0.45	7.35 ± 0.35*	4.14 ± 0.05	5.31 ± 0.04*
16:4	11.43 ± 0.88	20.53 ± 0.88*	33.93 ± 0.42	34.65 ± 0.34*
18:0	0.69 ± 0.02	0.64 ± 0.05*	0.89 ± 0.04	0.99 ± 0.11
18:1	1.01 ± 0.07	0.61 ± 0.04*	0.72 ± 0.01	0.78 ± 0.02*
18:2	0.41 ± 0.02	0.46 ± 0.03*	0.41 ± 0.01	0.40 ± 0.01
18:3	0.55 ± 0.03	0.61 ± 0.03*	0.66 ± 0.01	0.66 ± 0.02
18:4	4.21 ± 0.17	4.14 ± 0.36	2.63 ± 0.03	2.50 ± 0.03*
20:0	*n.d.*	*n.d.*	*n.d.*	*n.d.*
20:4	*n.d.*	*n.d.*	*n.d.*	*n.d.*
20:5	40.41 ± 0.41	40.67 ± 0.89	31.52 ± 0.70	29.43 ± 0.22*
22:0	*n.d.*	*n.d.*	*n.d.*	*n.d.*
22:6	4.06 ± 0.09	4.44 ± 0.19*	3.57 ± 0.09	3.92 ± 0.04*
24:0	*n.d.*	*n.d.*	*n.d.*	*n.d.*
24:1	0.51 ± 0.02	0.50 ± 0.03	0.49 ± 0.01	0.51 ± 0.02
Total SFAs	9.29 ± 0.08	9.75 ± 0.30*	9.34 ± 0.18	9.32 ± 0.15
Total MUFAs	8.29 ± 0.27	8.29 ± 0.51	9.80 ± 0.15	9.67 ± 0.08
Total PUFAs	82.42 ± 0.26	81.97 ± 0.23*	80.86 ± 0.33	81.02 ± 0.21

***** statistically significant difference before and after addition of CO_2 or flue gas (t-test, 95% level, α=0.05, n=6)

For both algal species, the calculated mean concentration of each fatty acid before and after addition of CO_2 and flue gas can be found in Appendix 6. Among the fatty acids, the main focus was the content of EPA (20:5), DHA (22:6) and total PUFAs. The desired result of the addition of CO_2 and flue gas was either increased or unchanged content of these fatty acids. If the algal biomass is to be used as fish feed for the aquaculture industry, the content of LC-PUFAs, especially omega-3 LC-PUFAs, should be as high as possible, and should not be considerably reduced by the addition of flue gas.

The fatty acid composition of *P. glacialis* before and after addition of CO_2 and flue gas is shown in Table 14. The predominant fatty acids were 16:1, 16:3, 16:4 and 20:5. These fatty acids amounted to a total of approximately 75% of total fatty acids. Individually, the remaining fatty acids constituted less than 5% of total fatty acids.

The addition of CO_2 resulted in many significant changes in the fatty acid composition of *P. glacialis*. The greatest and most noticeable changes were the reduction from 18.06% to 7.35% ($p < 0.001$) in the content of 16:3 n-4 and the increase from 11.43% to 20.53% ($p < 0.001$) in the content of 16:4 n-1. The content of DHA increased from 4.06% to 4.44% ($p = 0.003$), while the content of EPA did not change significantly. Total PUFAs decreased from 82.42% to 81.97% ($p = 0.01$). These results share a number of similarities with Artamonova et al.'s [28] findings. For *P. glacialis,* Artamonova et al. reported that the content of DHA increased from 3.90% to 5.75% ($p < 0.05$) and total PUFAs decreased from 62.89% to 58.42% ($p < 0.05$) in response to CO_2 aeration (20-25% CO_2), which is in accordance with the present study. However, Artamonova et al. demonstrated that the content of EPA was reduced from 26.59% to 23.66% ($p < 0.05$). A possible explanation for this inconsistency is the difference in CO_2 concentration between the two studies. In Artamonova et al.'s study, there were no major changes in the content of 16:3 and 16:4.

Addition of CO_2 and flue gas to *P. glacialis* appear to lead to different changes in the fatty acid composition. As a result of the addition of flue gas (containing 7-8% CO_2) from Finnfjord, the content of EPA decreased from 31.52% to 29.43% ($p < 0.001$), while the content of DHA increased from 3.57% to 3.92% ($p < 0.001$). Total PUFAs did not change significantly. In contrast to the algae samples with and without addition of CO_2, there were no major changes in the content of 16:3 and 16:4. At the time of writing, there have been a few studies published on the effect of addition of flue gas on fatty acid composition of microalgae, but all the studies used algal species with a low content of LC-PUFAs. The algal species in the present study have

a completely different fatty acid composition than the warm-water species used in other studies. Kao et al. [30], for instance, reported the relative content of 16:0, 16:1, 18:0, 18:1, 18:2, 18:3 and "others" as a result of addition of three types of flue gases from a steel plant (containing approx. 25% CO_2). Further, Kao et al. reported that the content of unsaturated fatty acids, which was 44.6% for the control (with added ambient air), decreased by the addition of coke-oven flue gas (30.7%), increased by the addition of hot stove flue gas (45.1%) and increased by the addition of power plant flue gas (51.8%). Aslam et al. [34] demonstrated an increase from 41.03% to 48.07% in the content of PUFAs of mixed microalgae consortia in response to addition of unfiltered coal fired flue gas (containing 5.5% CO_2). This indicates that the resulting fatty acid composition may vary depending on the composition of the flue gas.

The results of the present study suggest that the addition of air containing 3% CO_2 and flue gas have a small impact on the fatty acid composition of *P. glacialis*, and most importantly, the proportion of unsaturated fatty acids was not reduced by the addition of flue gas, i.e. the algae did not get a more saturated fatty acid profile. The content of PUFAs, including EPA, was generally high in the algae. In addition, the omega-3/omega-6 ratio was particularly high. Although there are still other factors to take into consideration, based on the lipid content and fatty acid profile, the algal biomass seems to be well-suited as fish feed for the aquaculture industry.

4.2.2 Fatty acid composition of *C. furcellatus* before and after addition of CO_2

Table 15 - Fatty acid composition of C. furcellatus before and after addition of CO_2. For each fatty acid, proportion of total fatty acids (mean ± SD) is presented. n.d.: not detectable.

Fatty acid	***Cf.* before CO_2 (% TFA)**	***Cf.* after CO_2 (% TFA)**
14:0	4.79 ± 0.25	4.39 ± 0.15*
16:0	5.29 ± 0.22	4.92 ± 0.12*
16:1 (1)	8.62 ± 0.26	8.04 ± 0.12*
16:1 (2)	0.48 ± 0.01	0.46 ± 0.01*
16:2 (1)	1.23 ± 0.04	1.15 ± 0.02*
16:2 (2)	3.20 ± 0.08	3.00 ± 0.03*
16:3	9.83 ± 0.25	9.21 ± 0.05*
16:4	6.29 ± 0.16	5.89 ± 0.04*
18:0	0.93 ± 0.15	0.87 ± 0.06
18:1	0.96 ± 0.04	0.88 ± 0.06*
18:2	0.44 ± 0.02	0.42 ± 0.01
18:3	0.38 ± 0.02	0.37 ± 0.01
18:4 (1)	0.55 ± 0.02	0.55 ± 0.02
18:4 (2)	0.55 ± 0.02	0.53 ± 0.02
20:0	*n.d.*	*n.d.*
20:4	*n.d.*	*n.d.*
20:5	55.44 ± 1.45	58.27 ± 0.34*
22:0	*n.d.*	*n.d.*
22:6	1.02 ± 0.03	1.05 ± 0.01
24:0	*n.d.*	*n.d.*
24:1	*n.d.*	*n.d.*
Total SFAs	11.01 ± 0.59	10.18 ± 0.18*
Total MUFAs	10.06 ± 0.32	9.38 ± 0.16*
Total PUFAs	78.93 ± 0.89	80.44 ± 0.31*

***** statistically significant difference before and after addition of CO_2 (t-test, 95% level, α=0.05, n=6)

The fatty acid composition of *C. furcellatus* before and after addition of CO_2 is shown in Table 15. The predominant fatty acids were 16:0, 16:1, 16:3, 16:4 and 20:5. These fatty acids amounted to a total of approximately 85% of total fatty acids. Individually, the remaining fatty acids constituted less than 5% of total fatty acids.

It appears that the addition of CO_2 affects the fatty acid composition of *P. glacialis* and *C. furcellatus* in different ways. For *C. furcellatus*, the addition of CO_2 resulted in an increase of both EPA and total PUFAs. The content of EPA increased from 55.44% to 58.27% ($p = 0.004$) and the content of total PUFAs increased from 78.93% to 80.44% ($p = 0.007$). There was no significant change in the content of DHA. In correspondence with these findings, for the algal species *Attheya longicornis*, Artamonova et al. [28] reported that the content of EPA increased from 19.09% to 20.98% (even though statistically insignificant) and the content of total PUFAs increased significantly from 48.63% to 49.26% in response to CO_2 aeration (20-25% CO_2). There was no significant change in the content of DHA. In Artamonova et al.'s study, the significance level was set to 0.05. In accordance with both studies, Wang et al. [32] reported that the addition of CO_2 (20-30% CO_2) resulted in an increase in the content of both EPA and total PUFAs of the species *Chaetoceros muelleri*. However, for *C. muelleri*, the content of PUFAs constituted less than 17% of total fatty acids. For the species *Scenedesmus obliquus*, Tang et al. [33] reported an increase in the content of both EPA and total unsaturated fatty acids as response to CO_2 aeration (5-50% CO_2). These findings by Tang et al. correspond well with the findings of the studies mentioned above.

It should be noted that not all studies reported whether the changes in lipid content and fatty acid composition were statistically significant. In the cases where it was reported, the p-value is presented.

Similar to the findings for *P. glacialis*, the results presented in Table 15 indicate that the addition of air containing 3% CO_2 has a small impact on the fatty acid composition of *C. furcellatus*.

At the time of writing, only a few algal species have been investigated regarding the effect of addition of CO_2 and flue gas. Knowledge about how the addition of CO_2 and flue gas affect the lipid content and fatty acid composition of microalgae is still new and should be studied further.

4.3 Structure determination of unsaturated fatty acids

Chromatograms of the picolinyl derivatives in three algae samples (*Pg.* with addition of CO_2, *Pg.* with addition of flue gas and *Cf.* with addition of CO_2) are shown in Figure 43 - 45. All the fatty acids which were quantified as FAMEs were also detected as picolinyl derivatives. For *C. furcellatus*, the picolinyl derivative of the fatty acid 24:1 was observed even though the methyl ester derivative of the fatty acid was not detected. The fatty acids that were present in the algae samples are listed in Table 16. All samples of *P. glacialis* contained the same fatty acids. The same goes for both samples of *C. furcellatus*.

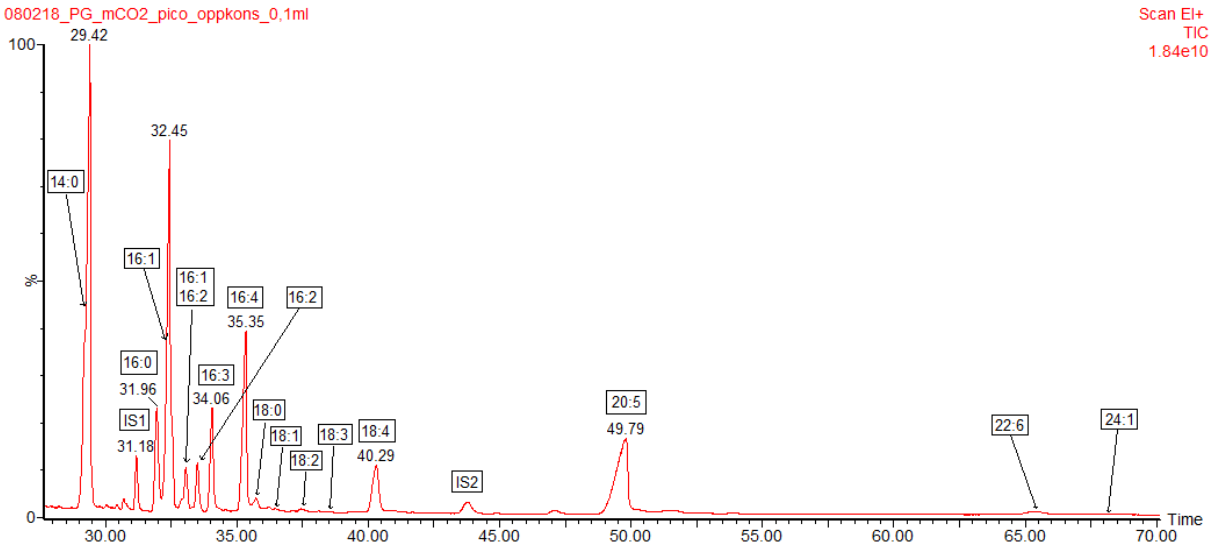

Figure 43 - Chromatogram of picolinyl derivatives in an algae sample of P. glacialis after addition of CO_2

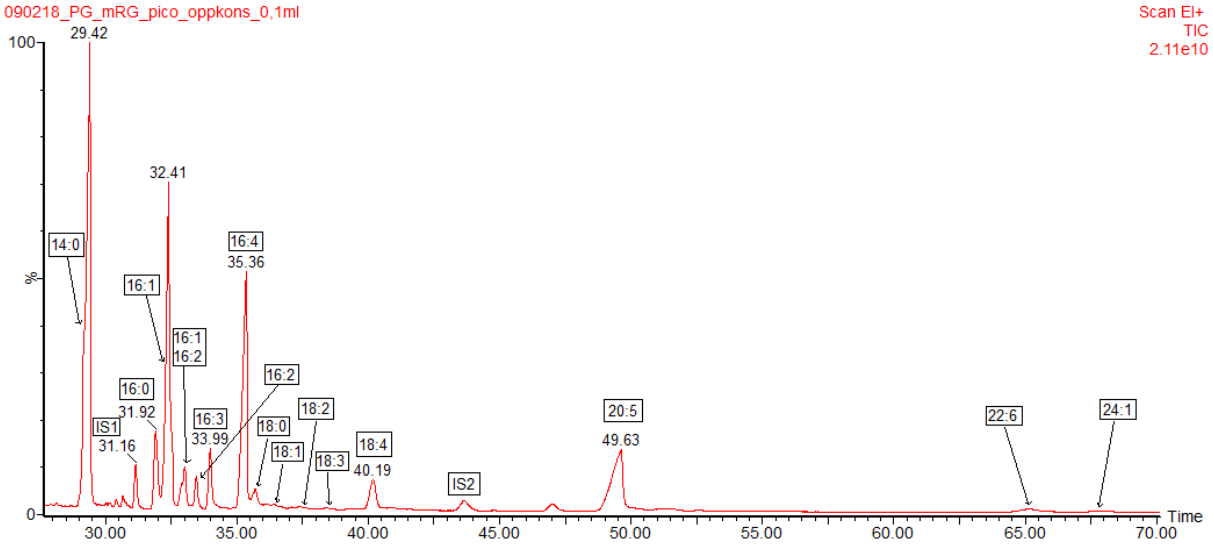

Figure 44 - Chromatogram of picolinyl derivatives in an algae sample of P. glacialis after addition of flue gas

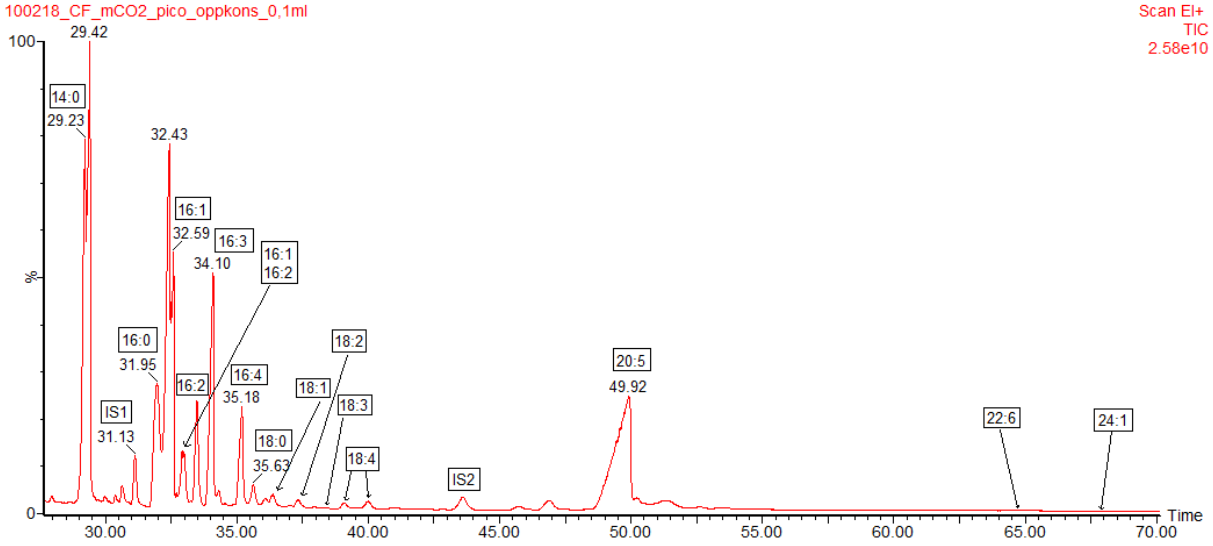

Figure 45 - Chromatogram of picolinyl derivatives in an algae sample of C. furcellatus after addition of CO_2

Table 16 – Fatty acids found in P. glacialis and C. furcellatus. Double bond positions of the fatty acids are presented as omega (n-x) and delta (Δ).

Fatty acid	**Double bond positions**			
	P. glacialis		***C. furcellatus***	
	Omega	**Delta**	**Omega**	**Delta**
14:0				
16:0				
16:1 (1)	n-7	Δ9	n-7	Δ9
16:1 (2)	n-5	Δ11	n-5	Δ11
16:2 (1)	n-7	Δ6,9	n-7	Δ6,9
16:2 (2)	n-4	Δ9,12	n-4	Δ9,12
16:3	n-4	Δ6,9,12	n-4	Δ6,9,12
16:4	n-1	Δ6,9,12,15	n-1	Δ6,9,12,15
18:0				
18:1	n-7	Δ11	n-7	Δ11
18:2	n-6	Δ9,12	n-6	Δ9,12
18:3	x	x	x	x
18:4 (1)	n-3	Δ6,9,12,15	n-4	Δ5,8,11,14
18:4 (2)	*n.d.*		n-3	Δ6,9,12,15
20:5	n-3	Δ5,8,11,14,17	n-3	Δ5,8,11,14,17
22:6	n-3	Δ4,7,10,13,16,19	n-3	Δ4,7,10,13,16,19
24:1	n-11	Δ13	(n-9)	(Δ15)

Since only one GC column was used, the retention order was the same for the picolinyl derivatives and the FAMEs. In Table 16, the fatty acids are listed by increasing retention time. For the TG-FAMEWAX column, it appeared that isomers were eluted according to their omega number; an isomer with a high omega number had shorter retention time than an isomer with a lower omega number. For fatty acid 18:3, the mass spectra were not interpretable and the structure remained thus unknown. However, considering the retention time of 18:3 in the algae samples in relation to the retention time of 18:3 n-3 in the standard samples, it can be assumed that the fatty acid had an omega number higher than 3.

The chemical structures of all the identified unsaturated fatty acids are shown in Figure 46. For both algal species, the mass spectra of the picolinyl derivatives of the fatty acids can be found

in Appendix 7 and 8. The chemical structures of the picolinyl derivatives of the unsaturated fatty acids are shown in Appendix 9. Fragment ions that reveal double bond positions are pointed out on these structures.

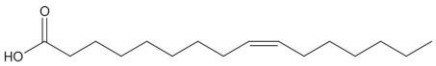

9(Z)-hexadecenoic acid (16:1 n-7)

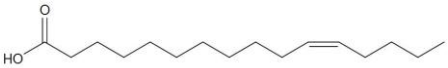

11(Z)-hexadecenoic acid (16:1 n-5)

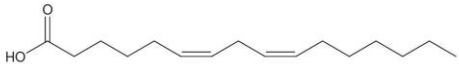

6(Z),9(Z)-hexadecadienoic acid (16:2 n-7)

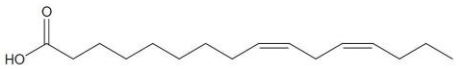

9(Z),12(Z)-hexadecadienoic acid (16:2 n-4)

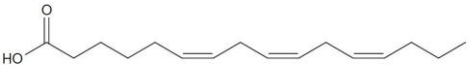

6(Z),9(Z),12(Z)-hexadecatrienoic acid (16:3 n-4)

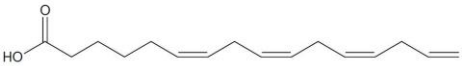

6(Z),9(Z),12(Z),15(Z)-hexadecatetraenoic acid (16:4 n-1)

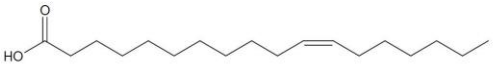

11(Z)-octadecenoic acid (18:1 n-7)

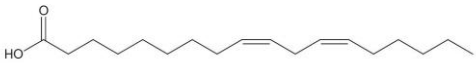

9(Z),12(Z)-octadecadienoic acid (18:2 n-6)

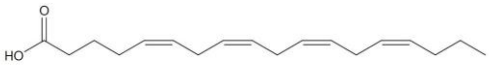

5(Z),8(Z),11(Z),14(Z)-octadecatetraenoic acid (18:4 n-4)

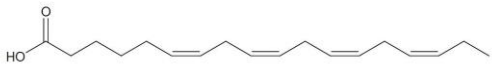

6(Z),9(Z),12(Z),15(Z)-octadecatetraenoic acid (18:4 n-3)

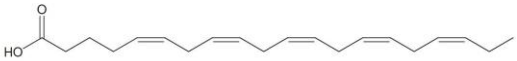

5(Z),8(Z),11(Z),14(Z),17(Z)-eicosapentaenoic acid (EPA, 20:5 n-3)

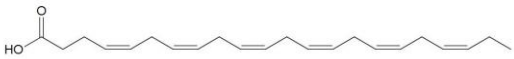

4(Z),7(Z),10(Z),13(Z),16(Z),19(Z)-docosahexaenoic acid (DHA, 22:6 n-3)

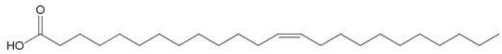

13(Z)-tetracosenoic acid (24:1 n-11)

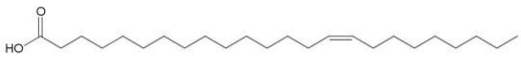

15(Z)-tetracosenoic acid (24:1 n-9)

Figure 46 – Chemical structure of all the identified unsaturated fatty acids in the algae

4.4 Determination of molecular ions using GC/MS with chemical ionization and selected ion recording

As mentioned earlier, when using EI, the molecular ion can be weak or missing for some of the FAMEs. This includes the methyl ester derivative of the fatty acid 18:4 n-4 (which was not present in the standard samples) in the samples of *C. furcellatus* (see Figure 41 and Figure 42). In Figure 47, the molecular ion of the FAME 18:4 n-4 (*m/z* = 290) is completely absent. Since this compound was eluted after 18:3 n-3 and before 18:4 n-3 (from the standard samples), it was not possible to determine whether this FAME was actually 18:3 or 18:4.

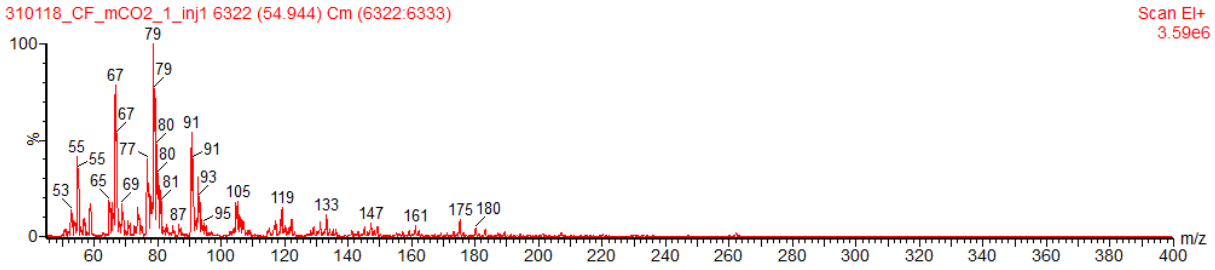

Figure 47 - Mass spectrum of the FAME 18:4 n-4. From a sample of C. furcellatus with EI and full scan mode.

In order to achieve more prominent molecular ions, analysis of a standard sample using CI and full scan mode was first attempted. This approach resulted in poor sensitivity (Figure 49) compared to EI and full scan mode (Figure 48), however, the peaks of the quasi-molecular ions were more intense (Figure 50).

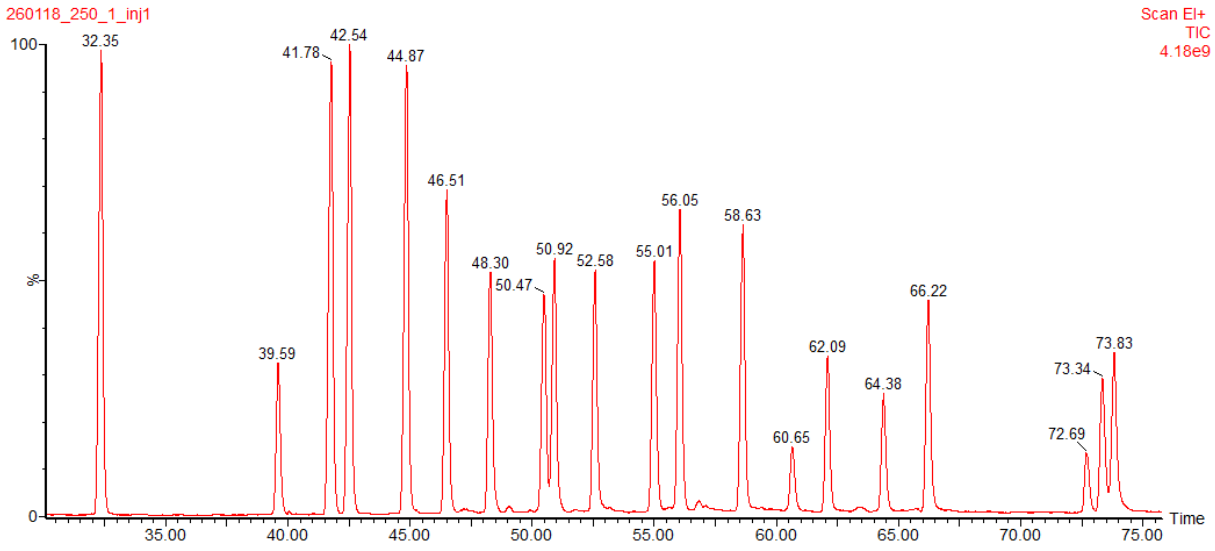

Figure 48 - Chromatogram of FAMEs in a 250 µg/mL standard sample. EI and full scan mode.

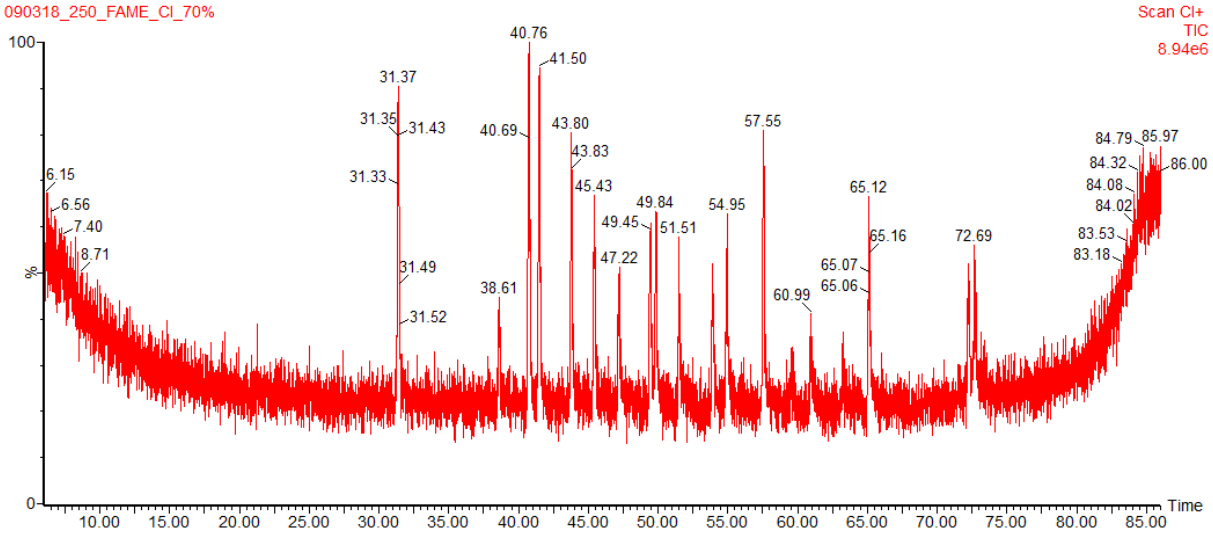

Figure 49 - Chromatogram of FAMEs in a 250 µg/mL standard sample. CI and full scan mode.

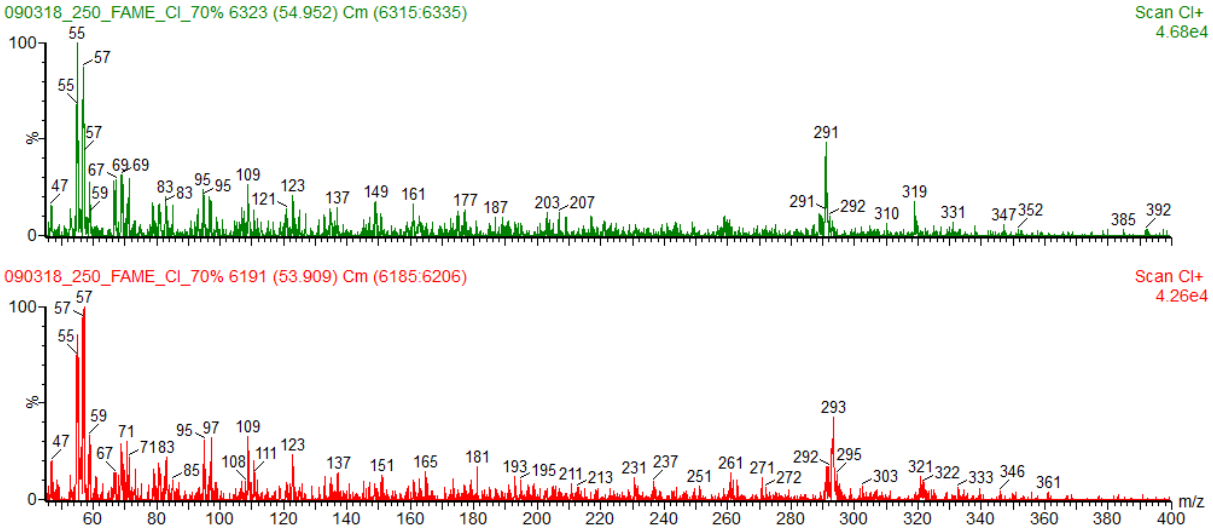

Figure 50 - Mass spectra of the FAMEs 18:4 ($[M+H]^+$ at m/z = 291), at the top, and 18:3 ($[M+H]^+$ at m/z = 293), at the bottom. From a standard sample with CI and full scan mode.

Furthermore, analysis using CI and selected ion recording (SIR) was tested. The result of this approach was highly improved sensitivity and selectivity. Figure 51 shows SIR chromatograms of some of the FAMEs in an algae sample of *P. glacialis*. SIR chromatograms of all the FAMEs can be found in Appendix 10. Since the chromatograms of all samples of *P. glacialis* were rather similar, only chromatograms for each algal species are presented.

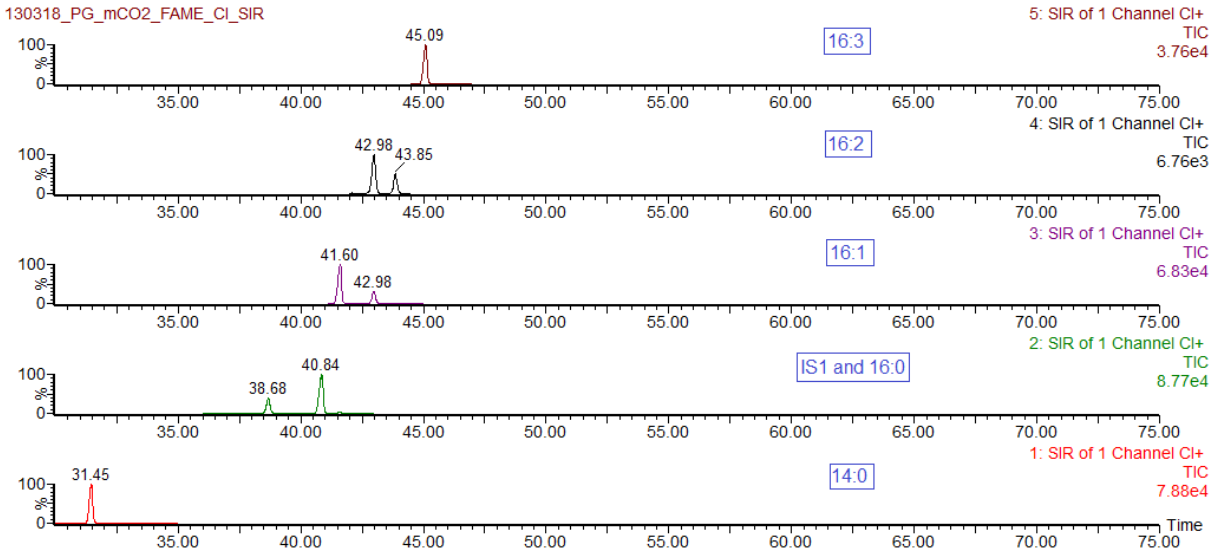

Figure 51 – SIR chromatograms of the following FAMEs: 14:0 (1), IS1 and 16:0 (2), 16:1 (3), 16:2 (4) and 16:3 (5). From an algae sample of P. glacialis.

These results confirmed the assumption that one peak contained both the FAMEs 16:1 n-5 and 16:2 n-7. The fatty acids 20:0 and 20:4 appeared to be present in *C. furcellatus*, but the amount of these fatty acids was modest. The presence of the fatty acid 24:1 in *C. furcellatus* was also confirmed.

Figure 52 shows the SIR chromatograms of the FAMEs 18:3 and 18:4 of both algal species. These chromatograms showed that *C. furcellatus* contained two isomers of 18:4, while *P. glacialis* contained only one 18:4 fatty acid. For *P. glacialis*, the peak of the FAME 18:3 with retention time 53.97 minutes was ignored due to the small amount, and because when using EI and full scan mode, it co-eluted with an unknown compound. For *C. furcellatus*, the peak of the FAME 18:3 with retention time 54.02 minutes was ignored because most of the peak area was from the isotope of 18:4 containing two ^{13}C atoms. Regarding the peak with retention time 51.88 minutes, it was excluded because it was not quantifiable when using EI and full scan mode.

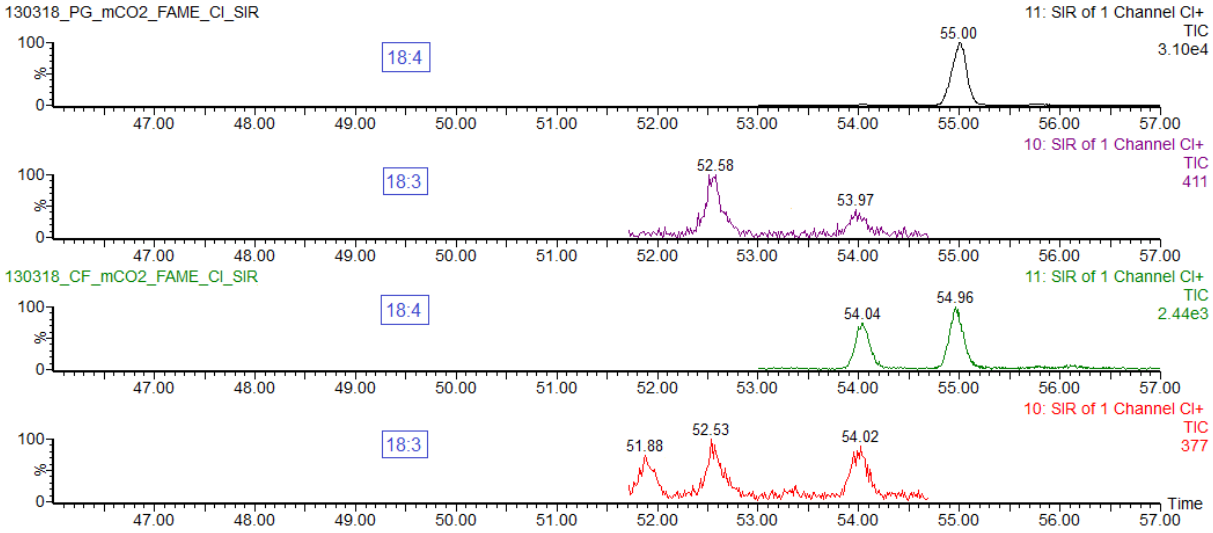

Figure 52 - SIR chromatograms of the FAMEs 18:3 and 18:4. From bottom to top: 18:3 in C. furcellatus, 18:4 in C. furcellatus, 18:3 in P. glacialis and 18:4 in P. glacialis.

As of today, there have been few articles published on the use of GC/MS with chemical ionization for analysis of fatty acids. In the present study, although CI and full scan mode provided poor sensitivity, the use of CI and SIR seemed to have potential for analysis of FAMEs. Even though this method cannot be used for localization of double bonds, it appeared to be useful for identification of molecular ions. In addition, the utilization of this method for quantitative analysis of FAMEs should be studied further.

4.5 Evaluation of GC/MS/MS method for fatty acid analysis

To determine whether tandem mass spectrometry could be useful for fatty acid analysis, a product ion scan approach was used to analyze standard samples of FAMEs and picolinyl derivatives. As for the ionization mode, both EI and CI were tested.

Regardless of collision energy, the use of chemical ionization was unsuccessful for analysis of both FAMEs and picolinyl derivatives. For the FAMEs, the sensitivity was poor and no interpretable fragmentation patterns were observed. An example of a mass spectrum is shown in Figure 53. For the picolinyl derivatives, the sensitivity was slightly better, but there was almost no fragmentation of the fatty acid chain. The fragment ion at *m/z* = 92 was the most prominent (see Figure 54).

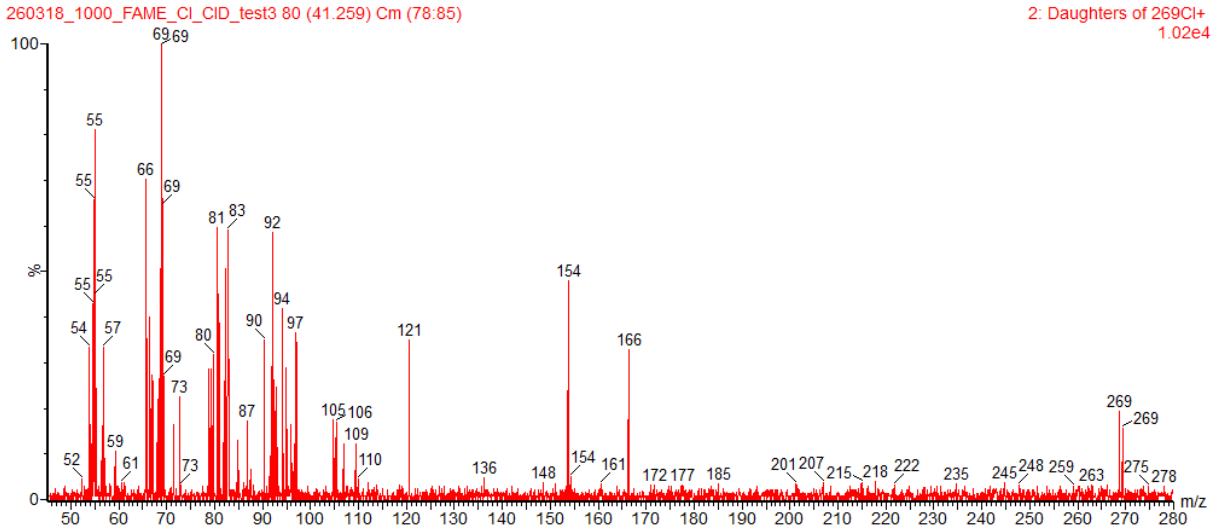

Figure 53 - Mass spectrum of the FAME 16:1. GC/MS/MS and CI. Collision energy is 40 V.

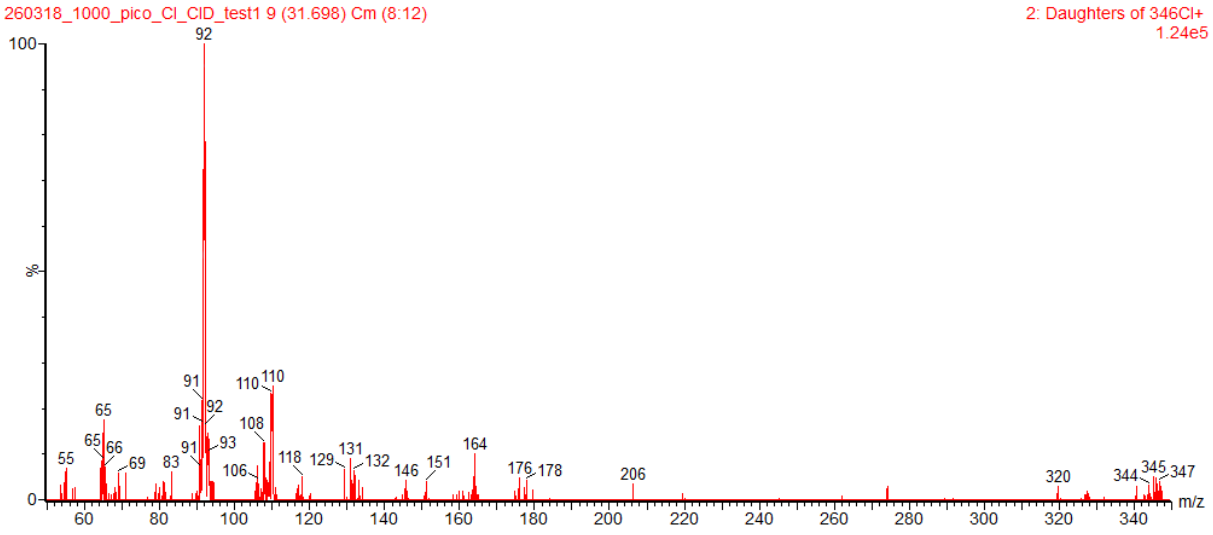

Figure 54 - Mass spectrum of the picolinyl derivative of 16:1. GC/MS/MS and CI. Collision energy is 40 V.

For finding fragmentation patterns, the use of electron ionization appeared more promising than chemical ionization. However, the sensitivity was poor for both FAMEs and picolinyl derivatives at all the tested collision energies. For the picolinyl derivatives, unlike when using CI, there was fragmentation of the fatty acid chain, but the mass spectra were less interpretable than when using full scan mode (see Figure 55). For the FAMEs, the mass spectra were messy and would not be useful for interpretation (see Figure 56).

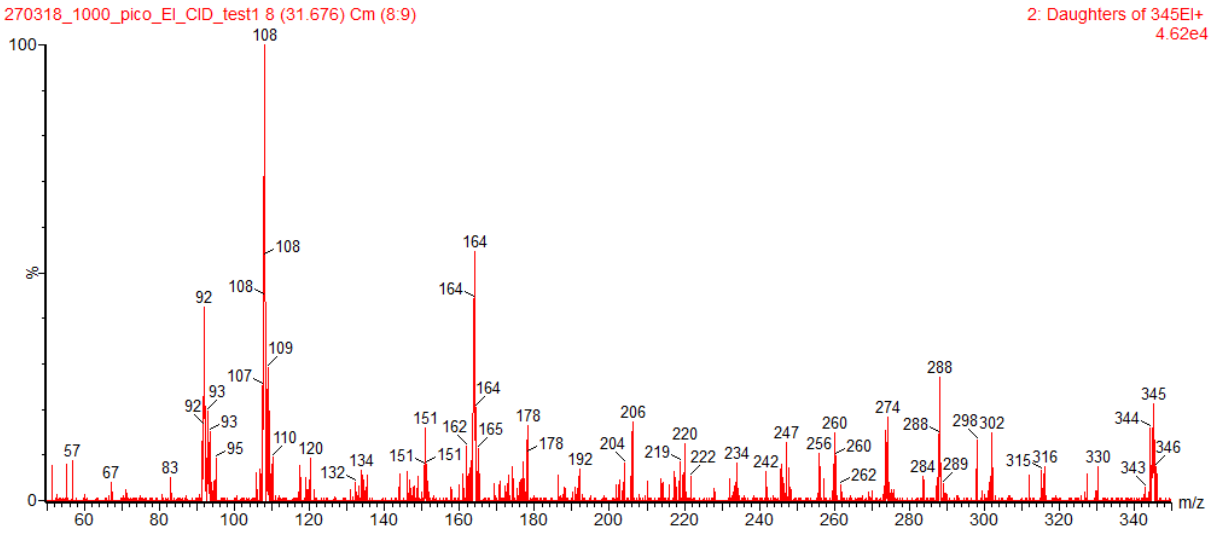

Figure 55 - Mass spectrum of the picolinyl derivative of 16:1. GC/MS/MS and EI. Collision energy is 15 V.

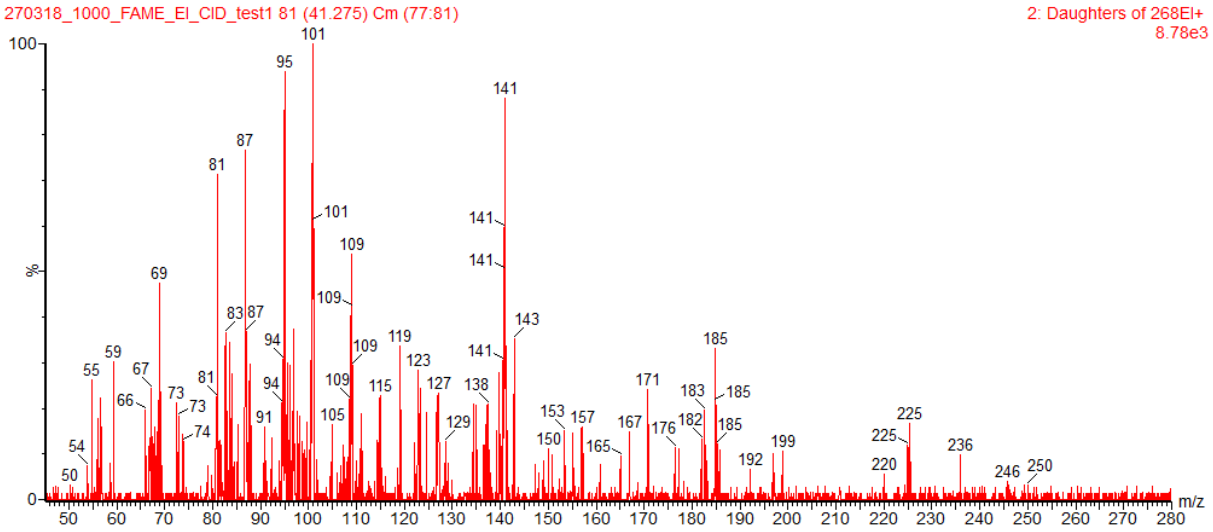

Figure 56 - Mass spectrum of the FAME 16:1. GC/MS/MS and EI. Collision energy is 15 V.

To conclude, GC/MS/MS with the product ion scan approach demonstrated here would not be useful for fatty acid analysis, neither for quantification nor identification.

For the time being, there are few publications on methodological approaches for analyzing fatty acid derivatives using GC/MS/MS, however, there is one well-known method for analysis of FAMEs. Van Pelt and Brenna [35] developed a technique for identification of FAMEs, including double bond localization, by covalent adduct chemical ionization tandem mass spectrometry (CACI-MS/MS). For chemical ionization, acetonitrile is used as reagent. When acetonitrile reacts with itself, the ion (*m/z* = 54) formed interacts with the double bonds of the fatty acid chain. By performing a product ion scan using $[M+54]^+$ as the precursor ion, two diagnostic ions, which locate the positions of the double bonds, emerge. Even FAMEs with up to six double bonds have highly characteristic mass spectra [36]. Considering that there is no need for further derivatization, this approach would be a good alternative for identification of the fatty acids in the algae samples. In that case, the same GC conditions could be applied for both quantification and identification of the FAMEs.

4.6 Limitations of the study

It is plausible that a number of limitations might have influenced the results of the estimation of lipid content and the quantification of the FAMEs.

There are several differences between the extraction method used and the Folch method [25]. Firstly, in this project, dichloromethane was used instead of chloroform. However, according to a study by Cequier-Sánchez et al. [37], there seemed to be no disadvantage of replacing chloroform with dichloromethane. Secondly, according to the Folch method, the proportions of chloroform, methanol and water should be roughly 8:4:3 (by volume), while in this project, these proportions were 2:1:3. Improper proportions of the solvents can lead to selective losses of lipids [38]. Thirdly, in the Folch method, the water contained 0.9% NaCl, while in this project, 5% NaCl water was used. The yield of lipids from the algae samples is uncertain and may have been influenced by these factors. However, for this extraction method, the yield from algal biomass has been measured previously [39]. Since the second extraction provided an increase of only roughly 20% in lipid content, an acceptable extraction yield was assumed.

The different fatty acids have variable solubility due to differences in chain length and degree of unsaturation. Obviously, there is also a difference in solubility between the fatty acids, FAMEs and picolinyl derivatives. From the lipid extraction and the methylation process, there is a possibility that the yield was different for the various fatty acids.

Five of the standard samples (50-1000 µg/mL) were prepared in the middle of December 2017, but due to problems with the GC/MS instrument, the samples were not analyzed before the end of January 2018. Meanwhile, the samples were stored in a freezer at -20 °C. Whether this significantly affected the FAMEs is unclear.

In the chromatogram of the FAMEs, even with a rather long temperature program, there was not complete separation between 18:0 and 18:1 and between 24:0 and 24:1. Therefore, when integrating the peak areas of these FAMEs in the standard samples, the integration was manually adjusted. Although this applied primarily to the highest concentrations, it may have affected the calibration curves of these FAMEs to some extent. In the algae samples, these peaks did not overlap due to the low concentration of these fatty acids.

Several of the unsaturated fatty acids in the algae samples did not have the same double bond positions as their corresponding fatty acid in the standard samples. This applied to the following fatty acids: 16:1 n-5, 16:2 n-7, 16:3, 18:1, 18:3, 18:4 n-4 and 24:1 n-11. Consequently, the

calibration curves may not have been optimal for quantification of these fatty acids. Another thing to mention is that the estimated concentrations of the fatty acid 16:4 were outside the calibration curve range, but this only applied to the algae samples of *P. glacialis* with and without addition of flue gas. The mean concentrations of the fatty acid were 1463.4 and 1472.5 µg/mL, while the calibration curve range was 10-1000 µg/mL. Linearity cannot be guaranteed beyond the calibration curve range, therefore, these estimated concentrations may be inaccurate. For the remaining fatty acids, however, the estimated concentrations were within the calibration curve ranges.

There were rather few parallels for the estimations of lipid content (n=3) and fatty acid composition (n=6) of the algae. In order for these estimates to be more representative for the actual lipid content and fatty acid composition of the algae, several rounds of cultivation of the algae are needed. The lipid extraction and methylation/transesterification should also have been carried out several times.

When using EI and full scan mode, it appeared to be several minor contaminations present in the algae samples. For most FAMEs, this did not seem to be a problem, however, there was an unknown compound that slightly overlapped with IS1, which could potentially have affected the quantification of half the FAMEs. For IS1, the integration of the peak was therefore manually adjusted. As mentioned, the approach for quantification of the peak containing both the FAMEs 16:1 n-5 and 16:2 n-7 was not optimal, but it provided a fair estimate. By using a more selective approach, for instance CI and SIR, for quantification of the FAMEs, the latter two problems might have been avoided.

5 Conclusion and future perspectives

The results of the study suggest that the addition of air containing 3% CO_2 and flue gas have a small impact on lipid content and fatty acid composition of the algae. Most importantly, the proportion of unsaturated fatty acids was not reduced by the addition of flue gas, and the lipid content was only slightly reduced. However, the algal growth rate was increased by the addition of flue gas, and seen from a fish feed production viewpoint this may outweigh the slightly lower lipid production in the algae. Several experiments are still needed to determine how the addition of flue gas affects the lipid content and fatty acid composition of the algae. Regarding the identification of picolinyl derivatives, the double bond positions of all the fatty acids in the algae, except 18:3, were determined.

The content of PUFAs, including EPA, were generally high in all the algae samples, and the omega-3/omega-6 ratio was also particularly high. Although there are still other factors to take into consideration, based on the lipid content and fatty acid profile, the use of algal biomass as fish feed for the aquaculture industry seems promising.

GC/MS with chemical ionization and selected ion recording appeared to be useful for determination of molecular ions of FAMEs. Since the method provided better sensitivity and selectivity compared to EI and full scan mode, the utilization of this method for quantification of FAMEs should be studied further. GC/MS/MS with the product ion scan approach tested in this project was, on the contrary, unsuccessful for analyzing both FAMEs and picolinyl derivatives. For identification of fatty acids, Van Pelt and Brenna's method using covalent adduct chemical ionization tandem mass spectrometry (CACI-MS/MS) for structure elucidation of FAMEs could be a convenient alternative considering that there is no need for further derivatization of the FAMEs. If using GC/MS with CI and SIR for quantification of FAMEs and CACI-MS/MS for identification of FAMEs, the same GC conditions and ionization mode can thus be applied for both quantitative analysis and identification. A combination of these methods is proposed for future work involving fatty acid analysis.

References

1. Ytrestøyl T, Aas TS, Åsgård T. Utilisation of feed resources in production of Atlantic salmon (Salmo salar) in Norway. Aquaculture. 2015;448(Supplement C):365-74.
2. Salem N, Jr., Eggersdorfer M. Is the world supply of omega-3 fatty acids adequate for optimal human nutrition? Current Opinion in Clinical Nutrition and Metabolic Care. 2015;18(2):147-54.
3. Henderson RJ, Hegseth EN, Park MT. Seasonal variation in lipid and fatty acid composition of ice algae from the Barents Sea. Polar Biology. 1998;20(1):48-55.
4. Nichols DS, Nichols PD, Sullivan CW. Fatty acid, sterol and hydrocarbon composition of Antarctic sea ice diatom communities during the spring bloom in McMurdo Sound. Antarctic Science. 1993;5(3):271-8.
5. Hauge JG, Aakvaag RK, Christensen TB. Biokjemi: en grunnbok. 4. ed. Oslo: Universitetsforlaget; 2001.
6. Certik M, Shimizu S. Biosynthesis and regulation of microbial polyunsaturated fatty acid production. Journal of Bioscience and Bioengineering. 1999;87(1):1-14.
7. Ander BP, Dupasquier CMC, Prociuk MA, Pierce GN. Polyunsaturated fatty acids and their effects on cardiovascular disease. Experimental & Clinical Cardiology. 2003;8(4):164-72.
8. Abedi E, Sahari MA. Long-chain polyunsaturated fatty acid sources and evaluation of their nutritional and functional properties. Food Science & Nutrition. 2014;2(5):443-63.
9. Guschina IA, Harwood JL. Algal lipids and effect of the environment on their biochemistry. In: Kainz M, Brett MT, Arts MT, editors. Lipids in Aquatic Ecosystems. New York: Springer New York; 2009. p. 1-24.
10. Nelson DL, Lehninger AL, Cox MM. Lehninger principles of biochemistry. 5. ed. New York: Freeman; 2008.
11. Throndsen J, Tangen K, Hasle GR. Norsk kystplanktonflora. Oslo: Almater Forlag; 2003.
12. Degerlund M, Eilertsen HC. Main Species Characteristics of Phytoplankton Spring Blooms in NE Atlantic and Arctic Waters (68–80° N). Estuaries and Coasts. 2010;33(2):242-69.
13. Mann DG, Vanormelingen P. An inordinate fondness? The number, distributions, and origins of diatom species. The Journal of Eukaryotic Microbiology. 2013;60(4):414-20.
14. Andersen RA. Diversity of eukaryotic algae. Biodiversity & Conservation. 1992;1(4):267-92.
15. de Baar HJW. von Liebig's law of the minimum and plankton ecology (1899–1991). Progress in Oceanography. 1994;33(4):347-86.
16. Kim J, Brown CM, Kim MK, Burrows EH, Bach S, Lun DS, et al. Effect of cell cycle arrest on intermediate metabolism in the marine diatom Phaeodactylum tricornutum. Proceedings of the National Academy of Sciences of the United States of America. 2017;114(38):E8007-E16.
17. Klok AJ, Martens DE, Wijffels RH, Lamers PP. Simultaneous growth and neutral lipid accumulation in microalgae. Bioresource Technology. 2013;134(Supplement C):233-43.
18. Richardson B, Orcutt DM, Schwertner HA, Martinez CL, Wickline HE. Effects of Nitrogen Limitation on the Growth and Composition of Unicellular Algae in Continuous Culture. Applied Microbiology. 1969;18(2):245-50.
19. Yao S, Brandt A, Egsgaard H, Gjermansen C. Neutral lipid accumulation at elevated temperature in conditional mutants of two microalgae species. Plant Physiology and Biochemistry. 2012;61(Supplement C):71-9.
20. Hansen S, Pedersen-Bjergaard S, Rasmussen KE. Introduction to Pharmaceutical Chemical Analysis. Chichester: Wiley; 2012.
21. Christie WW. Preparation of Ester Derivatives of Fatty Acids for Chromatographic Analysis [Internet]. 2011 [cited 2017 Dec 22]. Available from: http://lipidlibrary.aocs.org/Analysis/content.cfm?ItemNumber=40374.
22. Harvey DJ. Picolinyl esters for the structural determination of fatty acids by GC/MS. Molecular Biotechnology. 1998;10(3):251-60.
23. Pedersen-Bjergaard S, Rasmussen KE. Legemiddelanalyse. 2. ed. Bergen: Fagbokforlaget; 2010.
24. Dass C. Tandem Mass Spectrometry. Fundamentals of Contemporary Mass Spectrometry. Hoboken: John Wiley & Sons; 2006. p. 119-50.

25. Folch J, Lees M, Stanley GHS. A simple method for the isolation and purification of total lipids from animal tissues. Journal of Biological Chemistry. 1957;226(1):497-509.
26. Dubois N, Barthomeuf C, Bergé J-P. Convenient preparation of picolinyl derivatives from fatty acid esters. European Journal of Lipid Science and Technology. 2006;108(1):28-32.
27. Christie WW. 3-Pyridylcarbinol ('picolinyl') Esters of Fatty Acids - Archive of Mass Spectra [Internet]. 2017 [cited 2018 Apr 4]. Available from: http://www.lipidhome.co.uk/ms/pyrcarbinol/pyrcarb-arch/index.htm.
28. Artamonova EY, Vasskog T, Eilertsen HC. Lipid content and fatty acid composition of Porosira glacialis and Attheya longicornis in response to carbon dioxide (CO2) aeration. PLOS ONE. 2017;12(5):e0177703.
29. Yoo C, Jun S-Y, Lee J-Y, Ahn C-Y, Oh H-M. Selection of microalgae for lipid production under high levels carbon dioxide. Bioresource Technology. 2010;101(1, Supplement):S71-S4.
30. Kao C-Y, Chen T-Y, Chang Y-B, Chiu T-W, Lin H-Y, Chen C-D, et al. Utilization of carbon dioxide in industrial flue gases for the cultivation of microalga Chlorella sp. Bioresource Technology. 2014;166:485-93.
31. de Castro Araújo S, Garcia VMT. Growth and biochemical composition of the diatom Chaetoceros cf. wighamii brightwell under different temperature, salinity and carbon dioxide levels. I. Protein, carbohydrates and lipids. Aquaculture. 2005;246(1):405-12.
32. Wang X-W, Liang J-R, Luo C-S, Chen C-P, Gao Y-H. Biomass, total lipid production, and fatty acid composition of the marine diatom Chaetoceros muelleri in response to different CO2 levels. Bioresource Technology. 2014;161:124-30.
33. Tang D, Han W, Li P, Miao X, Zhong J. CO2 biofixation and fatty acid composition of Scenedesmus obliquus and Chlorella pyrenoidosa in response to different CO2 levels. Bioresource Technology. 2011;102(3):3071-6.
34. Aslam A, Thomas-Hall SR, Manzoor M, Jabeen F, Iqbal M, uz Zaman Q, et al. Mixed microalgae consortia growth under higher concentration of CO2 from unfiltered coal fired flue gas: Fatty acid profiling and biodiesel production. Journal of Photochemistry and Photobiology B: Biology. 2018;179:126-33.
35. Van Pelt CK, Brenna JT. Acetonitrile Chemical Ionization Tandem Mass Spectrometry To Locate Double Bonds in Polyunsaturated Fatty Acid Methyl Esters. Analytical Chemistry. 1999;71(10):1981-9.
36. Brenna JT, Tyburczy C. Identification of FAME Double Bond Location by Covalent Adduct Chemical Ionization (CACI) Tandem Mass Spectrometry [Internet]. 2018 [cited 2018 Apr 22]. Available from: http://lipidlibrary.aocs.org/Analysis/content.cfm?ItemNumber=40368.
37. Cequier-Sánchez E, Rodríguez C, Ravelo ÁG, Zárate R. Dichloromethane as a Solvent for Lipid Extraction and Assessment of Lipid Classes and Fatty Acids from Samples of Different Natures. Journal of Agricultural and Food Chemistry. 2008;56(12):4297-303.
38. Christie WW. Extraction of lipids from tissues - a beginner's guide [Internet]. 2011 [cited 2018 Apr 27]. Available from: http://lipidlibrary.aocs.org/History/content.cfm?ItemNumber=40362.
39. Svenning JB. Personal communication. 2018.

Appendix

Appendix 1: Preparation of standard solutions

Table 17 - Preparation of standard solutions. SS1 = stock solution 1 (1000 µg/mL), SS2 = stock solution 2 (100 µg/mL), IS solution = internal standard solution (100 µg/mL).

Concentration (µg/mL)	**SS1 (µL)**	**SS2 (µL)**	**IS solution (µL)**	**DCM (µL)**
10		10	100	890
25		25	100	875
50		50	100	850
100		100	100	800
250	25		100	875
500	50		100	850
1000	100		100	800

Appendix 2: Weight of algal biomass and lipids

Table 18 - Weight of algal biomass and lipids

Sample	Parallel	Weight of dry biomass (mg)	Weight of extracted lipids (mg)	Lipid content (%)
Pg. before CO_2	1	104.4	9.6	9.20
	2	100.6	9.2	9.15
	3	106.0	10.0	9.43
Pg. after CO_2	1	101.5	11.3	11.13
	2	101.7	10.4	10.23
	3	100.7	10.1	10.03
Pg. before flue gas	1	105.3	9.2	8.74
	2	100.3	8.3	8.28
	3	104.0	8.9	8.56
Pg. after flue gas	1	102.2	7.4	7.24
	2	100.5	7.1	7.06
	3	105.4	7.9	7.50
Cf. before CO_2	1	100.7	4.7	4.67
	2	107.2	4.0	3.73
	3	101.4	4.6	4.54
Cf. after CO_2	1	100.6	5.2	5.17
	2	100.4	4.7	4.68
	3	102.5	4.8	4.68

Appendix 3: Chromatograms of the FAMEs in the standard samples

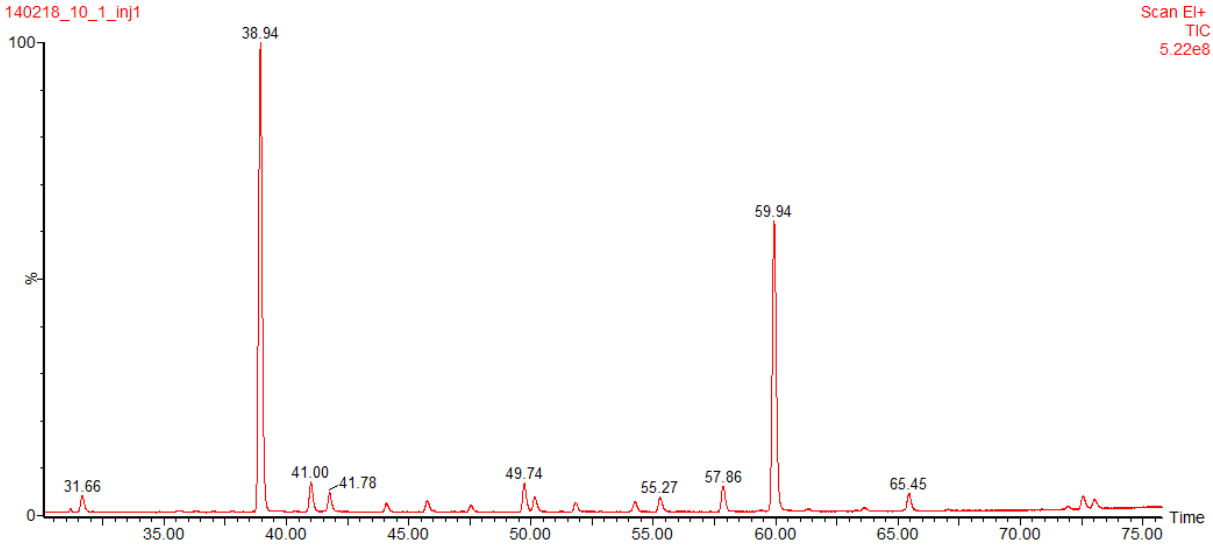

Figure 57 - Chromatogram of the FAMEs in a standard sample with concentration 10 µg/mL

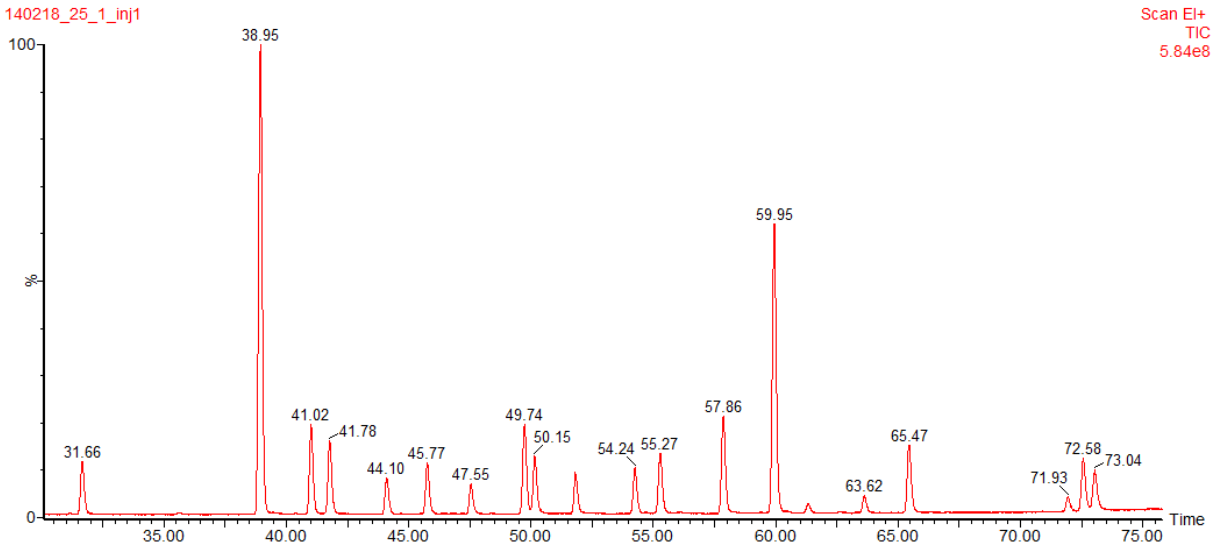

Figure 58 - Chromatogram of the FAMEs in a standard sample with concentration 25 µg/mL

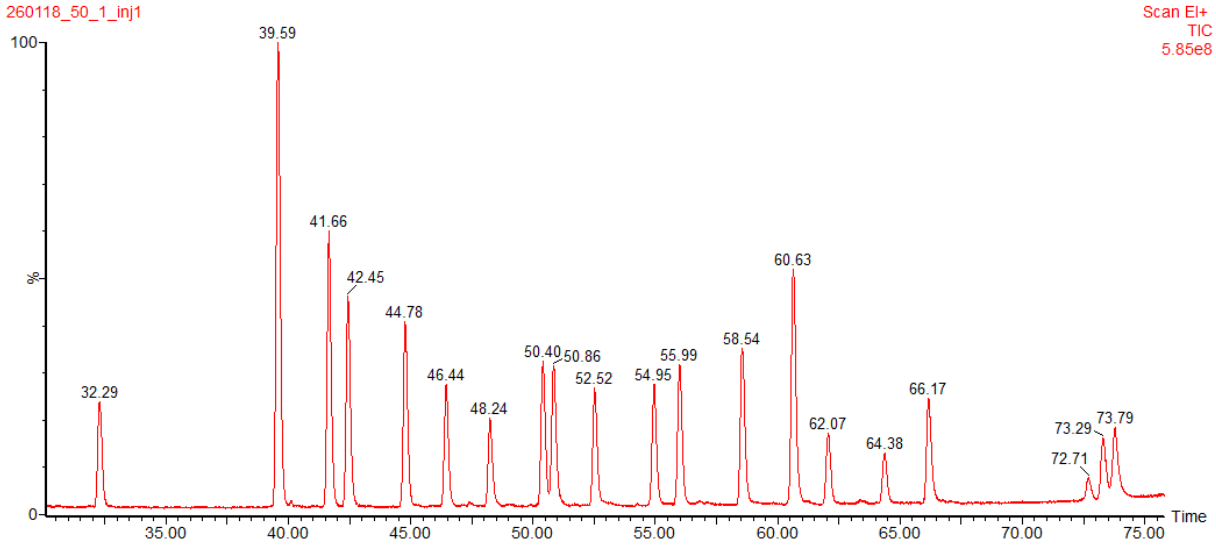

Figure 59 - Chromatogram of the FAMEs in a standard sample with concentration 50 µg/mL

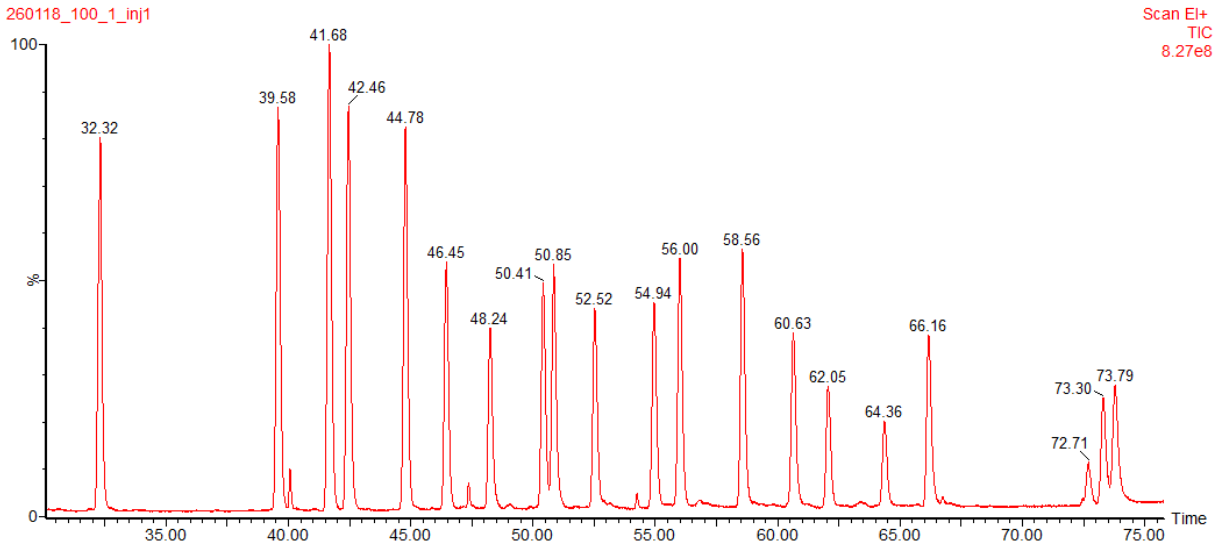

Figure 60 - Chromatogram of the FAMEs in a standard sample with concentration 100 µg/mL

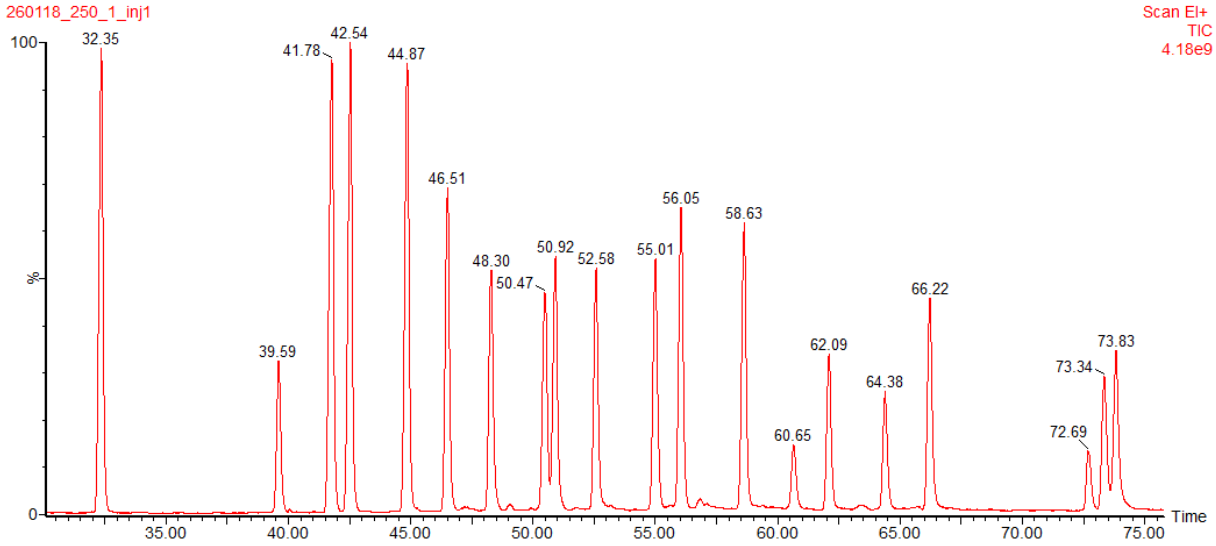

Figure 61 - Chromatogram of the FAMEs in a standard sample with concentration 250 µg/mL

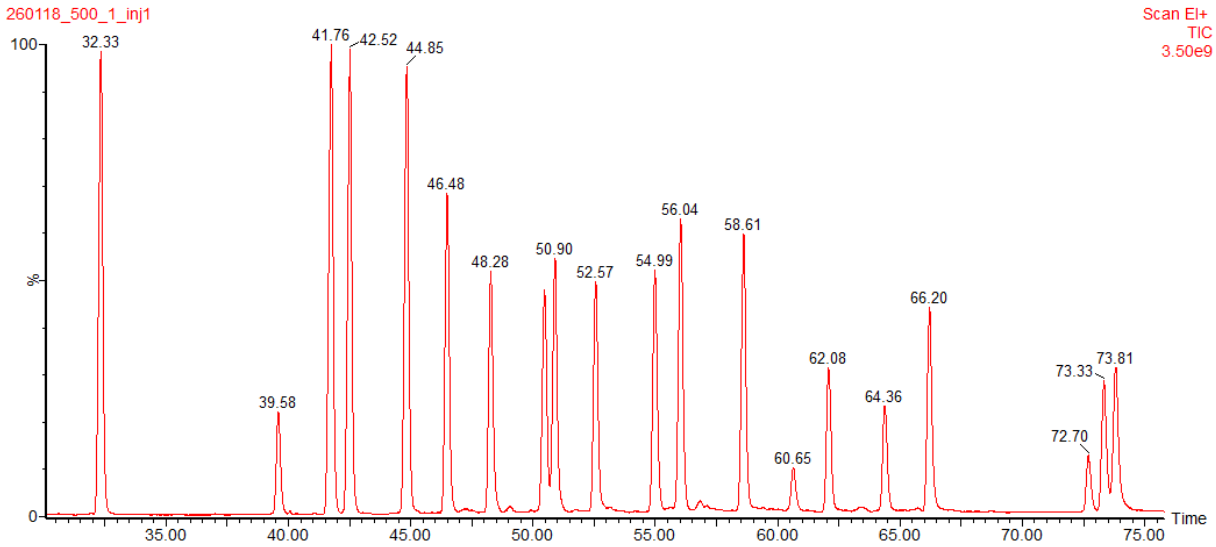

Figure 62 - Chromatogram of the FAMEs in a standard sample with concentration 500 µg/mL

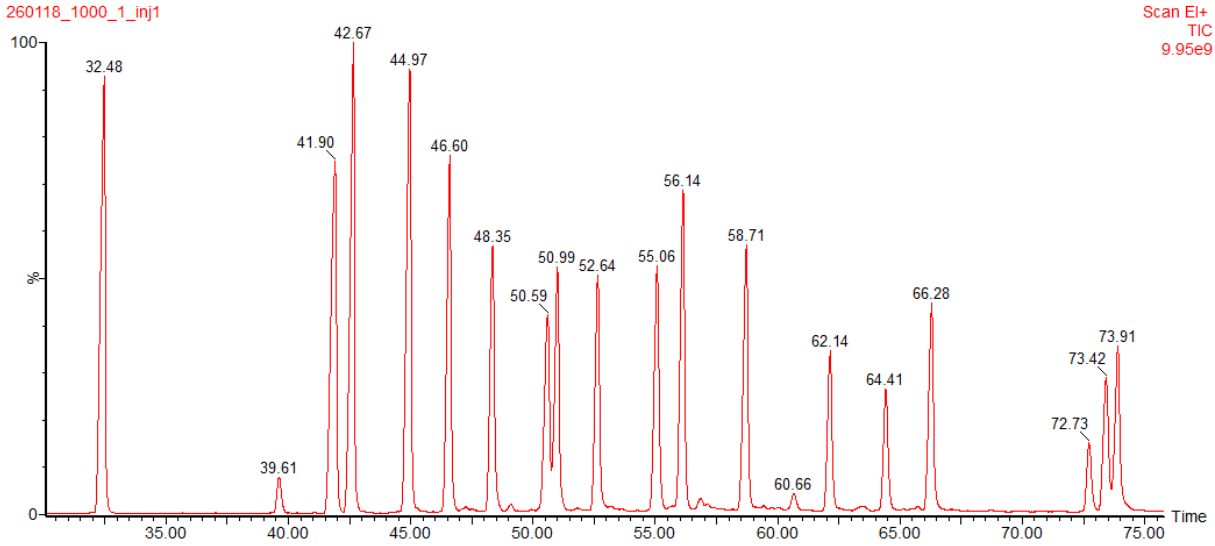

Figure 63 - Chromatogram of the FAMEs in a standard sample with concentration 1000 µg/mL

Appendix 4: Calibration curves

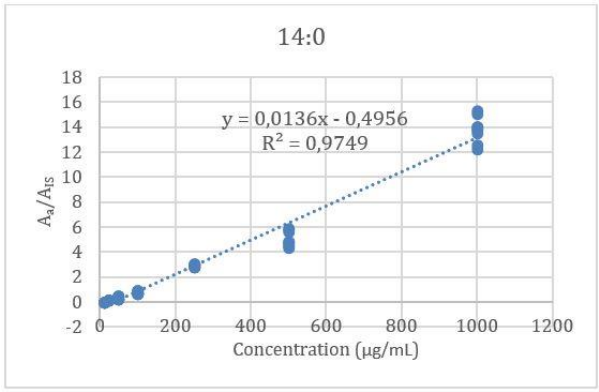

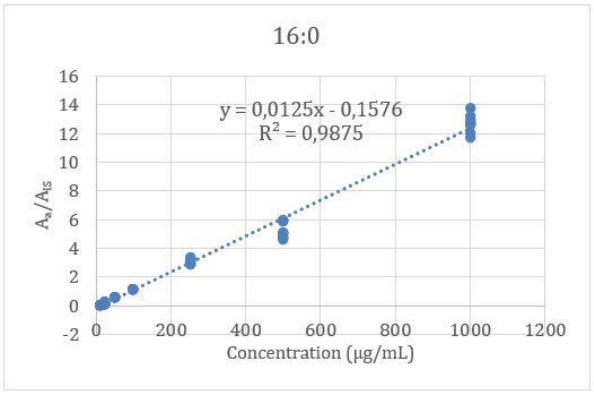

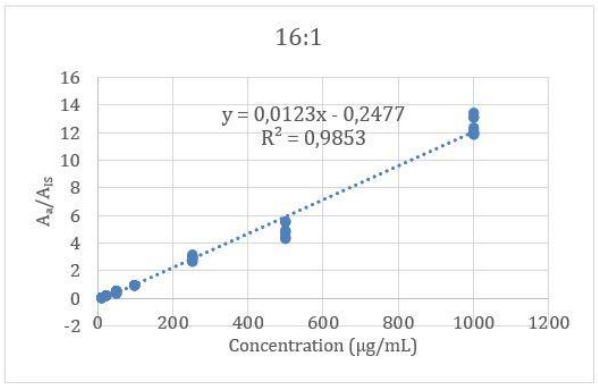

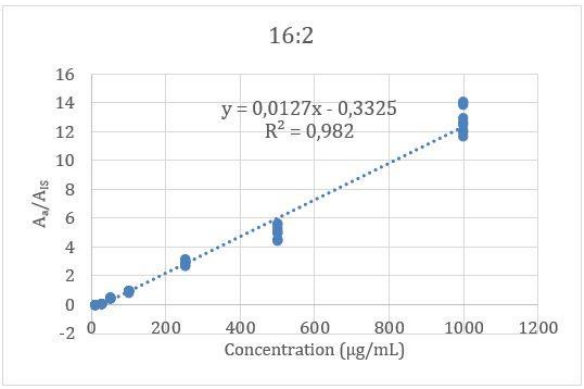

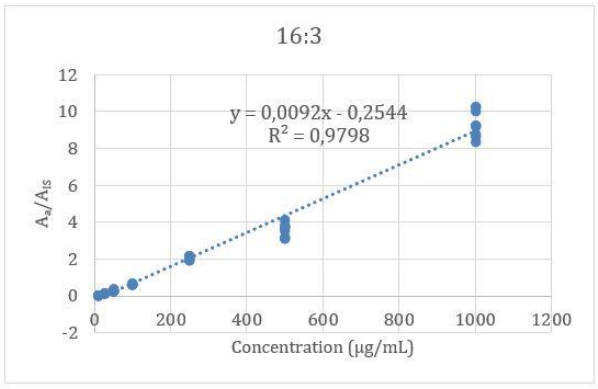

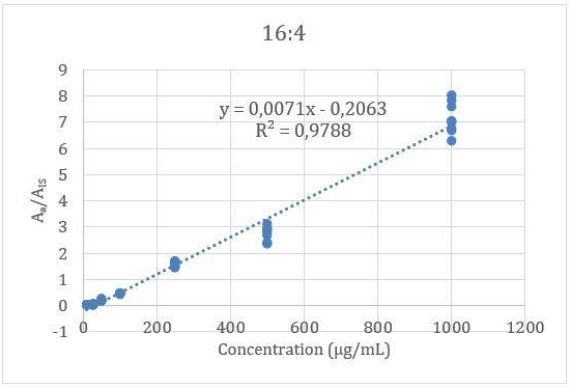

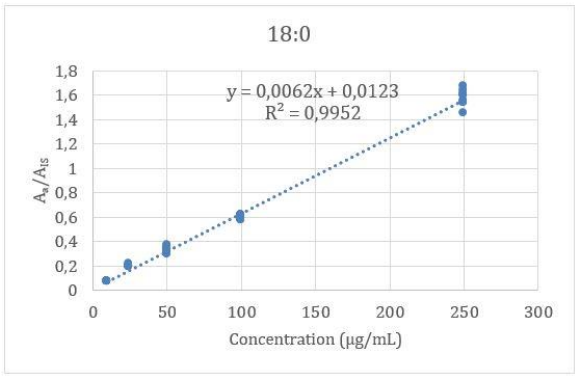

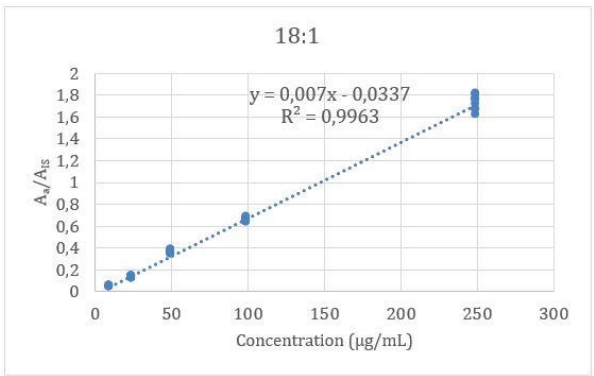

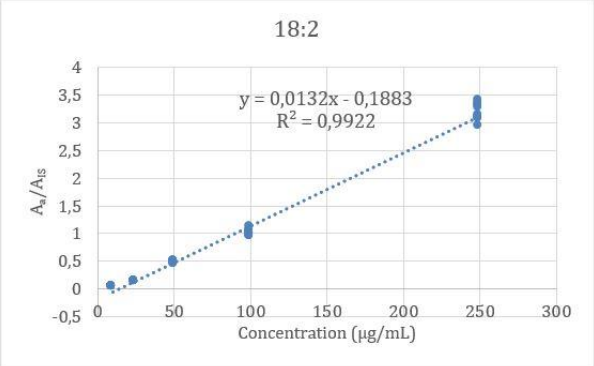
18:2
y = 0,0132x - 0,1883
R² = 0,9922
Aa/AIS
Concentration (µg/mL)

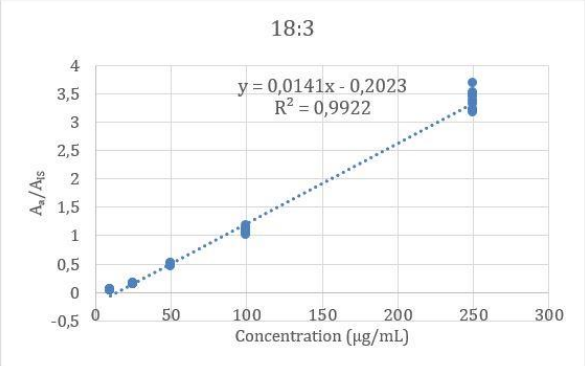
18:3
y = 0,0141x - 0,2023
R² = 0,9922
Aa/AIS
Concentration (µg/mL)

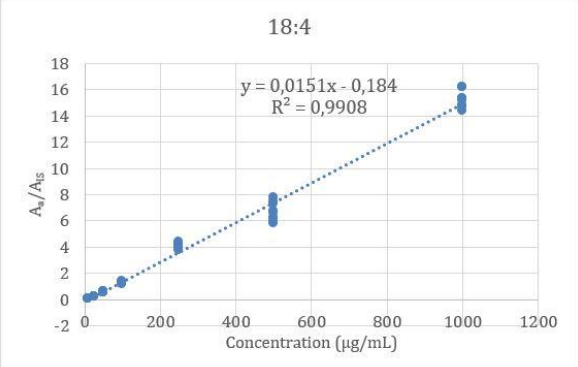
18:4
y = 0,0151x - 0,184
R² = 0,9908
Aa/AIS
Concentration (µg/mL)

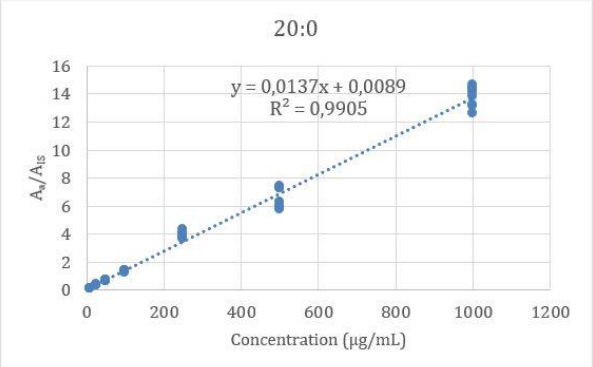
20:0
y = 0,0137x + 0,0089
R² = 0,9905
Aa/AIS
Concentration (µg/mL)

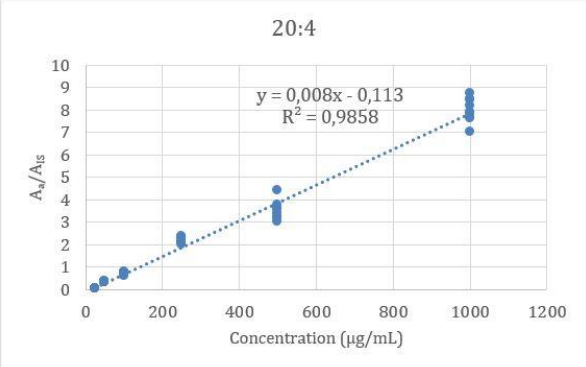
20:4
y = 0,008x - 0,113
R² = 0,9858
Aa/AIS
Concentration (µg/mL)

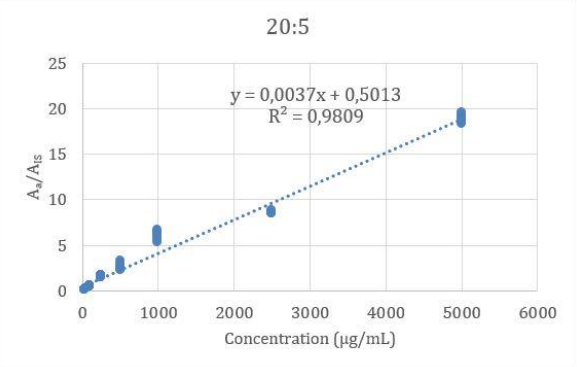
20:5
y = 0,0037x + 0,5013
R² = 0,9809
Aa/AIS
Concentration (µg/mL)

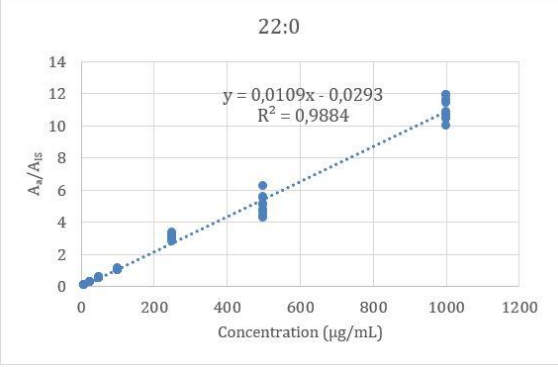
22:0
y = 0,0109x - 0,0293
R² = 0,9884
Aa/AIS
Concentration (µg/mL)

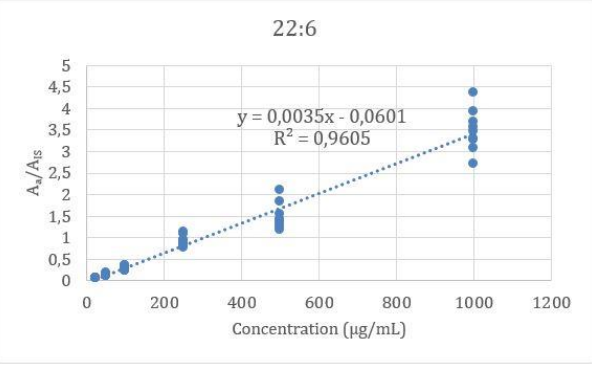
22:6
y = 0,0035x - 0,0601
R² = 0,9605
Aa/AIS
Concentration (µg/mL)

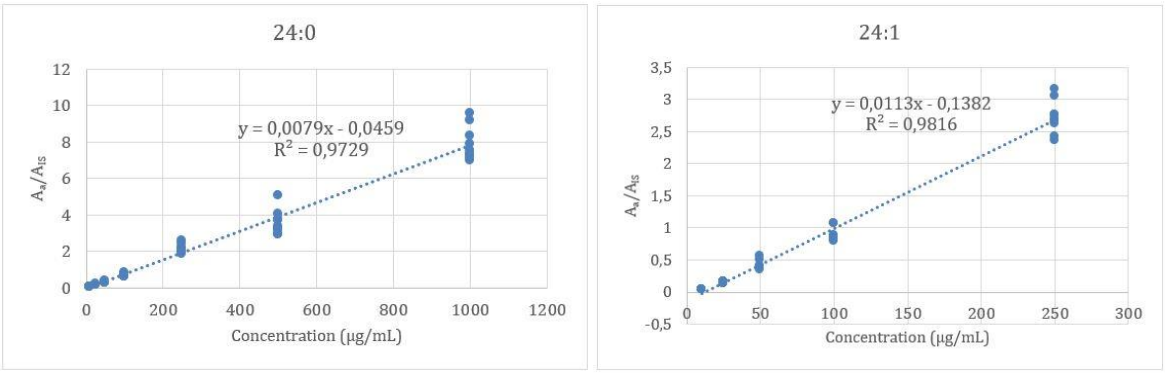

Figure 64 - Calibration curves of the FAMEs

Appendix 5: Estimated proportions of the peak containing 16:1 and 16:2

Table 19 - Estimated proportions of the peak containing both 16:1 n-5 and 16:2 n-7

Algae sample	**Peak area of molecular ion**		**Peak area of molecular ion /2.3**	**Proportion of the peak (%)**	
	16:1	**16:2**	**16:2**	**16:1**	**16:2**
Pg. before CO_2	56116	137135	59624	48.5	51.5
Pg. after CO_2	110581	95377	41468	72.7	27.3
Pg. before flue gas	101287	208387	90603	52.8	47.2
Pg. after flue gas	107806	249755	108589	49.8	50.2
Cf. before CO_2	44276	447373	194510	18.5	81.5
Cf. after CO_2	46393	465504	202393	18.6	81.4

Example:

56116 / (56116+59624) = 0.485

59624 / (59624+56116) = 0.515

Appendix 6: Calculated concentrations of each fatty acid

Table 20 - Calculated concentrations of each fatty acid in P. glacialis before and after addition of CO_2 and flue gas. The results are presented as mean ± SD (n=6). n.d.: not detectable.

Fatty acid	***Pg.* before CO_2 (µg/mL)**	***Pg.* after CO_2 (µg/mL)**	***Pg.* before flue gas (µg/mL)**	***Pg.* after flue gas (µg/mL)**
14:0	181.3 ± 7.0	193.8 ± 18.7	169.0 ± 4.2	161.4 ± 8.9
16:0	229.4 ± 10.2	198.0 ± 11.9	195.4 ± 6.6	192.2 ± 4.6
16:1 (1)	278.6 ± 21.3	226.0 ± 31.5	298.5 ± 9.4	280.0 ± 11.4
16:1 (2)	45.2 ± 0.6	82.8 ± 5.5	71.8 ± 1.6	76.0 ± 2.6
16:2 (1)	52.0 ± 0.6	49.0 ± 2.0	70.9 ± 1.4	80.8 ± 2.6
16:2 (2)	105.2 ± 8.0	112.2 ± 3.5	101.9 ± 2.2	95.6 ± 3.5
16:3	861.6 ± 13.0	316.6 ± 30.2	178.3 ± 3.9	225.7 ± 9.8
16:4	546.8 ± 58.6	882.9 ± 60.9	1463.4 ± 37.8	1472.5 ± 72.2
18:0	32.8 ± 1.5	27.2 ± 1.5	38.5 ± 2.1	42.1 ± 3.2
18:1	48.2 ± 5.1	26.3 ± 2.3	31.2 ± 0.9	33.3 ± 1.5
18:2	19.5 ± 0.4	19.7 ± 0.4	17.7 ± 0.2	17.0 ± 0.2
18:3	26.3 ± 1.0	26.2 ± 0.2	28.4 ± 0.4	28.1 ± 0.6
18:4	200.7 ± 4.2	178.0 ± 16.3	113.4 ± 1.6	106.2 ± 3.6
20:0	*n.d.*	*n.d.*	*n.d.*	*n.d.*
20:4	*n.d.*	*n.d.*	*n.d.*	*n.d.*
20:5	1929.4 ± 67.8	1748.3 ± 91.8	1359.2 ± 31.1	1250.5 ± 52.7
22:0	*n.d.*	*n.d.*	*n.d.*	*n.d.*
22:6	194.1 ± 9.2	190.8 ± 13.3	154.0 ± 3.3	166.3 ± 6.3
24:0	*n.d.*	*n.d.*	*n.d.*	*n.d.*
24:1	24.1 ± 0.8	21.3 ± 1.4	21.1 ± 0.7	21.5 ± 0.6

Table 21 - Calculated concentrations of each fatty acid in C. furcellatus before and after addition of CO_2. The results are presented as mean ± SD (n=6). n.d.: not detectable.

Fatty acid	***Cf.* before CO_2 (µg/mL)**	***Cf.* after CO_2 (µg/mL)**
14:0	358.3 ± 14.7	330.0 ± 23.1
16:0	395.9 ± 14.5	369.2 ± 17.9
16:1 (1)	645.1 ± 13.3	604.0 ± 26.3
16:1 (2)	35.6 ± 0.6	34.3 ± 0.5
16:2 (1)	92.0 ± 2.7	86.3 ± 2.1
16:2 (2)	239.7 ± 5.3	225.0 ± 7.8
16:3	735.4 ± 18.2	691.4 ± 27.4
16:4	470.7 ± 12.4	442.0 ± 16.3
18:0	69.3 ± 11.9	65.5 ± 4.7
18:1	72.0 ± 2.2	66.3 ± 4.8
18:2	32.7 ± 0.5	31.8 ± 0.9
18:3	28.3 ± 0.9	28.0 ± 0.8
18:4 (1)	41.3 ± 1.0	41.0 ± 1.0
18:4 (2)	40.9 ± 1.2	40.1 ± 1.3
20:0	*n.d.*	*n.d.*
20:4	*n.d.*	*n.d.*
20:5	4151.1 ± 214.8	4375.0 ± 172.4
22:0	*n.d.*	*n.d.*
22:6	76.1 ± 4.1	78.7 ± 2.4
24:0	*n.d.*	*n.d.*
24:1	*n.d.*	*n.d.*

Appendix 7: Mass spectra – *P. glacialis*

Regarding all the mass spectra, the entire *m/z* range is not presented, but all spectra had prominent fragment ions at *m/z* = 92, 108, 151 and 164.

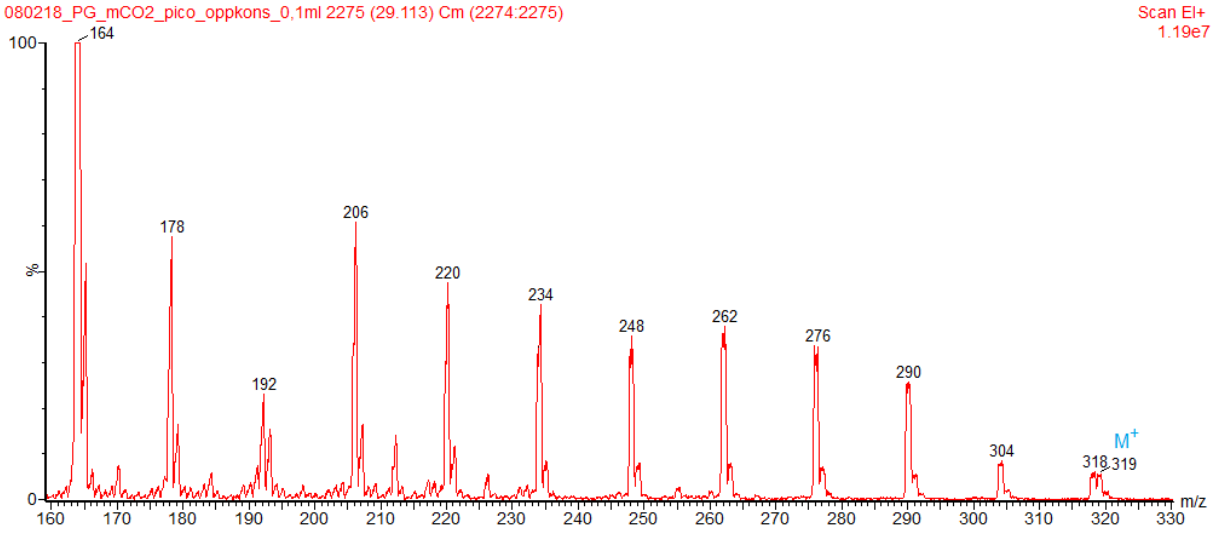

Figure 65 - Mass spectrum of 3-pyridylcarbinyl tetradecanoate (14:0).

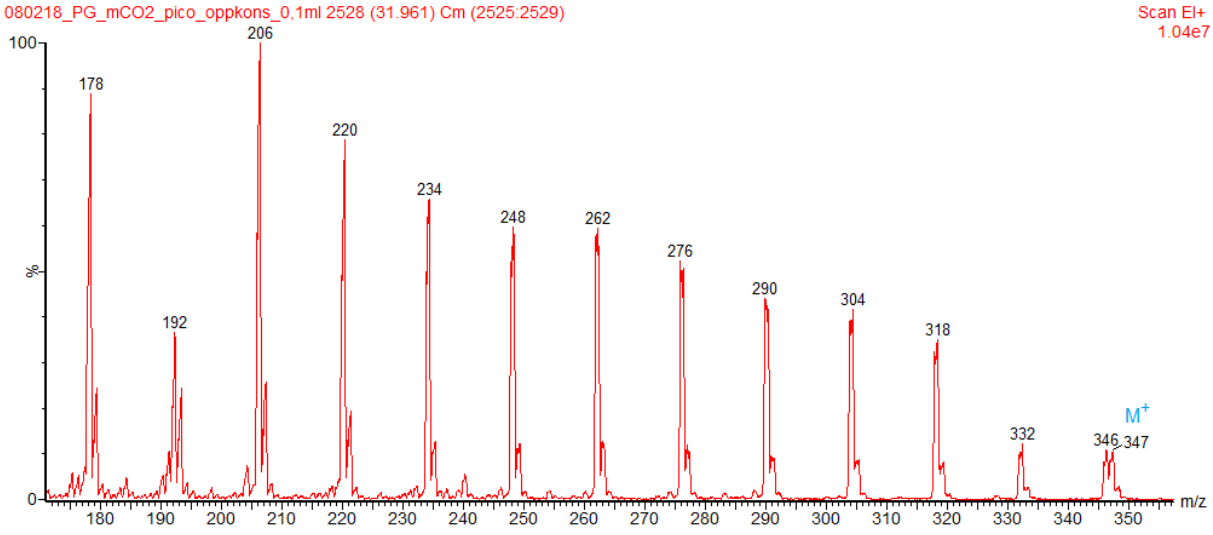

Figure 66 - Mass spectrum of 3-pyridylcarbinyl hexadecanoate (16:0).

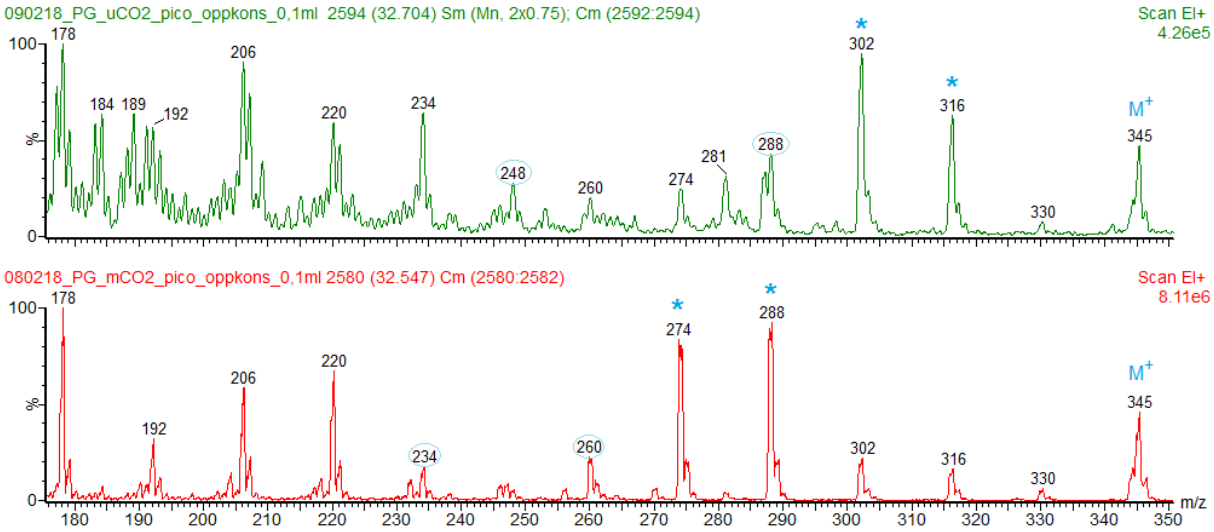

Figure 67 - Mass spectrum of 3-pyridylcarbinyl 11(Z)-hexadecenoate (16:1 n-5), at the top, and 3-pyridylcarbinyl 9(Z)-hexadecenoate (16:1 n-7), at the bottom. For 16:1 n-5, there is a gap of 40 amu between m/z = 248 and 288 and a prominent doublet at m/z = 302 and 316. For 16:1 n-7, there is a gap of 26 amu between m/z = 234 and 260 and a prominent doublet at m/z = 274 and 288. Structures of both fatty acid derivatives are shown in Figure 91 and Figure 92.

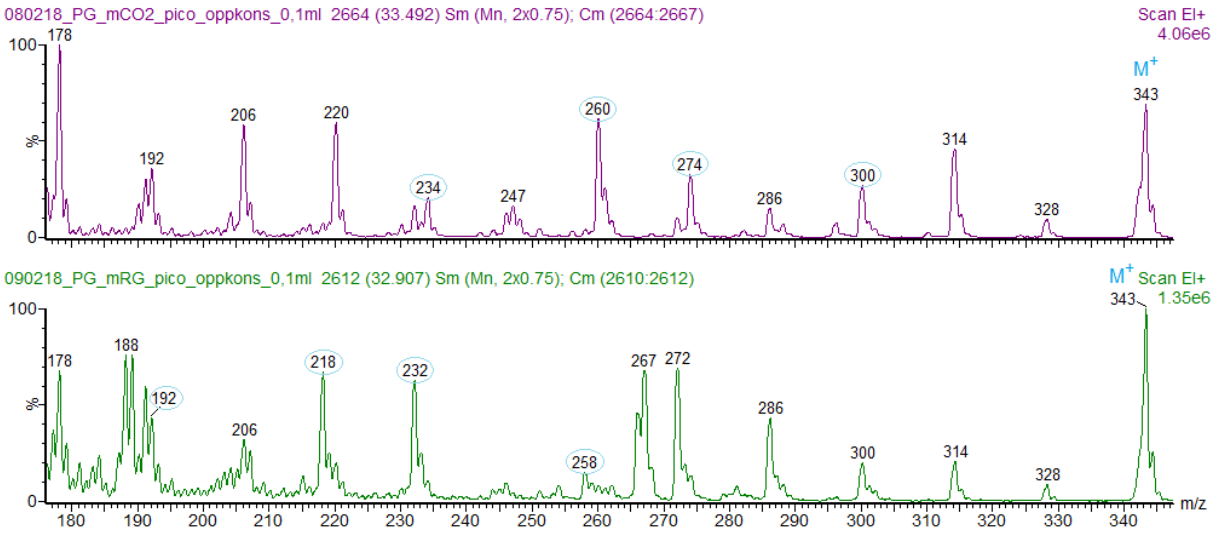

Figure 68 - Mass spectrum of 3-pyridylcarbinyl 9(Z),12(Z)-hexadecadienoate (16:2 n-4), at the top, and 3-pyridylcarbinyl 6(Z),9(Z)-hexadecadienoate (16:2 n-7), at the bottom. For 16:2 n-4, gaps of 26 amu are observed between m/z = 234 and 260 and m/z = 274 and 300. For 16:2 n-7, there are gaps of 26 amu between m/z = 192 and 218 and m/z = 232 and 258. Structures of both fatty acid derivatives are shown in Figure 93 and Figure 94.

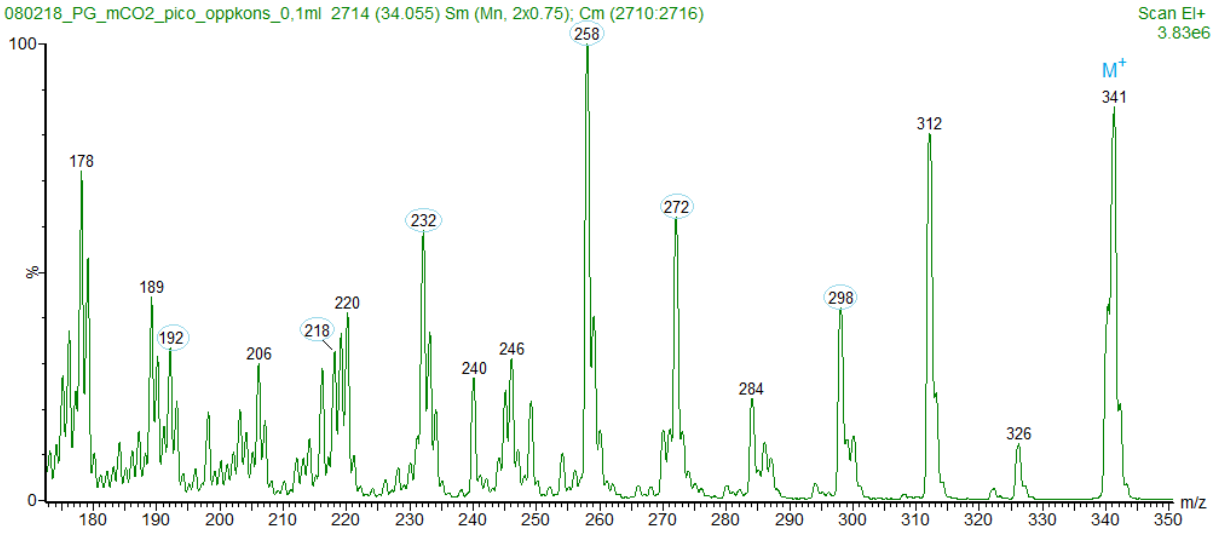

Figure 69 - Mass spectrum of 3-pyridylcarbinyl 6(Z),9(Z),12(Z)-hexadecatrienoate (16:3 n-4). Three gaps of 26 amu are observed between m/z = 192 and 218, m/z = 232 and 258 and m/z = 272 and 298. The structure is shown in Figure 95.

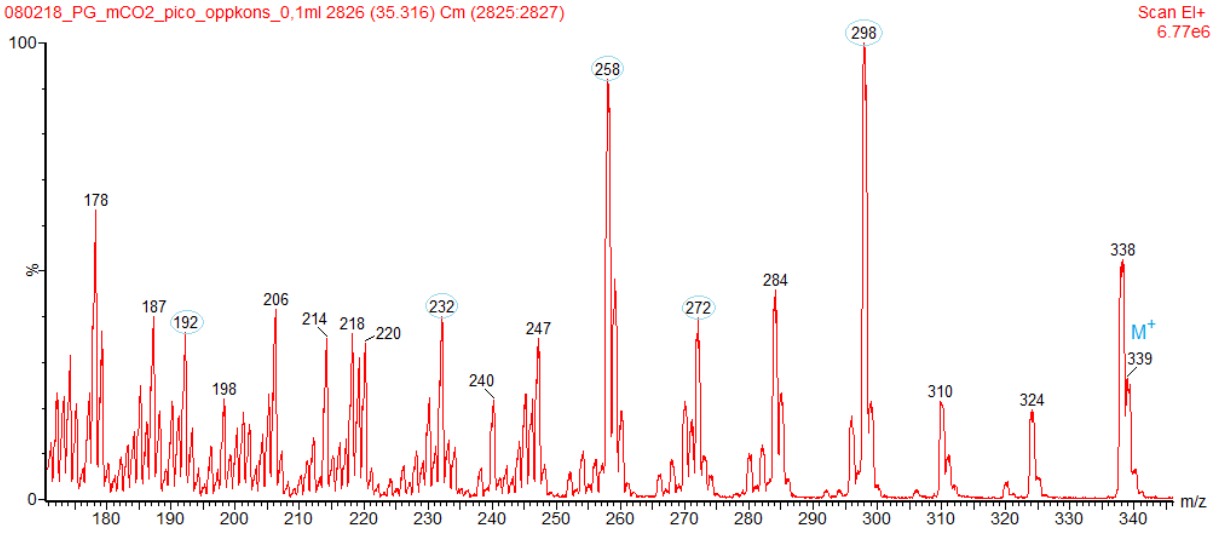

Figure 70 - Mass spectrum of 3-pyridylcarbinyl 6(Z),9(Z),12(Z),15(Z)-hexadecatetraenoate (16:4 n-1). There is a gap of 40 amu between m/z = 192 and 232 and two gaps of 26 amu between m/z = 232 and 258 and m/z = 272 and 298. Rearrangements caused by the terminal double bond make parts of the mass spectrum difficult to interpret. The structure is shown in Figure 96.

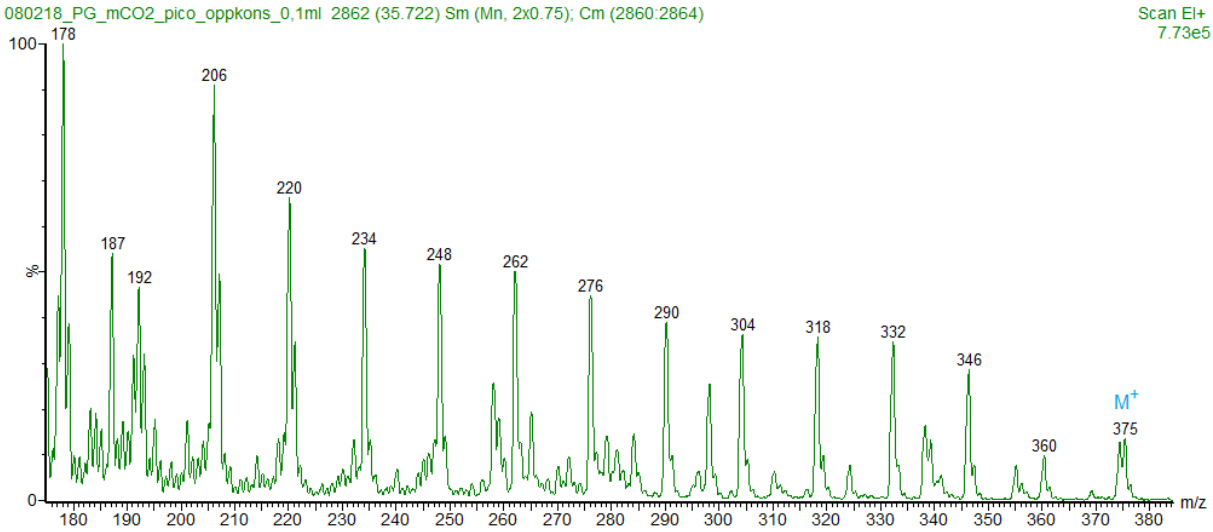

Figure 71 - Mass spectrum of 3-pyridylcarbinyl octadecanoate (18:0).

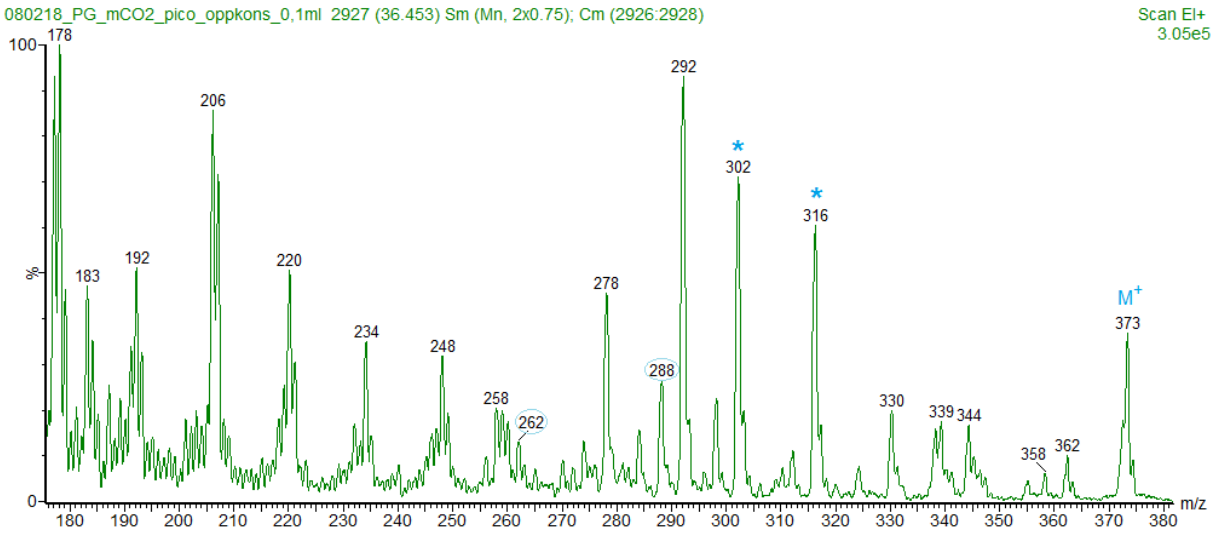

Figure 72 - Mass spectrum of 3-pyridylcarbinyl 11(Z)-octadecenoate (18:1 n-7). There is a gap of 26 amu between m/z = 262 and 288 and a prominent doublet at m/z = 302 and 316. The structure is shown in Figure 97.

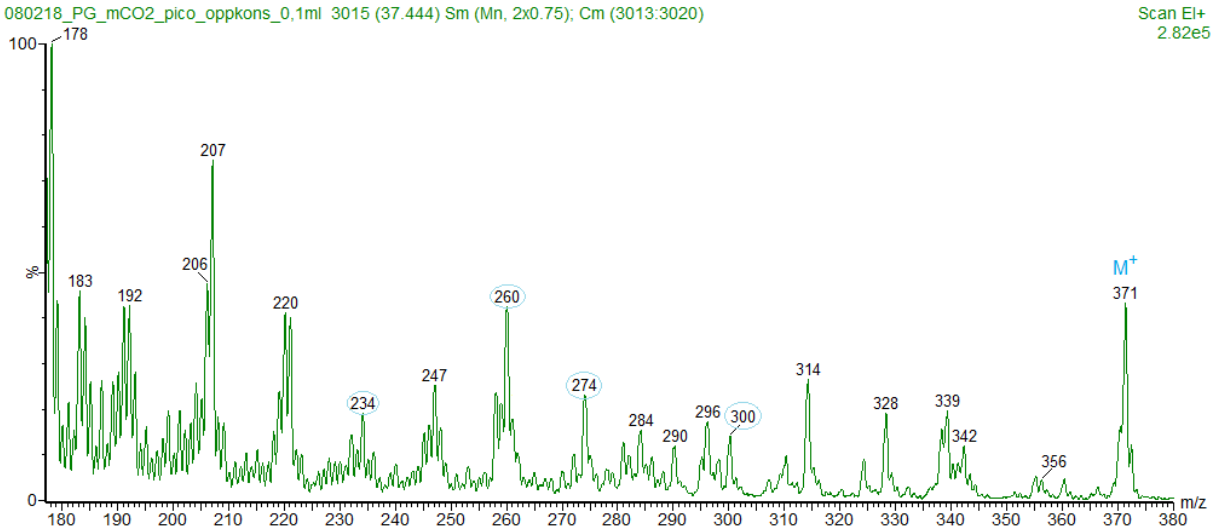

Figure 73 - Mass spectrum of 3-pyridylcarbinyl 9(Z),12(Z)-octadecadienoate (18:2 n-6). Two gaps of 26 amu are observed between m/z = 234 and 260 and m/z = 274 and 300. The structure is shown in Figure 98.

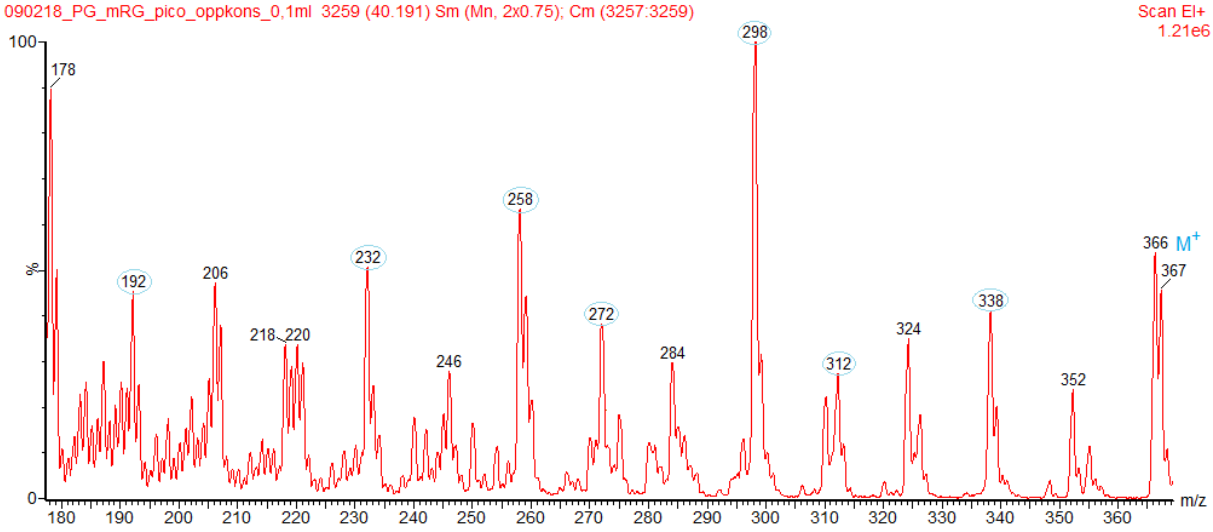

Figure 74 - Mass spectrum of 3-pyridylcarbinyl 6(Z),9(Z),12(Z),15(Z)-octadecatetraenoate (18:4 n-3). There is a gap of 40 amu between m/z = 192 and 232 and three gaps of 26 amu between m/z = 232 and 258, m/z = 272 and 298 and m/z = 312 and 338. The structure is shown in Figure 99.

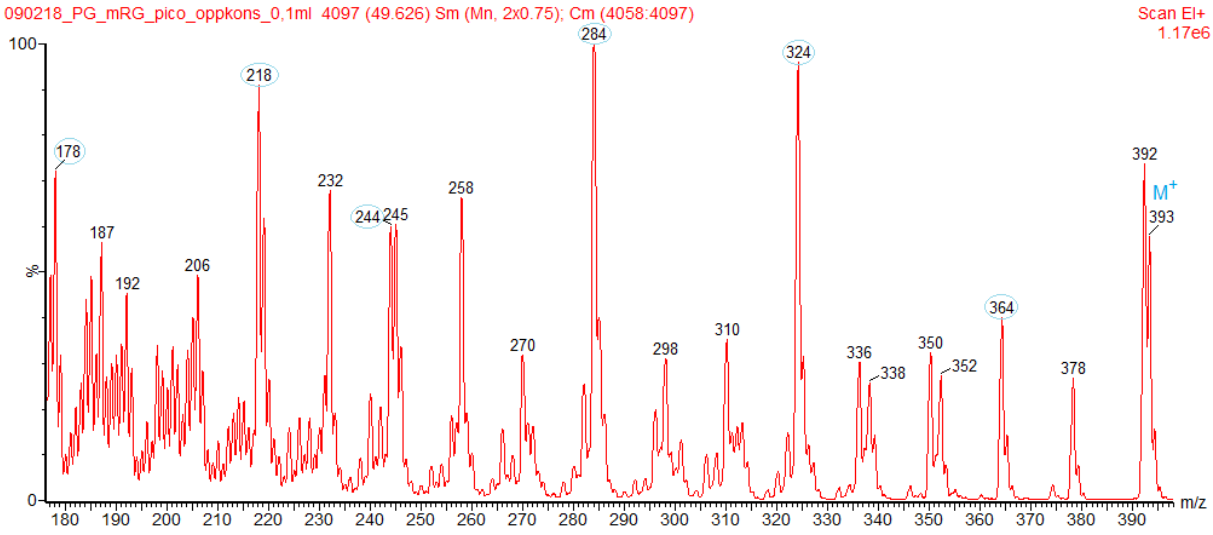

Figure 75 - Mass spectrum of 3-pyridylcarbinyl 5(Z),8(Z),11(Z),14(Z),17(Z)-eicosapentaenoate (20:5 n-3). There is a gap of 40 amu between m/z = 178 and 218, a gap of 26 amu between m/z = 218 and 244 and three gaps of 40 amu between m/z = and m/z = 244, 284, 324 and 364. The structure is shown in Figure 101.

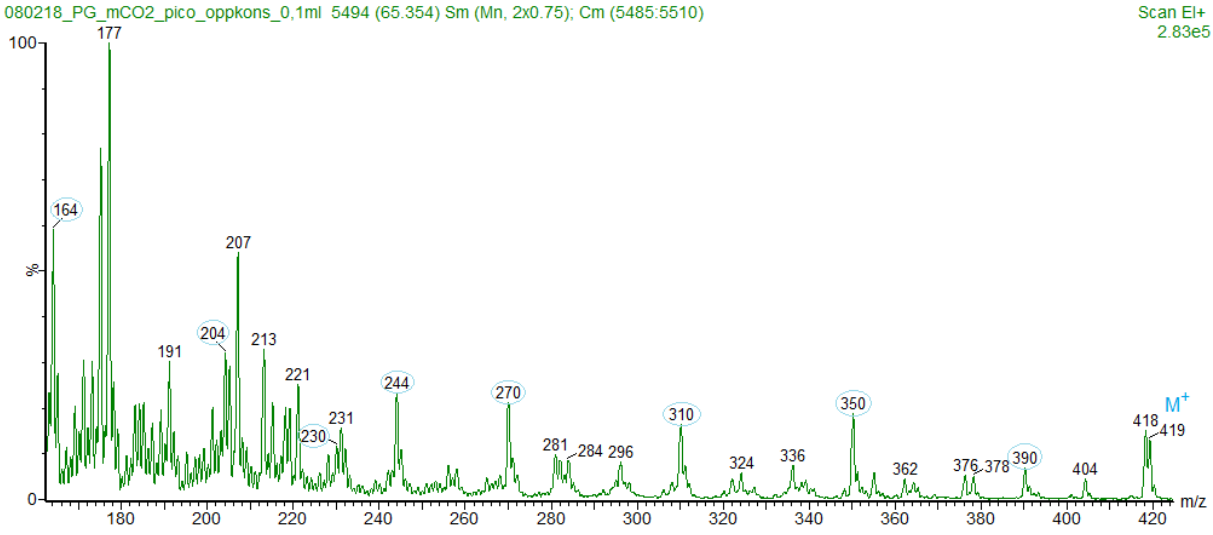

Figure 76 - Mass spectrum of 3-pyridylcarbinyl 4(Z),7(Z),10(Z),13(Z),16(Z),19(Z)-docosahexaenoate (22:6 n-3). There are six gaps of 40 amu between m/z = 164, 204 and 244 and m/z = 230, 270, 310, 350 and 390. The structure is shown in Figure 102.

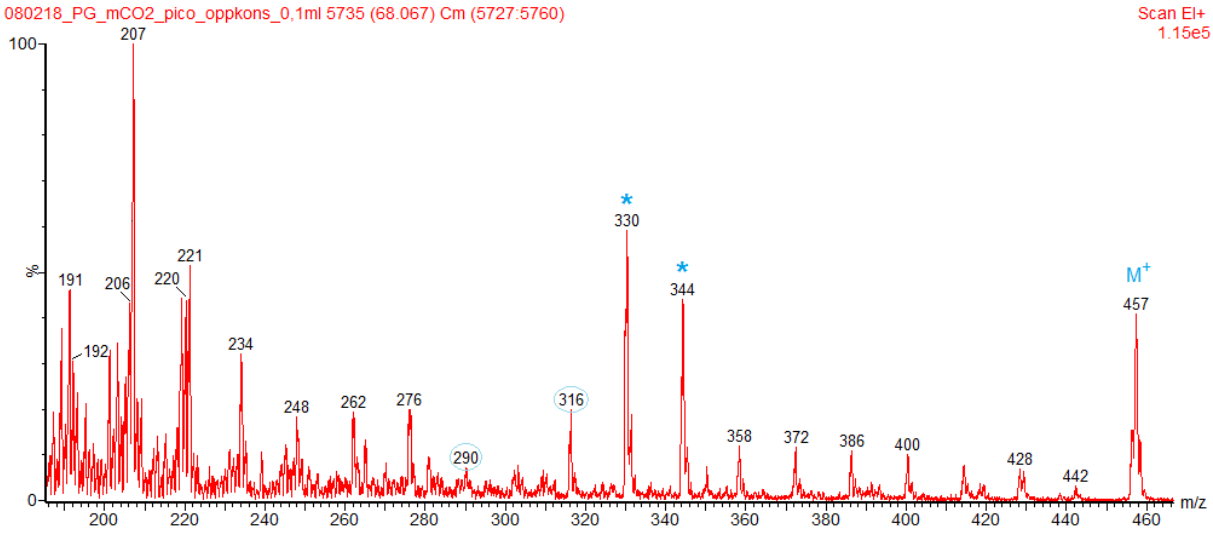

Figure 77 - Mass spectrum of 3-pyridylcarbinyl 13(Z)-tetracosenoate (24:1 n-11). There is a gap of 26 amu between m/z = 290 and 316 and a prominent doublet at m/z = 330 and 344. The structure is shown in Figure 104.

Appendix 8: Mass spectra – *C. furcellatus*

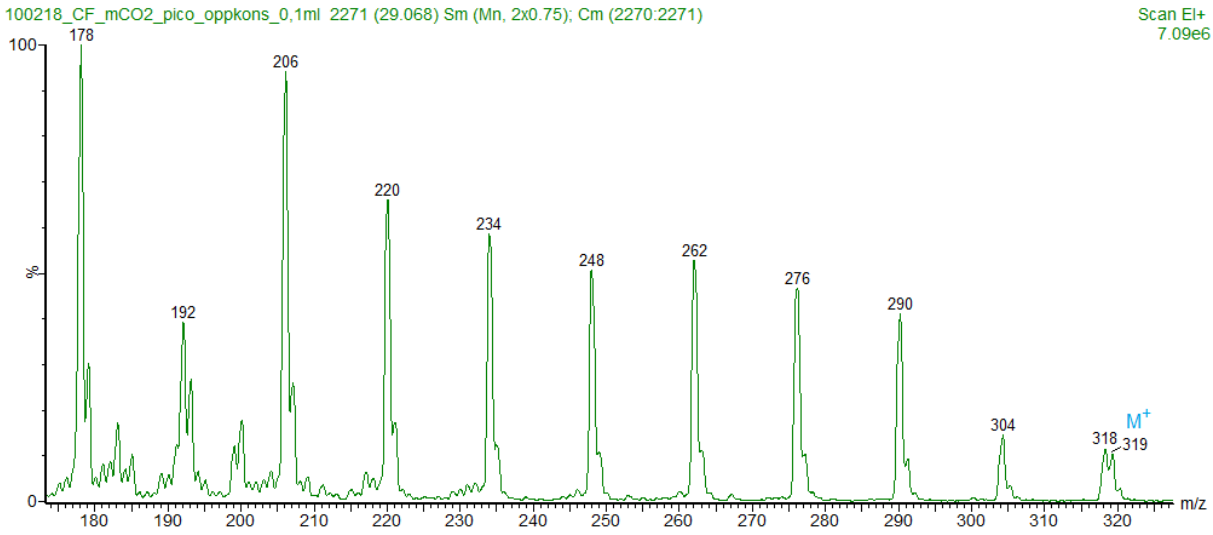

Figure 78 - Mass spectrum of 3-pyridylcarbinyl tetradecanoate (14:0).

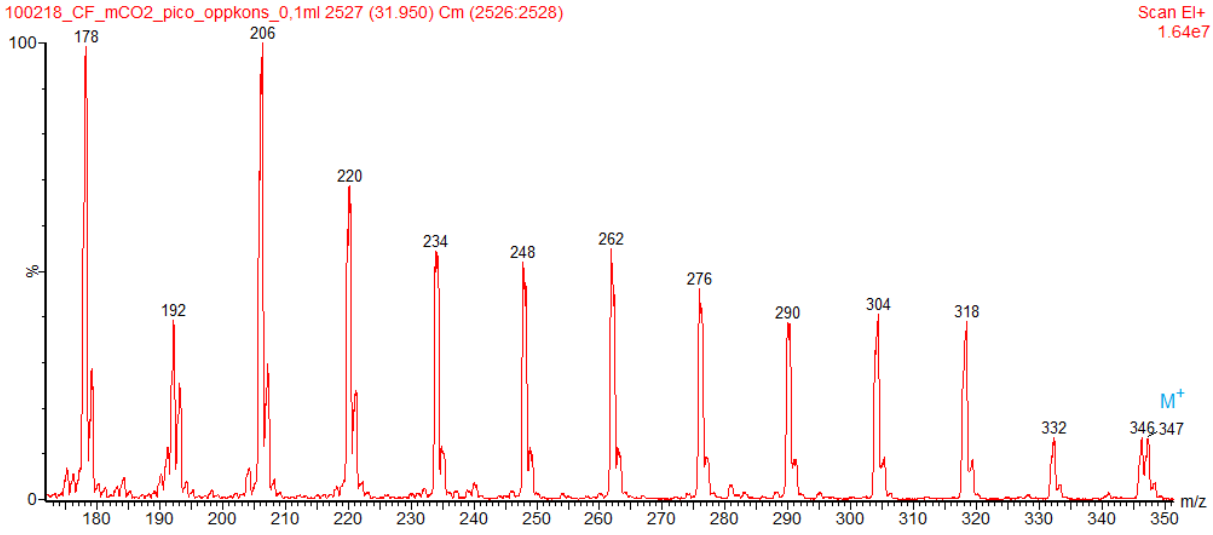

Figure 79 - Mass spectrum of 3-pyridylcarbinyl hexadecanoate (16:0).

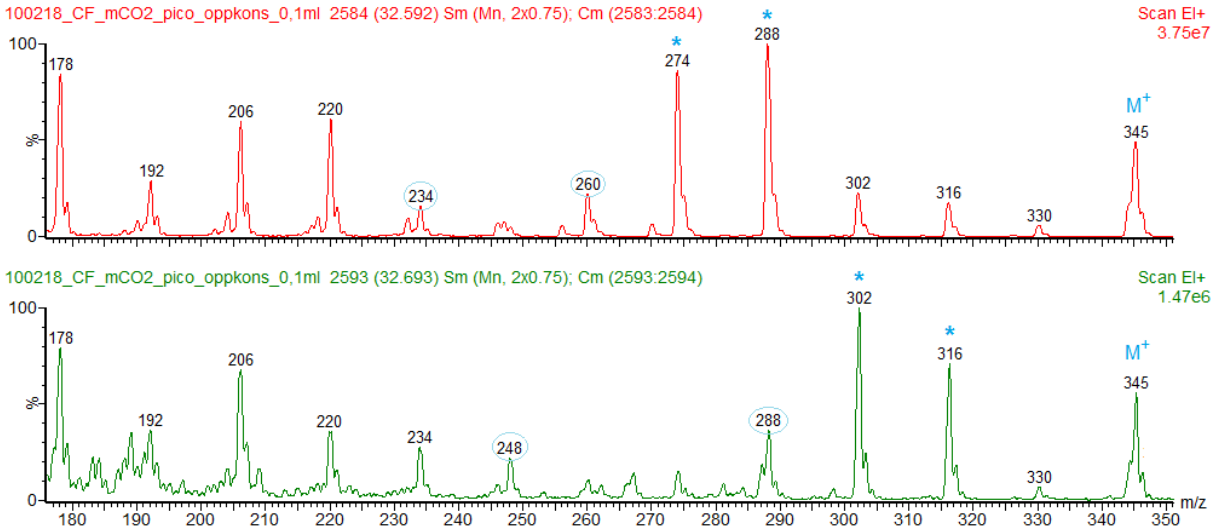

Figure 80 - Mass spectrum of 3-pyridylcarbinyl 9(Z)-hexadecenoate (16:1 n-7), at the top, and 3-pyridylcarbinyl 11(Z)-hexadecenoate (16:1 n-5), at the bottom. For 16:1 n-5, there is a gap of 40 amu between m/z = 248 and 288 and a prominent doublet at m/z = 302 and 316. For 16:1 n-7, there is a gap of 26 amu between m/z = 234 and 260 and a prominent doublet at m/z = 274 and 288. Structures of both fatty acid derivatives are shown in Figure 91 and Figure 92.

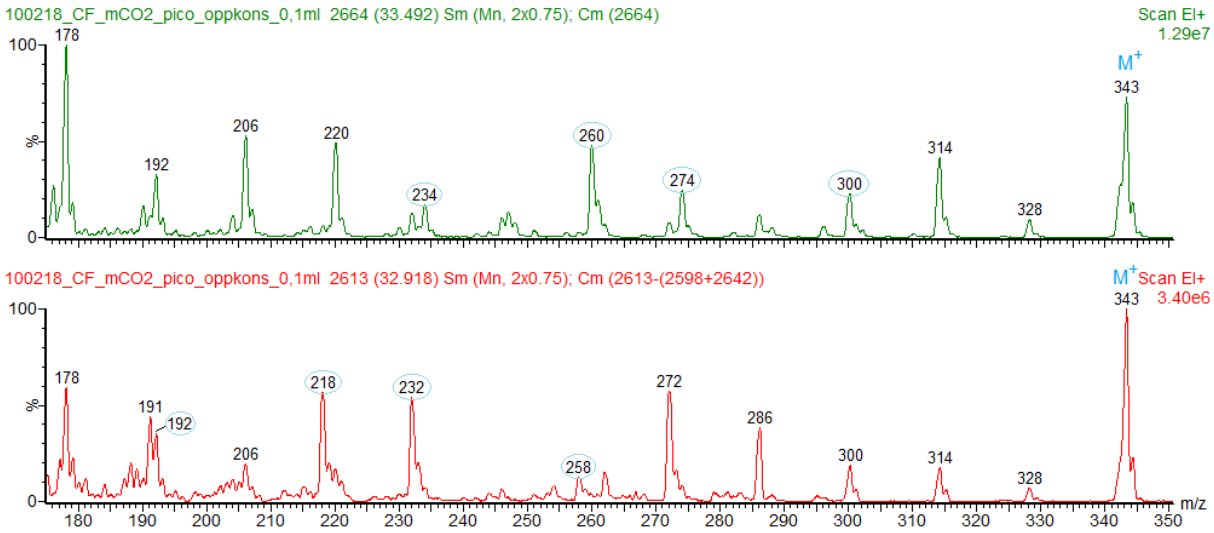

Figure 81 - Mass spectrum of 3-pyridylcarbinyl 9(Z),12(Z)-hexadecadienoate (16:2 n-4), at the top, and 3-pyridylcarbinyl 6(Z),9(Z)-hexadecadienoate (16:2 n-7), at the bottom. For 16:2 n-4, gaps of 26 amu are observed between m/z = 234 and 260 and m/z = 274 and 300. For 16:2 n-7, there are two gaps of 26 amu between m/z = 192 and 218 and m/z = 232 and 258. Structures of both fatty acid derivatives are shown in Figure 93 and Figure 94.

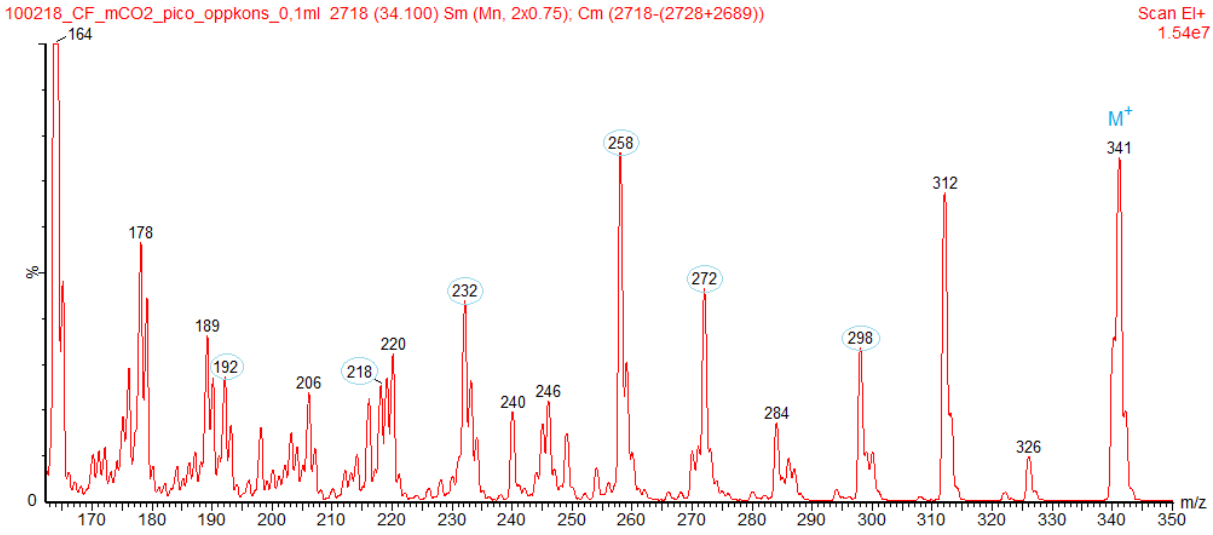

Figure 82 - Mass spectrum of 3-pyridylcarbinyl 6(Z),9(Z),12(Z)-hexadecatrienoate (16:3 n-4). Three gaps of 26 amu are observed between m/z = 192 and 218, m/z = 232 and 258 and m/z = 272 and 298. The structure is shown in Figure 95.

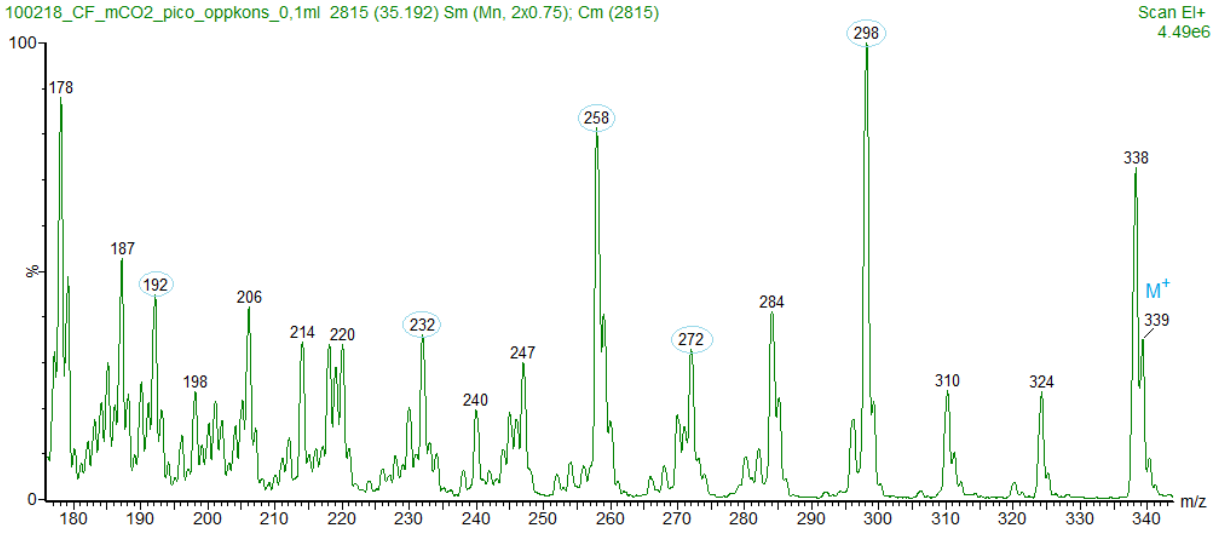

Figure 83 - Mass spectrum of 3-pyridylcarbinyl 6(Z),9(Z),12(Z),15(Z)-hexadecatetraenoate (16:4 n-1). There is a gap of 40 amu between m/z = 192 and 232 and two gaps of 26 amu between m/z = 232 and 258 and m/z = 272 and 298. Rearrangements caused by the terminal double bond make parts of the mass spectrum difficult to interpret. The structure is shown in Figure 96.

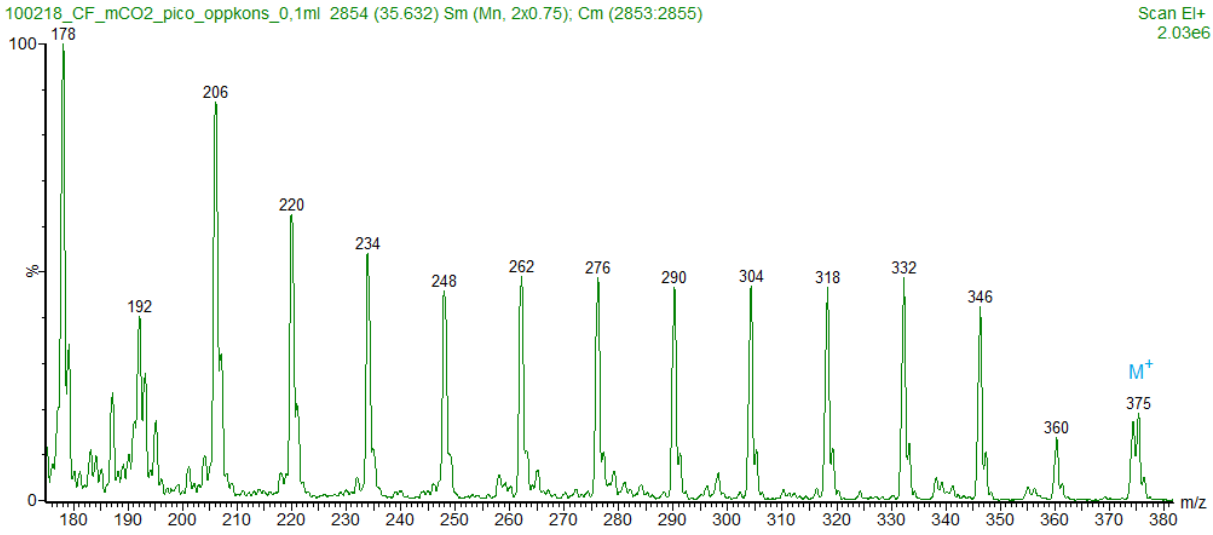

Figure 84 - Mass spectrum of 3-pyridylcarbinyl octadecanoate (18:0).

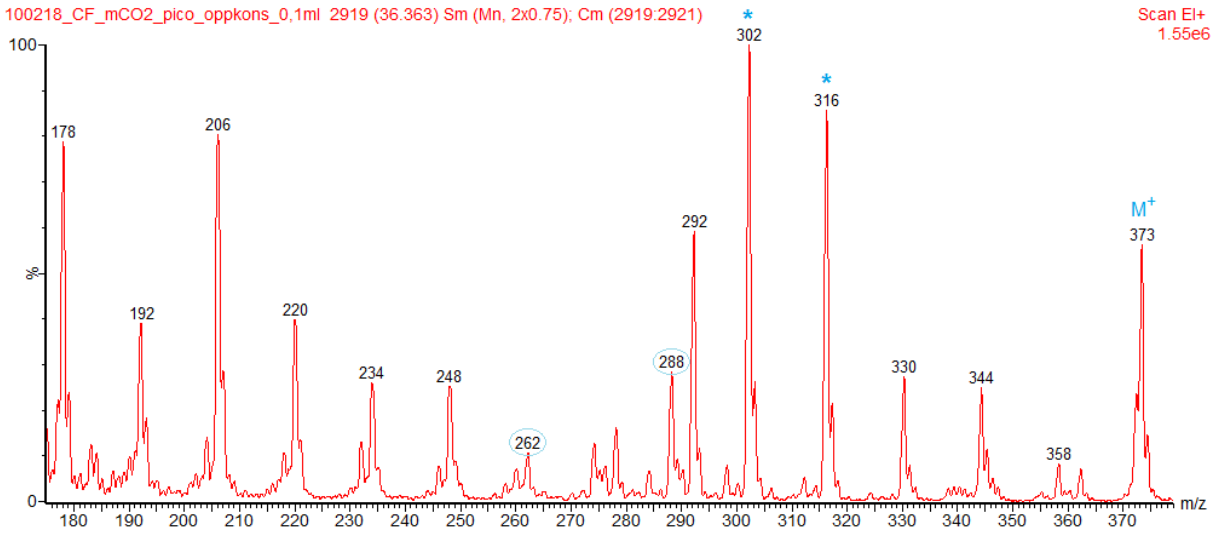

Figure 85 - Mass spectrum of 3-pyridylcarbinyl 11(Z)-octadecenoate (18:1 n-7). There is a gap of 26 amu between m/z = 262 and 288 and a prominent doublet at m/z = 302 and 316. The structure is shown in Figure 97.

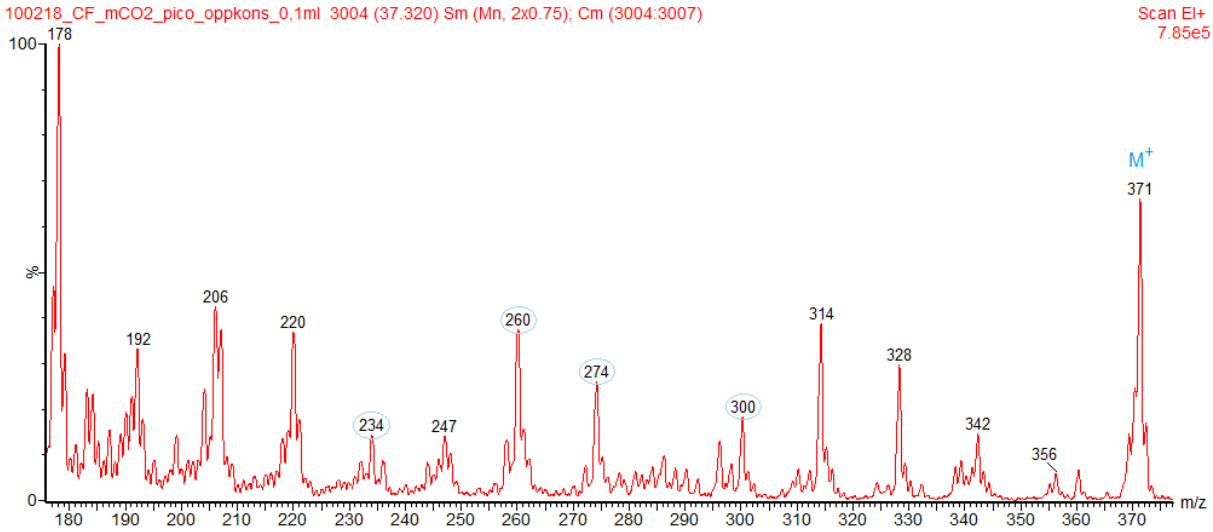

Figure 86 - Mass spectrum of 3-pyridylcarbinyl 9(Z),12(Z)-octadecadienoate (18:2 n-6). Two gaps of 26 amu are observed between m/z = 234 and 260 and m/z = 274 and 300. The structure is shown in Figure 98.

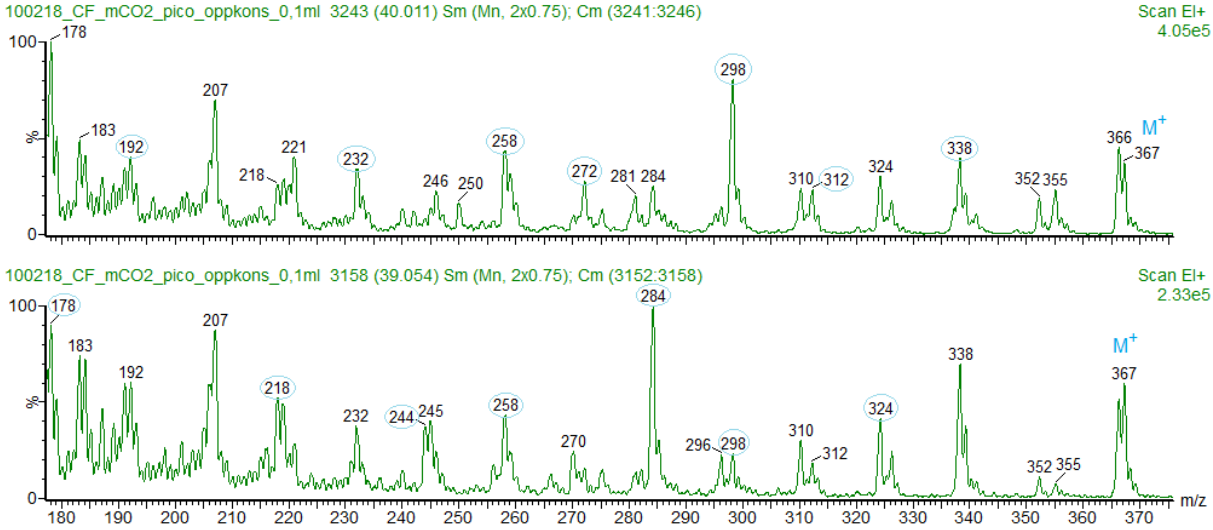

Figure 87 - Mass spectrum of 3-pyridylcarbinyl 6(Z),9(Z),12(Z),15(Z)-octadecatetraenoate (18:4 n-3), at the top, and 3-pyridylcarbinyl 5(Z),8(Z),11(Z),14(Z)-octadecatetraenoate (18:4 n-4), at the bottom. For 18:4 n-3, there is a gap of 40 amu between m/z = 192 and 232 and three gaps of 26 amu between m/z = 232 and 258, m/z = 272 and 298 and m/z = 312 and 338. For 18:4 n-4, there is a gap of 40 amu between m/z = 178 and 218 and three gaps of 26 amu between m/z = 218 and 244, m/z = 258 and 284 and m/z = 298 and 324. Structures of both fatty acid derivatives are shown in Figure 99 and Figure 100.

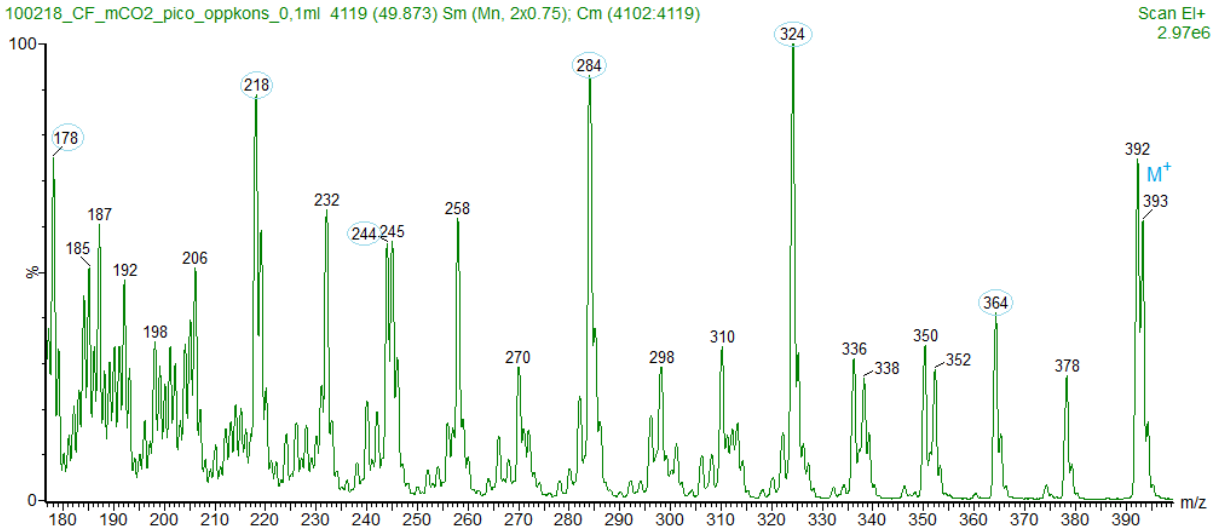

Figure 88 - Mass spectrum of 3-pyridylcarbinyl 5(Z),8(Z),11(Z),14(Z),17(Z)-eicosapentaenoate (20:5 n-3). There is a gap of 40 amu between m/z = 178 and 218, a gap of 26 amu between m/z = 218 and 244 and three gaps of 40 amu between m/z = and m/z = 244, 284, 324 and 364. The structure is shown in Figure 101.

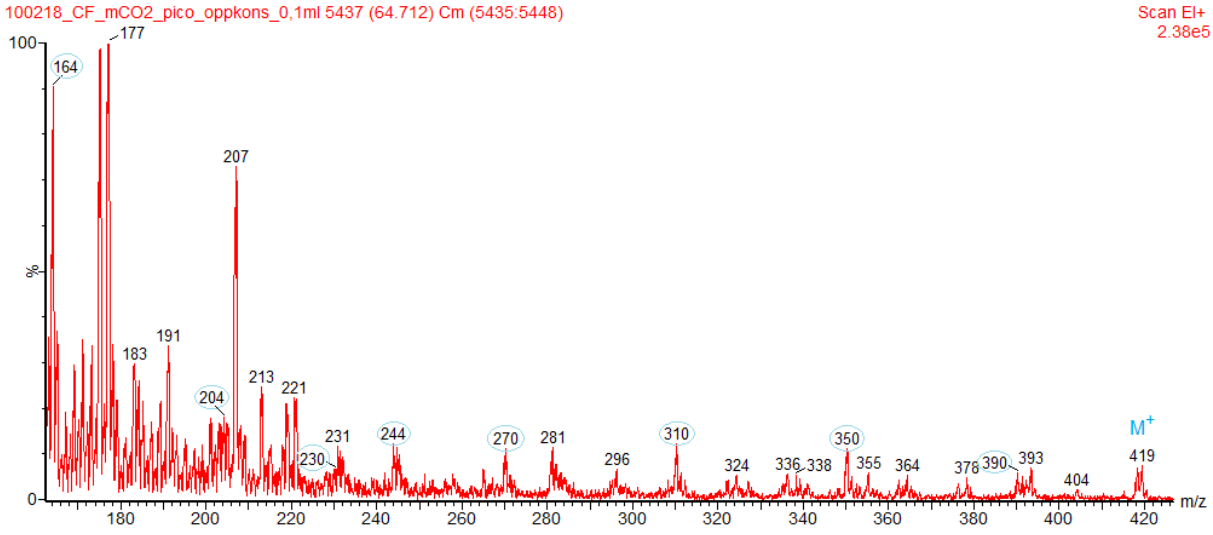

Figure 89 - Mass spectrum of 3-pyridylcarbinyl 4(Z),7(Z),10(Z),13(Z),16(Z),19(Z)-docosahexaenoate (22:6 n-3). There are six gaps of 40 amu between m/z = 164, 204 and 244 and m/z = 230, 270, 310, 350 and 390. The structure is shown in Figure 102.

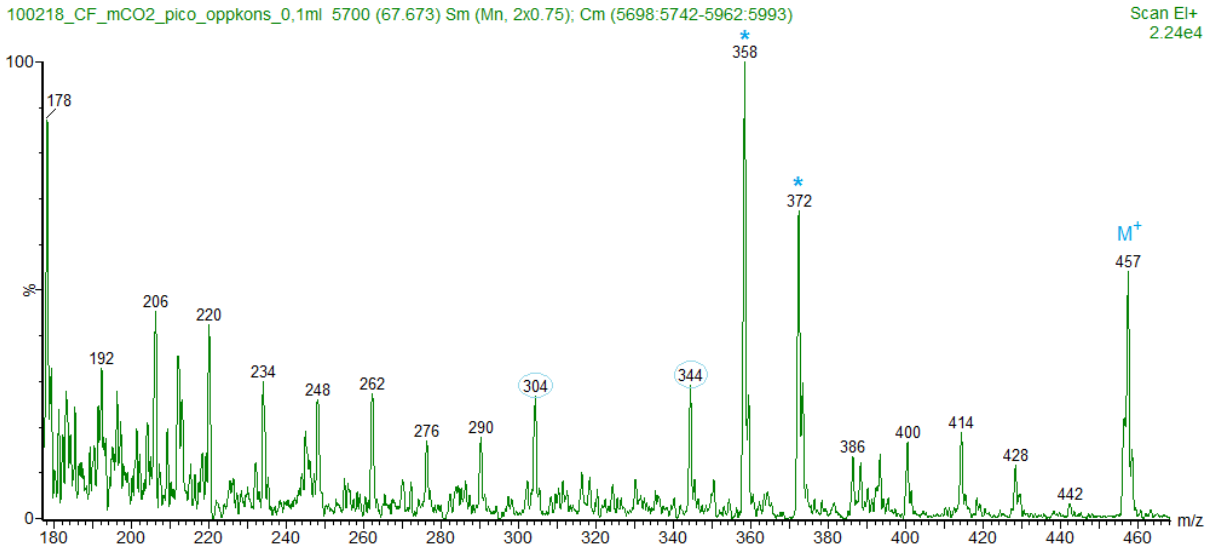

Figure 90 - Mass spectrum of 3-pyridylcarbinyl 15(Z)-tetracosenoate (24:1 n-9). There is a gap of 40 amu between m/z = 304 and 344 and a prominent doublet at m/z = 358 and 372. The structure is shown in Figure 103.

Appendix 9: Chemical structures of the picolinyl derivatives of the unsaturated fatty acids in the algae samples

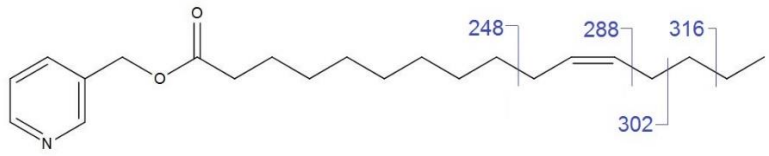

Figure 91 – 3-pyridylcarbinyl 11(Z)-hexadecenoate (16:1 n-5)

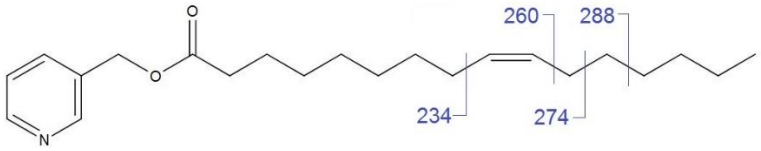

Figure 92 – 3-pyridylcarbinyl 9(Z)-hexadecenoate (16:1 n-7)

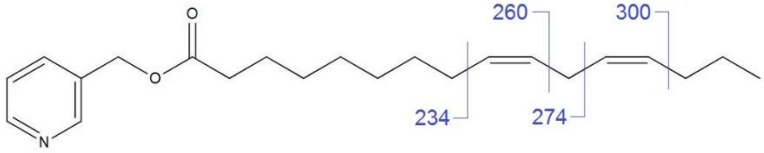

Figure 93 - 3-pyridylcarbinyl 9(Z),12(Z)-hexadecadienoate (16:2 n-4)

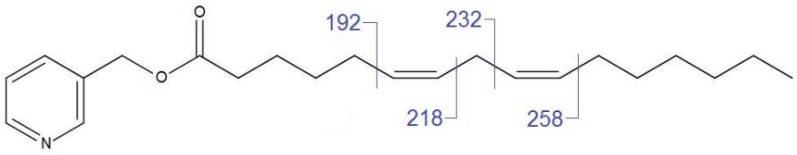

Figure 94 - 3-pyridylcarbinyl 6(Z),9(Z)-hexadecadienoate (16:2 n-7)

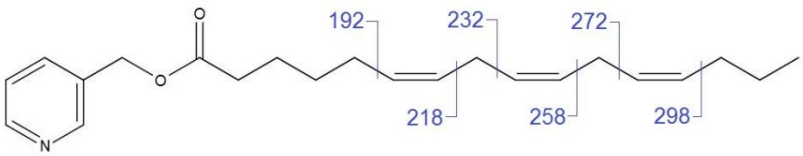

Figure 95 - 3-pyridylcarbinyl 6(Z),9(Z),12(Z)-hexadecatrienoate (16:3 n-4)

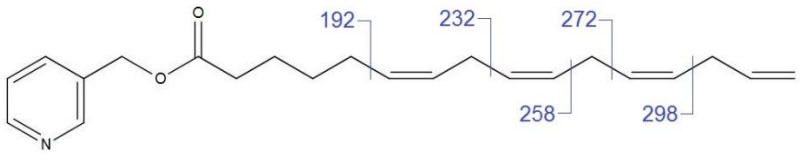

Figure 96 - 3-pyridylcarbinyl 6(Z),9(Z),12(Z),15(Z)-hexadecatetraenoate (16:4 n-1)

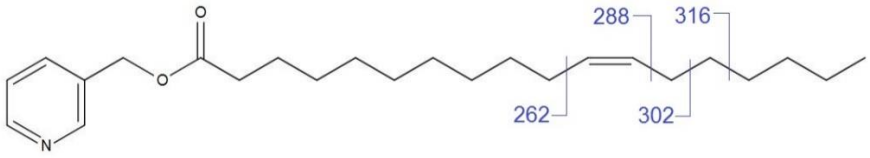

Figure 97 - 3-pyridylcarbinyl 11(Z)-octadecenoate (18:1 n-7)

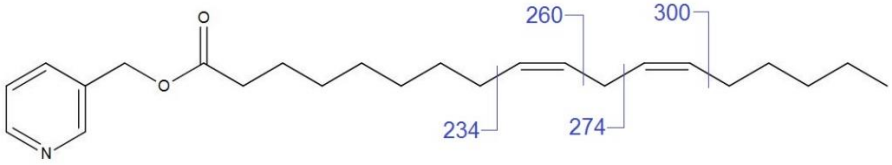

Figure 98 - 3-pyridylcarbinyl 9(Z),12(Z)-octadecadienoate (18:2 n-6)

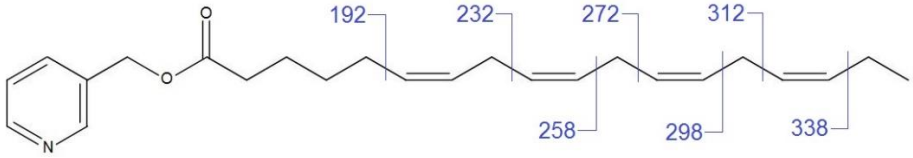

Figure 99 - 3-pyridylcarbinyl 6(Z),9(Z),12(Z),15(Z)-octadecatetraenoate (18:4 n-3)

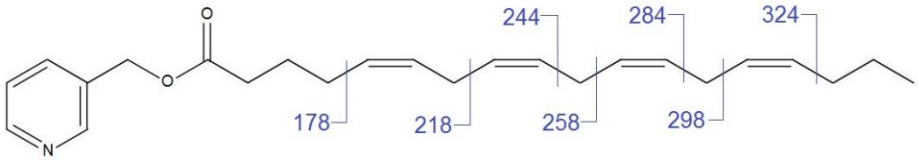

Figure 100 - 3-pyridylcarbinyl 5(Z),8(Z),11(Z),14(Z)-octadecatetraenoate (18:4 n-4)

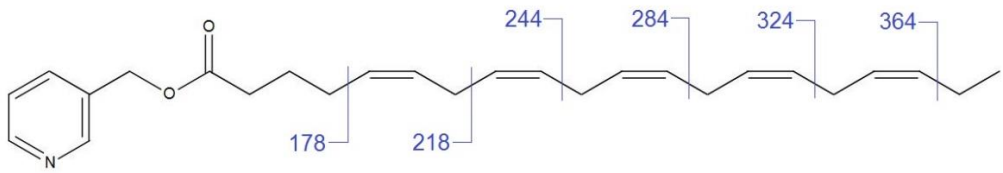

Figure 101 - 3-pyridylcarbinyl 5(Z),8(Z),11(Z),14(Z),17(Z)-eicosapentaenoate (20:5 n-3)

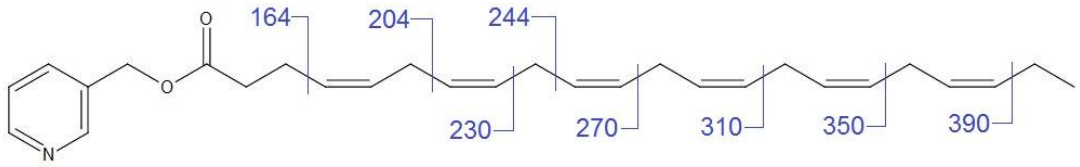

Figure 102 - 3-pyridylcarbinyl 4(Z),7(Z),10(Z),13(Z),16(Z),19(Z)-docosahexaenoate (22:6 n-3)

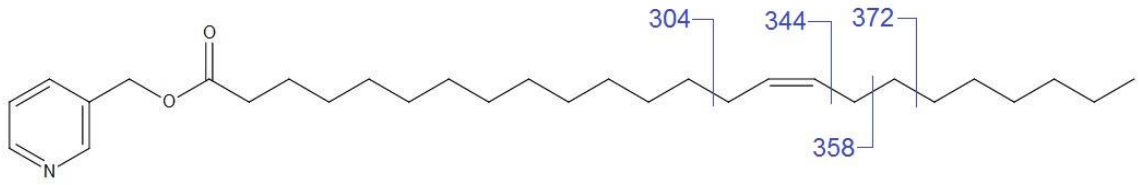

Figure 103 - 3-pyridylcarbinyl 15(Z)-tetracosenoate (24:1 n-9)

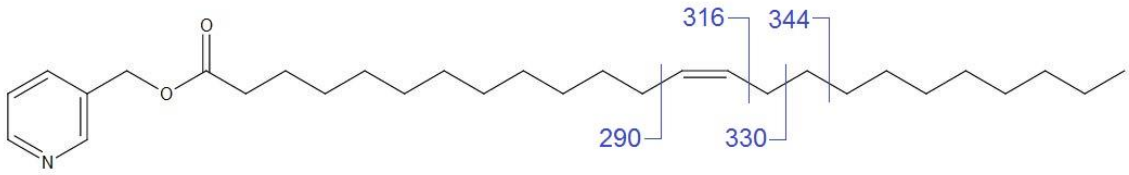

Figure 104 - 3-pyridylcarbinyl 13(Z)-tetracosenoate (24:1 n-11)

Appendix 10: SIR chromatograms of the FAMEs in the algae samples

Table 22 – Overview of SIR chromatograms

Chromatogram number	**FAME**	***m/z***
1	14:0	243.00
2	IS1 and 16:0	271.00
3	16:1	269.00
4	16:2	267.00
5	16:3	265.00
6	16:4	263.00
7	18:0	299.00
8	18:1	297.00
9	18:2	295.00
10	18:3	293.00
11	18:4	291.00
12	20:0	327.00
13	IS2	341.00
14	20:4	319.00
15	20:5	317.00
16	22:0	355.00
17	22:6	343.00
18	24:0	383.00
19	24:1	381.00

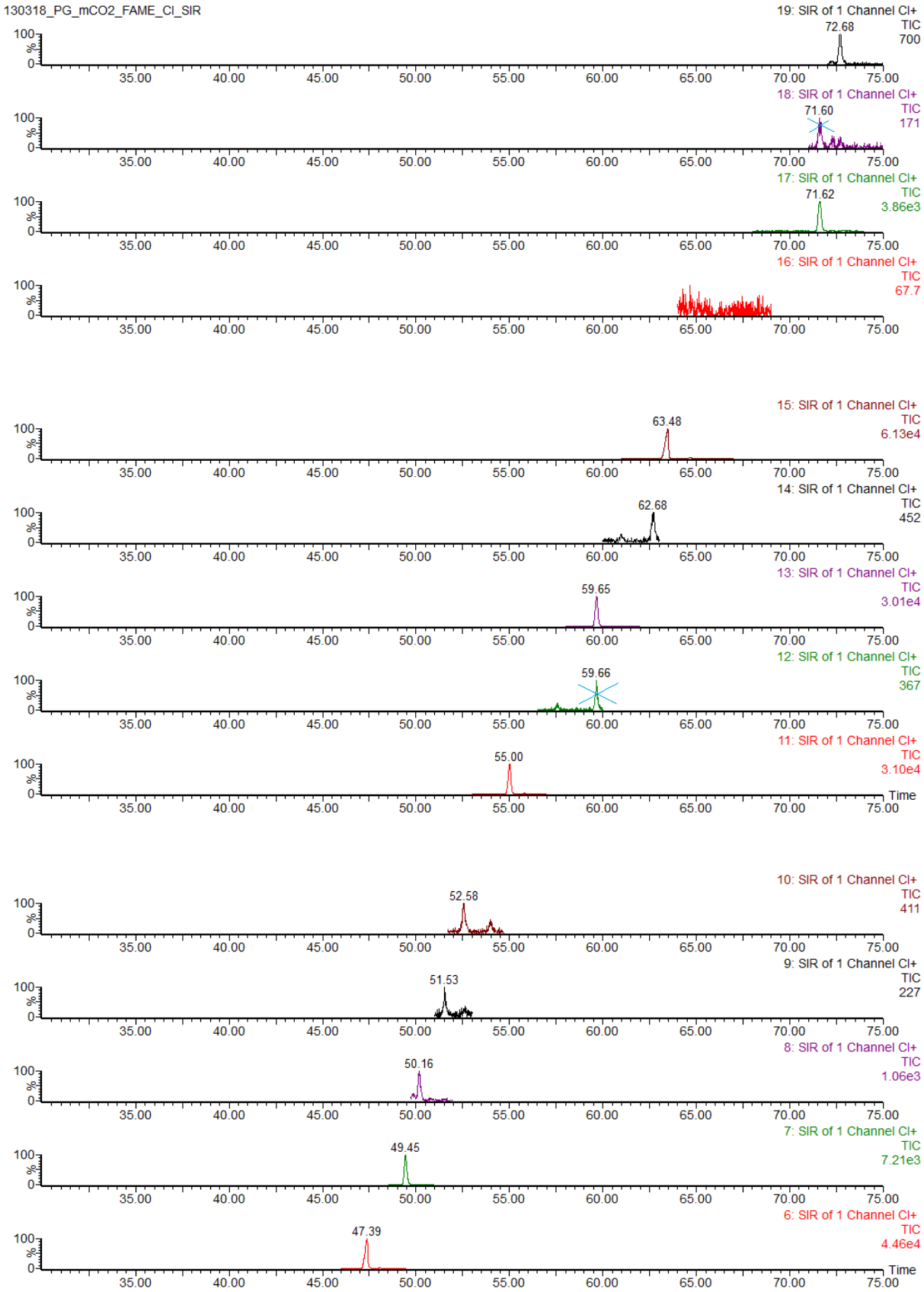
130318_PG_mCO2_FAME_Cl_SIR
19: SIR of 1 Channel Cl+
TIC
700
72.68
18: SIR of 1 Channel Cl+
TIC
171
71.60
17: SIR of 1 Channel Cl+
TIC
3.86e3
71.62
16: SIR of 1 Channel Cl+
TIC
67.7
15: SIR of 1 Channel Cl+
TIC
6.13e4
63.48
14: SIR of 1 Channel Cl+
TIC
452
62.68
13: SIR of 1 Channel Cl+
TIC
3.01e4
59.65
12: SIR of 1 Channel Cl+
TIC
367
59.66
11: SIR of 1 Channel Cl+
TIC
3.10e4
55.00
10: SIR of 1 Channel Cl+
TIC
411
52.58
9: SIR of 1 Channel Cl+
TIC
227
51.53
8: SIR of 1 Channel Cl+
TIC
1.06e3
50.16
7: SIR of 1 Channel Cl+
TIC
7.21e3
49.45
6: SIR of 1 Channel Cl+
TIC
4.46e4
47.39
100
%
0
35.00
40.00
45.00
50.00
55.00
60.00
65.00
70.00
75.00
Time

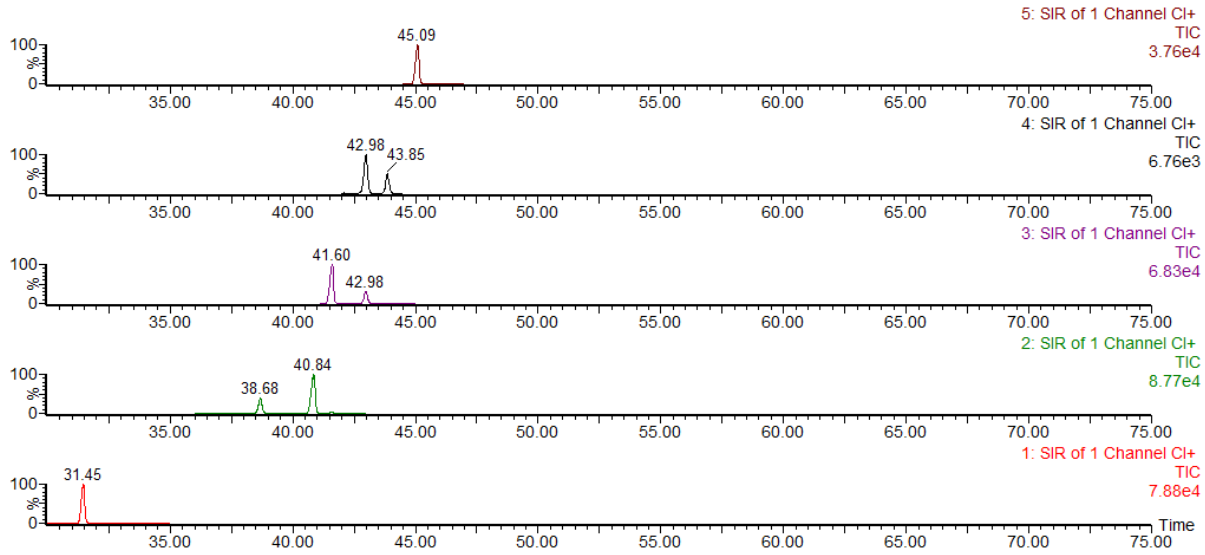

Figure 105 – SIR chromatograms of the FAMEs in an algae sample of P. glacialis (after addition of CO_2)

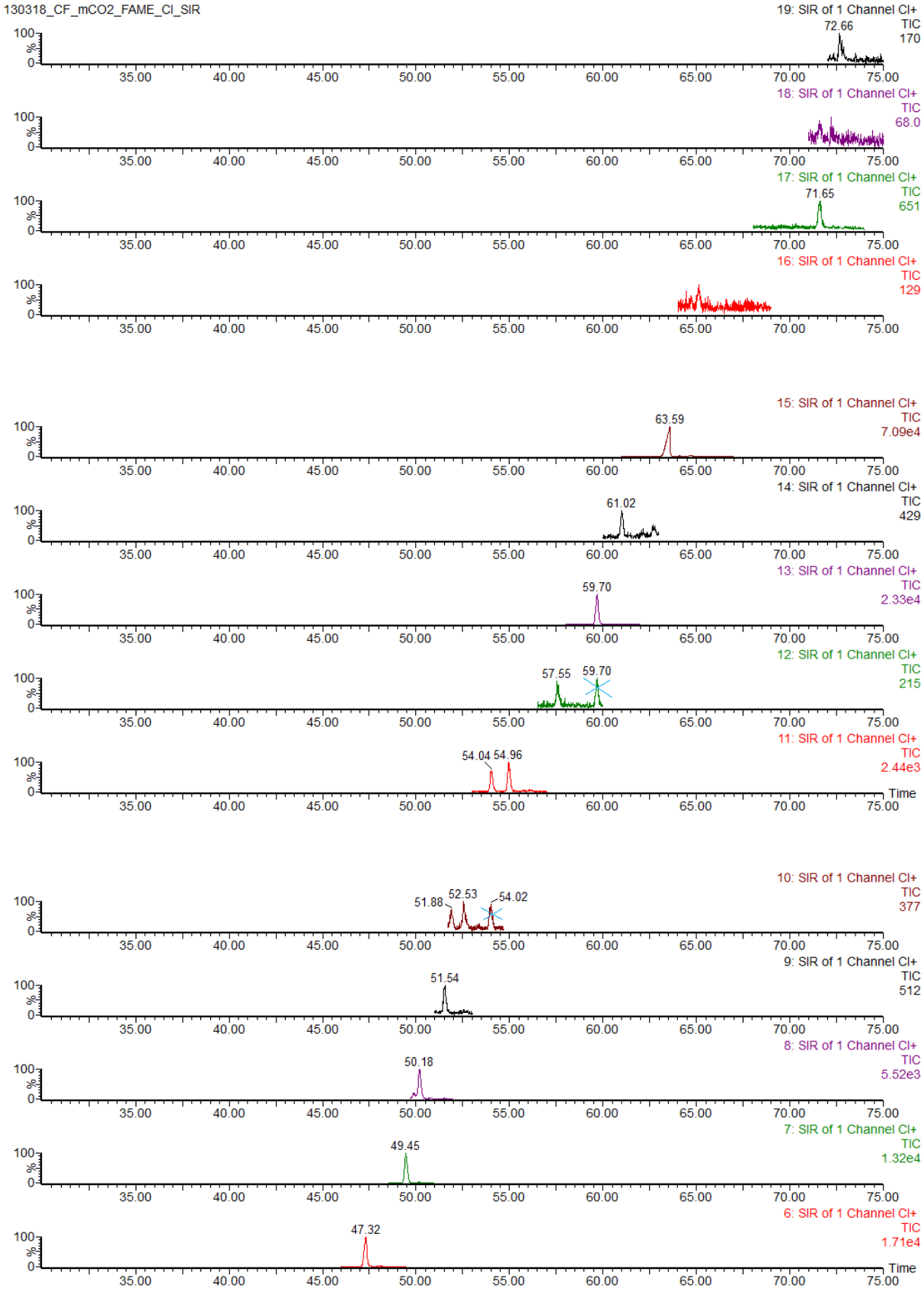
130318_CF_mCO2_FAME_CI_SIR
19: SIR of 1 Channel CI+
TIC
170
72.66
18: SIR of 1 Channel CI+
TIC
68.0
17: SIR of 1 Channel CI+
TIC
651
71.65
16: SIR of 1 Channel CI+
TIC
129
15: SIR of 1 Channel CI+
TIC
7.09e4
63.59
14: SIR of 1 Channel CI+
TIC
429
61.02
13: SIR of 1 Channel CI+
TIC
2.33e4
59.70
12: SIR of 1 Channel CI+
TIC
215
57.55
59.70
11: SIR of 1 Channel CI+
TIC
2.44e3
54.04
54.96
10: SIR of 1 Channel CI+
TIC
377
51.88
52.53
54.02
9: SIR of 1 Channel CI+
TIC
512
51.54
8: SIR of 1 Channel CI+
TIC
5.52e3
50.18
7: SIR of 1 Channel CI+
TIC
1.32e4
49.45
6: SIR of 1 Channel CI+
TIC
1.71e4
47.32
%
100
0
35.00
40.00
45.00
50.00
55.00
60.00
65.00
70.00
75.00
Time

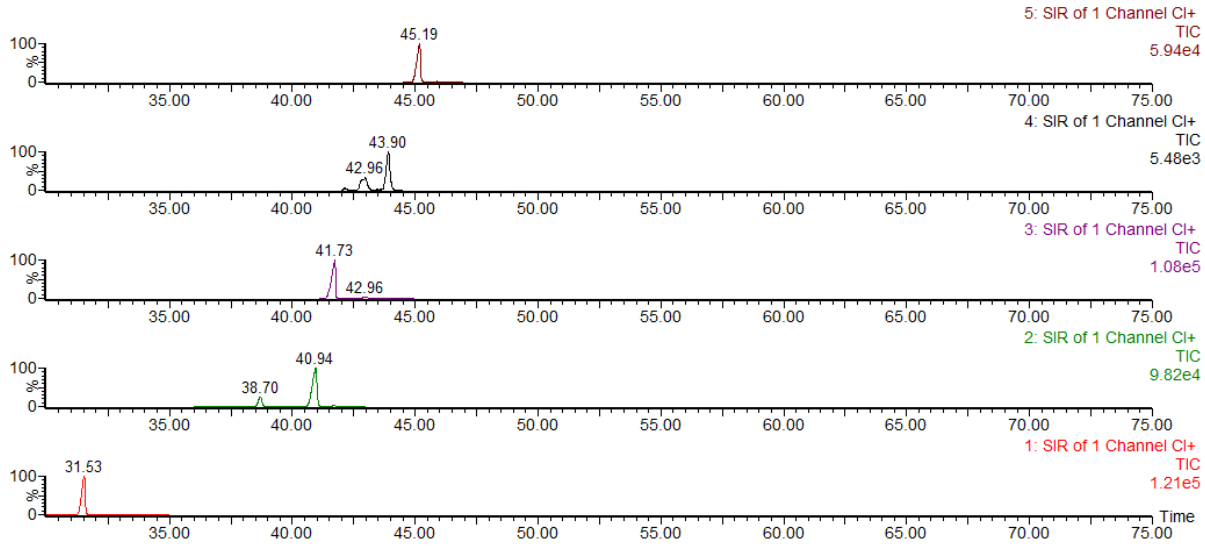

Figure 106 - SIR chromatograms of the FAMEs in an algae sample of C. furcellatus (after addition of CO_2)